UNIVERSIDAD AUTÓNOMA DE BAJA CALIFORNIA

Instituto de Ciencias Agrícolas

Instituto de Investigaciones en Ciencias Veterinarias

“Bacterias y nanopartículas de plantas autóctonas: aislamiento, caracterización y evaluación de sus propiedades antimicrobianas”

T E S I S

QUE COMO REQUISITO PARCIAL

PARA OBTENER EL GRADO DE:

DOCTOR EN CIENCIAS AGROPECUARIAS

PRESENTA

M.C. Ali Abdelmoteleb Abdelaziem Abdallah Gera

DIRECTOR

Dr. en C. Daniel González Mendoza

Co-DIRECTOR

Dra. en C. Rosalba Troncoso Rojas

Mexicali, B.C. Abril del 2018

La presente tesis "Bacterias y nanopartículas de plantas autóctonas: aislamiento, caracterización y evaluación de sus propiedades antimicrobianas" realizada por el **M.C. Ali Abdelmoteleb Abdelaziem Abdallah Gera**, dirigido por el Dr. en C. Daniel González Mendoza y la Co-Directora Dra. en C. Rosalba Troncoso Rojas, ha sido evaluada y aprobada por el Comité Particular abajo indicado, como requisito parcial para obtener el grado de:

Doctor en Ciencias Agropecuarias

Comité Particular

Dr. Daniel González Mendoza
Director de Tesis

Dra. Rosalba Troncoso Rojas
Co-Director de Tesis

Dr. Onécimo Grimaldo Juárez
Sinodal

Dr. Dagoberto Durán Hernández
Sinodal

Dra. Silvia Mónica Avilés-Marín
Sinodal

AGRADECIMIENTOS

Le agradecemos a Dios por darnos fuerza para superar todos los obstáculos, que se nos presentaron en la realización de éste trabajo.

Me gustaría que estas líneas sirvieran para expresar mi más profundo y sincero agradecimiento a todas aquellas personas que con su ayuda han colaborado en la realización del presente trabajo, en especial al **Dr. Daniel González-Mendoza director de mi tesis**, por haber aceptado la dirección del presente trabajo y brindarme la oportunidad de trabajar con él, durante este proceso me han ofrecido su completo apoyo, paciencia, tiempo, conocimientos y sobre todo por esa gran amistad que me brindó y me brinda, por escucharme y aconsejarme siempre, sin su apoyo y guía la presente tesis nunca se hubiera llevado a cabo. Todo lo que he aprendido en el transcurso de este tiempo, me acompañaran el resto de mi vida profesional y personal, con la que me encuentro en deuda por el ánimo infundido y la confianza en mí depositada, por los momentos en los que más que un profesor se comportó como un amigo, por compartir conmigo muchos momentos tanto alegres como tristes.

Dra. Rosalba Troncoso Rojas Co-Director de Tesis, no tengo palabras para agradecer su apoyo siempre, su energía positiva , sus consejos, y por brindarme la oportunidad de vivir la experiencia de la investigación al lado de personas tan brillantes y preparadas como ustedes, fue un honor, los admiro y los quiero mucho. Por tener siempre tendida su mano amiga, por escucharme, en fin, por darme cariño y amistad desde el día en que me conoció. Le agradezco la confianza, apoyo y dedicación de tiempo a mis asesores **Dr. Onécimo Grimaldo Juárez, Dr. Dagoberto Duran-Hernández** y **Dra. Monica Aviles-Marin**, por sus conocimientos y la colaboración brindada durante toda la tesis y sobre todo en ésta última etapa. Por todos los momentos compartidos, por los ánimos y cariño que me dan, un honor que sean mis asesores de tesis.

A **mi familia**, por ayudarme en esta semejante tarea y por estar siempre unidos en las buenas y en malas. Siempre serán la luz que ilumine mi camino. Me han ayudado a ser mejor persona y a llevar a cabo este trabajo, y luchar juntas contra las reveses de la

vida. Mil Gracias a todos, sin ustedes no habría llegado a esta instancia, ocupan un lugar especial en mi corazón.

De igual manera mi más sincero agradecimiento a mis amigos **Rafael Jordán (El farmacéutico)** y **Alejandro Sánchez (El Capitán)** personas que desde el primer momento me brindaron todo el apoyo, colaboración y cariño sin ningún interés, son las personas por las cuales hoy por hoy puedo afirmar que, a pesar de haber venido solo a continuar mis estudios, jamás me he sentido así, porque ellos han estado a mi lado cada día durante estos años.

A la **Secretaría de las Relaciones Exteriores (SER)** ya que a través de sus becas he podido llevar a cabo la presente Tesis Doctoral. A las autoridades del **Instituto de Ciencias Agrícolas de la Universidad Autónoma de Baja California (ICA-UABC)** por haberme permitido llevar a cabo mis estudios de postgrado. A la secretaria del coordinador de posgrado **Sandra Rojas** por su amistad.

A todas las personas del Laboratorio de Biotecnología, es especial con quienes compartí gran cantidad de tiempo y han hecho muy ameno el desarrollo del presente trabajo: en especial, **Tania Elisa González** (buena amiga y compañera de investigación).

A mis amigos y compañeros por su amistad, acertados consejos, con quienes compartí momentos inolvidables: Paola Melissa Ruiz Romero.

A todos, mi mayor reconocimiento y gratitud

Ali Abdelmoteleb

INDICE GENERAL

LISTA DE FIGURAS

LISTA DE TABLAS

ABREVIATURAS

°C	Degrees Celsius
4-Me-U	4-methylumbelliferone
4-MU-β-(GlcNAc)3	4-methylumbelliferyl-β-D-N, N', N''-triacetylchitotrioside
U	Unite
PCR	Polymerase Chain Reaction
ANOVA	Variance analysis
SD	Standard deviation
$Ca_3(PO_4)_2$ / (TCP)	Tri-calcium phosphate
Ca	Calcium
SI	Solubilization index
CFU	Colony forming unites
cDNA	Complementary DNA
rpm	Revolutions per minute
UV	Ultraviolet.
DEPC	Diethylpyrocarbonate
DNA	Deoxyribonucleic acid
RNA	Ribonucleic acid
DNS	3,5 Dinitrosalicylic acid
dNTP´s	Deoxynucleoside triphosphates
EDTA	Ethylenediaminetetraacetic acid
NCBI	National Center for Biotechnology Information
bp	base pairs

Fm	Maximum fluorescence
Fv	Variable fluorescence
ISR	Induced systemic resistance
g	Gram
mg	Milligram
µg	Microgram
ng	Nano-gram
L	Liter
ml	Milliliter
µl	Microliter
cm	Centimeter
mm	Millimeter
nm	Nanometer
mMol/ mM	Millimolar
µmol / µM	Micromole
h , hr / hrs	Hour/ Hours
min	Minute
USA	United States of America
V/ V	Volume / Volume
W/ V	Weight / Volume
$MgCl_2$	Magnesium chloride
$MgSO_4$	Magnesium sulphate
P	Phosphate
$CaCl_2$	Calcium chloride
K_2HPO_4	Dipotassium hydrogen phosphate
NaH_2PO_4	Monosodium phosphate
Na_2HPO_4	Disodium phosphate
$MgSO_4.7H_2O$	Magnesium Sulfate, Heptahydrate
$MnSO_4.4H_2O$	Manganese Sulfate Tetrahydrate
$(NH_4)_2SO_4$	Ammonium Sulfate
NaCl	Sodium chloride
KCl	Potassium chloride
$FeSO_4$	Ferric sulphate
NaOH	Sodium hydroxide
DW	Deionized water
H_2O	Water
Na_2CO_3	Sodium carbonate
MW	Molecular weight
rDNA	Ribosomal Deoxyribonucleic acid
ROS	Reactive oxygen species
EDS	Energy dispersive X-ray spectrometers
AgNPs	Silver nanoparticles
NPs	Nanoparticles
Ag	Silver
NaOCl	Sodium Hypochlorite
SEM	Scanning Electron Microscope
kV, keV	kilovolts

DLS	Dynamic light scattering
SPR	Surface plasmon resonance
C	Carbon
Cl	Chlorine
O	Oxygen
ζ	Zeta potential
%	Percentage
mV	Mega volte
$AgNO_3$	Silver nitrate
ppm	Parts per million
g_s	Stomata conductance
SDS	Sodium dodecyl sulfate
PVK	Pikovskaya's medium
SMA	Skimmed milk agar
PDA	Potato dextrose agar
PDB	Potato dextrose broth
Sp.	Specie
TAE	Tris acetate EDTA
Tris-HCl	Hydroxymethyl-hydrochloride
LR	Lateral roots
n	Number of replicates

CAPITULO I (CHAPTER I)

INTRODUCCIÓN GENERAL

1.1 Introducción

A nivel mundial, el interés por el control o manejo biológico de enfermedades de las plantas se incrementó al reconocerse los problemas de contaminación ambiental del planeta, como resultado del uso excesivo y a veces indiscriminado de los plaguicidas sintéticos. Los sistemas agrícolas son afectados por plagas y enfermedades que causan disminución en la producción y por lo tanto grandes pérdidas económicas. El tratamiento de éstas comúnmente se realiza utilizando indiscriminadamente plaguicidas y fungicidas que aumentan los costos de producción e impactan negativamente el medio ambiente. La búsqueda de sostenibilidad ha llevado a realizar estudios con microorganismos antagonistas como agentes de control, que tienen la capacidad de producir metabolitos biológicamente activos capaces de interferir en la supervivencia o desarrollo de los patógenos (Layton *et al*., 2011). Los microorganismos patógenos en las plantas influyen de forma negativa sobre la producción de alimentos y la estabilidad de los ecosistemas. Debido al uso indiscriminado de compuestos químicos como un método de protección de las cosechas, ha incrementado los efectos negativos como el desarrollo de cepas patógenas resistentes a estos compuestos, además del impacto ambiental que ellos ocasionan (Gerhardson, 2002). Por otra parte, se ha observado que la aplicación de compuestos químicos en la agricultura es insuficiente para ejercer el control de patógenos en cultivos de importancia económica (Johri *et al*., 2003).

Una alternativa para disminuir la contaminación ocasionada por el uso de agroquímicos sintéticos en el manejo de fitopatógenos es la utilización de microorganismos antagonistas del género *Bacillus,* que son considerados los más eficaces por sus propiedades de inhibición de fitopatógenos en el sistema radicular de las plantas, así como por su capacidad para estimular la promoción del crecimiento de las plantas, induciendo así mayor rendimiento a corto plazo. Dada la gran diversidad y potencial tanto en el suelo como en la rizósfera, se considera a éste microorganismo como un colonizador eficaz. Por tal motivo, el uso de rizobacterias para el control biológico provee una herramienta potencial en el control de fitopatógenos (Hernández-Suárez *et*

al., 2010). Asimismo, el costo de los agroquímicos y la demanda de los consumidores por productos libre de los mismos impulsó el desarrollo de nuevas tecnologías más amigables con el ambiente, como el control biológico. Entre los grupos bacterianos más estudiados como biocontroladores están las bacterias del género *Bacillus* que colonizan agua, aire y suelos. *Bacillus subtilis* no es patogénico o toxigénico para humanos, animales o plantas, y produce biomoléculas que tienen una fuerte capacidad antibiótica y antifúngica. Según las condiciones de cultivo, algunos miembros de este género bacteriano producen biopelículas, las cuales representan una comunidad interdependiente y pueden estar conformadas por una sola especie o una comunidad derivada de múltiples especies, que pueden adherirse sobre una gran variedad de superficies bióticas y abióticas (Sarti y Miyazaki, 2013).

Las especies del género *Bacillus* presentan ventajas para su utilización en la Biotecnología Agrícola como son la presencia de endosporas, la motilidad que le facilita la colonización de la planta, la capacidad de producir sustancias promotoras del crecimiento vegetal, sideróforos, solubilización de fosfatos y de sustancias responsables de su actividad antagónica e inhibidora, todo lo cual abre las perspectivas de su utilización en la agricultura sostenible con la consecuente preservación del medio ambiente (Tejera-Hernández *et al*., 2011). El género *Bacillus*, pertenece a la familia *Bacillaceae*, una de las familias bacterianas con mayor actividad bioquímica referenciada en la literatura científica que abarca tanto su utilización dentro de las actuales políticas de control biológico como el uso de los productos de su metabolismo para la industria. Son bacilos aerobios y anaerobios facultativos, gram positivos, producen endosporas con morfología oval o cilíndrica que le permite resistir condiciones desfavorables en el ambiente, son móviles por la presencia de flagelos laterales, son catalasa positiva, presentando hemólisis variable y un crecimiento activo en un rango de pH entre 5.5 - 8.5 (Layton *et al*., 2011). Una de las especies de *Bacillus* más representativa ha sido *Bacillus subtilis* por su efecto antagonista y por la capacidad que posee de producir compuestos fungicidas como la iturina, antibiótico de naturaleza lipopeptídica muy estudiado en el control biológico (Ragazzo-Sánchez *et al.*, 2011). Los efectos antagónicos de *B. subtilis* se relacionan con al menos cinco mecanismos: 1) parasitismo directo, donde las bacterias se mueven hacia las esporas en germinación y

se adhieren a la superficie por medio de la polaridad; 2) producción de antibióticos extracelulares como bacilomicina, iturina, micosubtilina y zwittermicina; 3) producción de enzimas líticas como quitinasa, proteasa, β-1,3 glucanasa y celulosa; 4) competencia por los nutrientes en el hospedante, que causa estrés por nutrientes e inanición en el hongo en germinación; y 5) estimulación de defensas del hospedante a través de la resistencia sistémica inducida por medio de la ruta del ácido jasmónico (Ruiz-Sánchez *et al*., 2016).

La producción de compuestos antimicrobianos es muy común entre las bacterias y los hongos. Estos compuestos son sintetizados y excretados con el objetivo de eliminar la competencia que pueda existir en su hábitat natural. En muchos sistemas de control biológico, uno o más antibióticos desempeñan un papel importante en la supresión de enfermedades. Además, se han realizado estudios moleculares que han sido efectivos para determinar esta capacidad presente en algunas bacterias, debido a la fácil obtención de mutantes defectivos en la producción de estos compuestos (Hu *et al*., 2007). El género *Bacillus* ha sido estudiado ampliamente respecto a la producción de antibióticos. En este sentido, se ha reportado que especies como *Bacillus subtilis* produce la fengicina, con elevado potencial de aplicación en la industria-biofarmacéutica (Steller y Vater, 2000), y *Bacillus cereus* que tiene la capacidad de producir zwitermicina A, un antibiótico que no solo suprime el crecimiento de hongos fitopatógenos que afectan a cultivos de interés agrícola, sino que también potencia la acción insecticida de las toxinas proteicas producidas por *B. thuringiensis* (Emmert *et al*., 2004). El efecto biocontrolador resulta como producto de diversos mecanismos, entre ellos la antibiosis que ejerce *Bacillus subtilis* con la producción de péptidos, lipopéptidos y fosfolípidos que se utilizan como agentes terapéuticos contra bacterias patógenas y hongos. Estos compuestos tienen origen peptídico y pueden ser sintetizados o no en el ribosoma. Entre las sustancias que no son sintetizados en el ribosoma se destacan los lipopéptidos como el surfactin, iturin, y fengycin. El ribosoma realiza la síntesis durante el crecimiento activo de las bacterias, a diferencia de los que no son sintetizados por el ribosoma que se producen después del crecimiento bacteriano (Joshi and Gardener, 2006). La actividad antimicrobiana de los lipopéptidos se da por la interacción con la membrana de las células diana, en la cual se modifica la

permeabilidad y la composición de los lípidos de la membrana con la formación de pequeñas vesículas y la agregación de partículas intramembranosas, de esta forma inhiben el crecimiento del micelio y el desarrollo de los hongos (Aranda *et al*., 2005; Gong *et al*., 2006). Las variaciones en la longitud y ramificación de las cadenas de ácidos grasos, así como las sustituciones de aminoácidos permiten la diferenciación de los lipopéptidos identificados hasta ahora en *Bacillus subtilis,* los cuales se dividen en tres grupos: la familia de surfactin, iturin y fengycin. Estos antibióticos presentan estructuras de tipo terciario y cuaternario (Nagórska *et al*., 2007).

La producción de enzimas líticas es otro de los mecanismos de acción de algunos microorganismos con actividad antagonista. Entre algunas de estas enzimas podemos encontrar a las quitinasas, glucanasas, celulasas y proteasas (Pal y Gardener, 2006). La quitina es un polímero de mayor abundancia en la naturaleza y que ocupa el segundo lugar después de la celulosa, se encuentra como compuesto estructural en la pared celular de los hongos y en el exoesqueleto de algunos insectos (Macagnan *et al*., 2008). Algunos microorganismos como por ejemplo las bacterias utilizan las enzimas quitinasas para llevar a cabo antagonismo contra fitopatógenos, el modo de acción va dirigido a la hidrólisis de este polímero actuando en los enlaces de carbono C_1 y C_4 de las unidades consecutivas de la N-acetil-β-D-glucosamina, afectando la estructura de la pared celular de los patógenos ocasionando la muerte por lisis celular. Las enzimas proteasas también presentan un efecto hidrolítico en las proteínas de la pared celular de los patógenos, afectando la estabilidad y permeabilidad de esta estructura ocasionando una lisis. Este tipo de enzimas al igual que muchas otras pueden ser evaluadas tanto de forma cualitativa como cuantitativa. La forma cualitativa es mediante diversos medios selectivos que emplean un sustrato especifico como: carboximetilcelulosa, quitina, leche, etc. los cuales son agregados al medio de cultivo para estimular a las bacterias y estas excreten enzimas para degradarlo, formando un halo alrededor de la colonia bacteriana, así se puede observar la producción de las diferentes enzimas y realizar una selección (Subba-Rao 1999; Gomaa 2012). La cuantificación de las enzimas quitinasas y glucanasas puede realizarse en medios líquidos con sustratos específicos como N-acetilglucosamina o con polímeros como laminarina, quitina o paredes celulares de hongos para estimular la inducción de las

enzimas. Posteriormente, se puede cuantificar mediante reacción colorimétrica (El-Katatny *et al*., 2001).

Por otro lado, una nueva herramienta para el control de enfermedades tanto en humanos como en plantas es el uso de nanotecnología, ya que su creciente desarrollo en las últimas décadas ha abierto nuevas posibilidades en el campo de la ciencia y su aplicación abarca desde la electrónica, telecomunicaciones, bioquímica, medicina y biología, entre muchas otras áreas. Específicamente, el uso de nanopartículas (NPs) de diferentes metales se visualiza que tienen un gran potencial en agricultura, por ejemplo para la formulación de nano encapsulados con bioinsecticidas, biofungicidas o biofertilizantes (Rangaraj *et al*., 2014). En los últimos años las nanopartículas de plata (AgNPs) han sido objeto de una variedad de estudios, principalmente debido a la relación que existe entre su tamaño con las propiedades ópticas, electrónicas y magnéticas. En la escala nanométrica (10-100 nm), las AgNPs presentan un comportamiento de las propiedades físicas, químicas y biológicas que no son comparables con mismas partículas de mayor escala, además de su sorprendente actividad antimicrobiana (Chen y Schluesener, 2008). En la actualidad, las AgNPs han encontrado aplicaciones importantes en electrónica, marcadores celulares, en catálisis química, biosensores, biotecnología, bioingeniería, medicina, ingeniería textil, tratamiento del agua y otros productos de consumo a base de plata. Sin embargo, una de las aplicaciones donde se han enfocado una buena parte de la investigación es en sus destacadas propiedades como agentes bactericidas o fungicidas. Debido a su fuerte actividad bactericida las AgNPs se han utilizado en el control de infecciones, recubrimientos de varios materiales textiles, además de usarse en el tratamiento de heridas y quemaduras (Ledezma *et al*., 2014).

Para la producción de nanopartículas metálicas, como en el caso de las nanopartículas de plata, se han propuesto diferentes estrategias de síntesis, entre las que se incluye, la síntesis química mediante microemulsión, reducción química, irradiación ultrasónica, síntesis electroquímica y más recientemente la aplicación de métodos biológicos que hacen uso de microorgansimos propios de las plantas y extractos de las mismas. La síntesis biológica de nanopartículas también denominada “síntesis verde” ha permitido la formación de nanoestructuras metálicas a partir del uso de bacterias, hongos, plantas

o sus extractos, por lo que esta forma de síntesis representa una alternativa presumiblemente no tóxica, amigable con el medio ambiente y que además su uso en algunas ocasiones iguala o sobrepasa las expectativas de las nanopartículas sintetizadas por métodos físicos y químicos, en cuanto a costo y características de las nanopartículas obtenidas (Ledezma *et al*., 2014). Desde un punto de vista químico, la síntesis de nanopartículas en disolución (disolución coloidal) requiere del empleo de métodos que permitan obtener un control preciso sobre el tamaño y la forma de las nanopartículas, para así obtener un conjunto de partículas monodispersas que presenten una propiedad determinada. En general, la síntesis de nanopartículas metálicas en disolución se lleva a cabo mediante el empleo de los siguientes componentes: i) precursor metálico; ii) agente reductor; iii) agente estabilizante. El mecanismo de formación de las disoluciones coloidales a partir de la reducción de iones de plata consta de dos etapas: nucleación y crecimiento. El proceso de nucleación requiere una alta energía de activación mientras que el proceso de crecimiento requiere una baja energía de activación. El tamaño y la forma de las nanopartículas dependerá de las velocidades relativas de estos procesos, que pueden ser controladas a través de la modificación de los parámetros de reacción (concentración, temperatura, pH, poder reductor, etc.) (Ledezma *et al*., 2014).

Actualmente, los dos campos de trabajo más activos relacionados con las nanopartículas de plata son el estudio y aplicación de sus propiedades ópticas y biomédicas. Las propiedades ópticas de las nanopartículas de los metales nobles se basan en la oscilación colectiva de electrones de conducción libres como resultado de su interacción con la radiación electromagnética. El campo eléctrico de la radiación electromagnética induce la formación de un dipolo en la nanopartícula, creándose en ésta una fuerza restauradora que intenta compensar ese efecto, resultando en una longitud de onda de resonancia que confiere el color característico a las disoluciones coloidales de nanopartículas de metales nobles. En relación con esta propiedad se han desarrollado interesantes aplicaciones relacionadas principalmente con la detección de especies químicas, orgánicas o inorgánicas, o biológicas. Otras propiedades como SERS (Surface Enhanced Raman Scattering) o MEF (Metal Enhanced Fluorescence) están siendo ampliamente estudiadas (Monge, 2009).

La plata es una alternativa prometedora para el control de fitopatógenos, debido a la resistencia de ciertas bacterias a los antibióticos como resultado del abuso de ellos, lo cual es un problema real. Como se ha reportado, las nanopartículas de plata son un antimicrobiano muy efectivo (Madhumathi *et al*., 2010); dado que las partículas de metal en el intervalo de tamaño nanométrico presentan propiedades físicas que son diferentes del ion de plata, proporcionando propiedades notables como aumento de la actividad catalítica (Singh *et al*., 2008). El mecanismo de acción antimicrobiana de los iones de plata libre se puede describir de la siguiente manera, los iones de plata forman compuestos insolubles con los grupos sulfhidrilo de la pared celular de las bacterias y hongos: que son componentes esenciales de las enzimas responsables del metabolismo energético y el transporte de electrolitos. Estos iones bloquean la cadena respiratoria de las bacterias y entran en la célula uniéndose al ADN bacteriano. Por lo que se han utilizado para crear distintos productos médicos como los catéteres donde su citotoxicidad, hemo-compatibilidad y la trombogenicidad de estos materiales impregnados con plata, se ha determinado y muestran excelentes resultados (Samuel y Guggenbichler, 2004). Con respecto a las nanopartículas de plata, se han recubierto superficies o incorporado a diversos materiales, ya que las nanopartículas de plata tienen diferentes aplicaciones biomédicas por su alto efecto antimicrobiano, y su actividad biocida demostrada contra ambas especies de bacterias, tanto Gram positivas como Gram negativas. Además, las nanopartículas de plata presentan una toxicidad nula en tejidos humanos al utilizarse en bajas concentraciones, por lo que son ampliamente utilizadas en el área médica como acondicionadores de tejidos, catéteres, cubierta de materiales así como en algunos materiales dentales (Liu *et al*., 2010; Allaker, 2010). Estas nanopartículas liberan iones de plata en las células aumentando su actividad bactericida; así como debido a su tamaño, las nanopartículas de plata poseen mejor y mayor superficie de contacto con las bacterias; es por ello que su actividad antibacteriana es alta (más que la de los iones plata en disolución), incluso en concentraciones muy bajas (Madhumathi *et al*., 2010). Singh *et al*. (2008) también hace mención de los efectos antibacterianos de las nanoparticulas de plata a bajas concentraciones. Se ha demostrado una relación inversa entre la actividad antimicrobiana y el tamaño de las nanopartículas, mencionándose en estudios que

existe una mayor actividad antibacteriana en nanopartículas de pequeño tamaño a diferencia de las de mayor tamaño; aunque la disminución en el tamaño de las nanopartículas conlleva a un incremento en su citotoxicidad (Liu *et al*., 2010; Allaker, 2010).

Los mecanismos de la actividad antimicrobiana de los metales de nanopartículas no se conoce completamente, pero existen estudios que han demostrado que la carga positiva del ion metálico es fundamental para la actividad antimicrobiana, lo cual permite la atracción electrostática entre la carga negativa de la membrana celular de las bacterias y las nanopartículas cargadas positivamente (Kim *et al*., 2007). Otros apuntan distintos mecanismos como la acción inhibitoria de los iones de plata sobre los microorganismos, ya que el ADN pierde su capacidad de replicarse (Allaker, 2010). Se ha demostrado que las nanopartículas de plata causan la inactivación de bacterias y evitan la replicación bacteriana *in-vitro* (Liao *et al*., 2010). Además, la alteración de la homeostasis del calcio juega un papel importante en las condiciones patológicas y toxicológicas siendo un signo temprano del daño celular, ya que los iones de calcio tienen el potencial para activar las enzimas catabólicas como la fosfolipasa, las proteasas y estas aumentan la toxicidad. Por lo que en los estudios de Asharani (2009), se señala que el estrés oxidativo, el calcio y el agotamiento de ATP se producen en las células tratadas con nanopartículas de plata (Asharani *et al*., 2009). Otro de los mecanismos de actividad antimicrobiana se realiza por medio de los iones de plata que afectan a las enzimas de membrana respiratoria. Mientras que en el estudio de Sondi y Salopek-Sondi (2004), demostraron cambios estructurales y daños a las membranas bacterianas, lo que resulta en la muerte celular. Estos estudios sugieren que todo el azufre que contienen las proteínas y enzimas, son clave en la membrana o dentro de las células así como los elementos que tienen fósforo, como el ADN, siendo los probables sitios preferenciales de unión para las nanopartículas de plata. Kim sugiere que las nanopartículas de plata inhiben las enzimas respiratorias en la célula bacteriana y de esta manera facilita la generación de radicales libres para dar paso al daño de la membrana (Kim *et al*., 2007).

1.2 Hipótesis

El uso de nanoparticulas obtenidas a partir de extractos de *Pluchea sericea* y *Prosopis glandulosa*, y la aplicación de metabolitos secundarios de *Bacillus subtilis* aislada de la rizosfera de *P. juliflora* pueden inhibir el crecimiento y proceso de replicacion celular de microorganismos de importancia agricola.

1.3 Objetivo

Aislar y caracterizar de *Bacillus subtilis* como solubilizador de fosfatos y agente antagonista de rizósfera obtenido de las plantas nativas (*Prosopis juliflora*), del valle Mexicali, México. Así mismo, sintetizar y caracterizar nanopartículas de plata a partir de extracto de *Pluchea sericea* y *Prosopis glandulosa,* con potencial antimicrobiano.
Para alcanzar este objetivo general, se consideraron los siguientes **objetivos específicos**:

1. Aislar e identificar cepas de *Bacillus subtilis* de rizósfera de *Prosopis juliflora* como plantas nativas en el valle de Mexicali, B.C.
2. Evaluar cualitativamente y cuantitativamente la actividad de solubilización de fosfatos minerales (fosfato tricálcico).
3. Determinar la capacidad antagónica de una cepa de *Bacillus subtilis* y su sobrenadante frente a varios hongos fitopatógenos.
4. Determinar el nivel de expresión de los genes que codifican a lipopéptidos antibióticos en una cepa de *Bacillus subtilis* (ALICA) nativa.
5. Determinar cuantitativamente el nivel de actividad enzimática de enzimas líticas producidas por *Bacillus subtilis* como quitinasa 1,3-β-glucanasa y proteasa, y cuantificar el nivel de expresión de los genes que codifican para esas enzimas.
6. Caracterizar las nanopartículas de plata obtenidas de extractos de *Pluchea sericea* y *prosopis glandulosa.*
7. Evaluar la actividad antimicrobiana de las nanopartículas de plata.

1.4 Literatura citada

Allaker R P. 2010. The use of nanoparticles to control oral biofilm formation. Journal of Dental Research, 89(11):1175-1186.

Aranda F J, Jose´ A. Teruel J A and Ortiz A. 2005. Further aspects on the hemolytic activity of the antibiotic lipopeptide iturin A. Biochimica et Biophysica Acta, 1713: 51 – 56.

Asharani PV, Hande M P and Valiyaveettil S. 2009. Anti-proliferative activity of silver nanoparticles. BMC Cell Biology, 17;10:65.PMID: 19761582. Doi: 10.1186/1471-2121-10-65.

Chen X and Schluesener H J. 2008. Nanosilver: a nanoproduct in medical application. Toxicology Letters, 176(1):1-12.

El-Katatny M H, Gudelj M, Robra K H, Elnaghy M A and Gübitz G M. 2001. Characterization of a chitinase and an endo-beta-1,3-glucanase from *Trichoderma harzianum Rifai* T24 involved in control of the phytopathogen *Sclerotium rolfsii*. Applied Microbiology and Biotechnology, 56(1-2):137-143.

Emmert E A B, Klimowicz A K, Thomas M G and Handelsman J. 2004. Genetics of Zwittermicin A Production by Bacillus cereus. Applied and Environmental Microbiology, 70(1):104-113.

Gerhardson B. 2002. Biological substitutes for pesticides. Trends in Biotechnology, 20:338-343.

Gomaa E Z. 2012. Chitinase production by *Bacillus thuringiensis* and *Bacillus licheniformis*: Their potential in antifungal biocontrol. The Journal of Microbiology, 50: 103–111.

Gong M, Wang J D, Zhang J, Yang H, Lu X F, Pei Y and Cheng J Q. 2006. Study of the antifungal ability of *Bacillus subtilis* strain PY-1 in vitro and identification of its antifungal substance (iturin A). Acta Biochimica et Biophysica Sinica (Shanghai), 38(4):233-240.

Hernández-Suárez M, Hernández-Castillo F D, Lira-Saldivar R H and Gallegos-Morales G. 2010. Biocontrol de *Rhizoctonia* solani y *Fusarium* sp. Con Microencapsulados de Bacillus subtilis y su Efecto en Crecimiento y Rendimiento de Tomate

(*Lycopersicon esculentum* Mill.). Revista Agraria -Nueva Epoca- Año VII · Vol. 7 · Nos. 1, 2, 3: 17- 25.

Hu L B, Shi Z Q, Zhang T and Yang Z M. 2007. Fengycin antibiotics isolated from B-FS01 culture inhibit the growth of *Fusarium moniliforme* Sheldon ATCC 38932. FEMS Microbiology Letters. 272 (1):91-98.

Johri B N, Sharma A and Virdi J S. 2003. Rhizobacterial diversity in India and its influence on soil and plant health. Advances in Biochemical Engineering/Biotechnology, 84:49-89.

Joshi R and Gardener B B M. 2006. Identification and Characterization of Novel Genetic Markers Associated with Biological Control Activities in *Bacillus subtilis*. Phytopathology, 96 (2): 145- 154.

Kim J S, Kuk E, Yu K N, Kim J H, Park S J, Lee H J, Kim S H, Park Y K and Park Y H. 2007. Antimicrobial effects of silver nanoparticles. Nanomedicine: Nanotechnology, Biology and Medicine.; 3(1):95-101.

Layton C, Maldonado E, Monroy L, Corrales L C and Sánchez L C .2011. *Bacillus* spp; perspectiva de su efecto biocontrolador mediante antibiosos en cultivos afectados por fitopatógenos. NOVA-Publicación Científica en Ciencias Biomédicas, 9(15): 177-187.

Ledezma A, Romero J, Hernández M, Moggio I, Arias E and Padrón G. 2014. Síntesis biomimética de nanopartículas de plata utilizando extracto acuoso de nopal (*Opuntia* sp.) y su electrohilado polimérico. Superficies y Vacío 27(4):133-140.

Liao J, Anchun M, Zhu Z and Quan Y. 2010. Antibacterial titanium plate deposited by silver nanoparticles exhibits cell compatibility. International Journal of Nanomedicine, 5:337-342.

Liu H L, Dai S A, Fu K Y, Hsu S H. 2010. Antibacterial properties of silver nanoparticles in three different sizes and their nanocomposites with a new waterborne polyurethane. International Journal of Nanomedicine, 5:1017-1028.

Macagnan D, Romeiro R S, Pomella A W V and Souza J T. 2008. Production of lytic enzymes and siderophores, and inhibition of germination of basidiospores of *Moniliophthora (ex Crinipellis) perniciosa* by phylloplane actinomycetes. Biological control 47: 309- 314.

Madhumathi K. Sudheesh Kumar P T, Abhilash S, Sreeja V, Tamura H, Manzoor K, Nair S V and Jayakumar R. 2010. Development of novel chitin/nanosilver composite scaffolds for wound dressing applications. Journal of Materials Science: Materials in Medicine, 21(2):807-813.

Monge M. 2009. Nanopartículas de plata: métodos de síntesis en disolución y propiedades bactericidas. Anales de Química, 105(1): 33−41.

Nagórska K, Bikowski M and Obuchowski M. 2007. Multicellular behaviour and production of a wide variety of toxic substances support usage of *Bacillus subtilis* as a powerful biocontrol agent. Acta biochimica Polonica, 54(3):495-508.

Pal K K and Gardener B M. 2006. Biological control of plant pathogens. The plant health 10: 1094- 1117.

Ragazzo-Sánchez J A, Robles-Cabrera A, Lomelí-González L, Luna-Solano G and Calderón-Santoyo M. 2011. Selección de cepas de *Bacillus* spp. Productoras de antibióticos aisladas de frutos tropicales. Revista Chapingo, Serie Horticultura, 17(1), p. 5-11.

Rangaraj S, Gopalu K, Muthusamy P, Rathinam Y, Venkatachalam R and Narayanasamy K. 2014. Augmented biocontrol action of silica nanoparticles and *Pseudomonas fluorescens* bioformulant in maize (*Zea mays* L.). RSC Advances, 4: 8461–8465.

Ruiz-Sánchez E, Mejía-Bautista M A, Serrato-Díaz A, Reyes-Ramírez A, Estrada-Girón Y and Valencia-Botín A J. 2016. Antifungal activity and molecular identification of native strains of *Bacillus subtilis*. AGROCIENCIA 50 (2): 133- 148.

Samuel U and Guggenbichler J P. 2004. Prevention of catheter-related infections: the potential of a new nano-silver impregnated catheter. International Journal of Antimicrobial Agents, Supplement 1: 75-78.

Sarti G C and Miyazaki S S. 2013. *Bacillus subtilis* crude extracts with antifungal activity against soybean (*Glycine max*) phytopathogens and *Bradyrhizobium japonicum* coinoculation effect. AGROCIENCIA, 47 (4): 373- 383.

Singh M, Singh S, Prasad S and Gambhir I S. 2008. Nanotechnology in medicine and antibacterial effect of silver nanoparticles; Digest Journal of Nanomaterials and Biostructures, 3 (3): 115 - 122.

Sondi I and Salopek-Sondi B. 2004. Silver nanoparticles as antimicrobial agent: a case study on *E. coli* as a model for Gram-negative bacteria. Journal of Colloid and Interface Science, 275(1):177-182.

Steller S and Vater J. 2000. Purification of the fengycin synthetase multienzyme system from *Bacillus subtilis* b213. Journal of Chromatography B, 737: 267–275.

Subba-Rao N S. 1999. Soil Microbiology: Fourth Edition of Soil Microorganisms and Plant Growth: 271-276, 292-298.

Tejera-Hernández B, Rojas-Badía M M and Heydrich-Pérez M. 2011. Potencialidades del género *Bacillus* en la promoción del crecimiento vegetal y el control biológico de hongos fitopatógenos. Revista CENIC Ciencias Biológicas, 42(3): 131-138.

CAPITULO II (CHAPTER II)

BIOCONTROL OF *Fusarium* spp., CAUSAL AGENTS OF DAMPING-OFF IN COTTON PLANTS BY NATIVE *Bacillus subtilis* ISOLATED FROM *Prosopis juliflora*

2.1 Abstract

The present study was conducted to evaluate the application of native phosphate solubilizing *Bacillus* sp., isolated from *Prosopis juliflora* rhizosphere in the biocontrol of three different *Fusarium* species. The native *Bacillus* sp. was further confirmed as *B. subtilis* using the Polymerase Chain Reaction (PCR). The results showed that the phosphate solubilizing ability of *B. subtilis* strain ALICA was tested in liquid medium with 0.5% $Ca_3(PO_4)_2$, and maximum of the value of soluble phosphate was 202.02 µg/mL after 3 days of incubation. On the other hand, the growth inhibition of *Fusarium solani, F. equiseti* and *F. oxysporum* were more evident in cell-free medium filtrates with respect to dual medium with a range of percentage inhibition from 51, 66 and 47% after 5 days, respectively . Our result of the DNA-PCR amplification of the lipopeptide genes from *B. subtilis* strain ALICA, showed 94% identity with subtilosin and subtilisin of different *Bacillus* spp. This result turns *B. subtilis* strain ALICA into a potential alternative for the biological control of *Fusarium* species present in the soil of transgenic insect-resistant cotton plants in Mexico.

Keywords: *Bacillus subtilis*; Phosphate solubilization; Antifungal; Biocontrol; *Fusarium* spp.

2.2 Introduction

As result of beneficial impacts of transgenic cotton on yields and pesticide use, the commercial cultivation of *Bacillus thuringiensis* (Bt) cotton has been increasing since in the last 34 years in Mexico, principally in Baja California and the Comarca Lagunera (Terán-Vargas *et al*., 2005). However, diseases caused by fungi represent serious problems of cotton production in Mexico and others countries (Lutfunnessa and Shamsi,

2011; González-Soto *et al*., 2015). In this sense, recent studies showed that *Fusarium* wilt represent the principal disease in soil of transgenic insect-resistant cotton plants in Mexico (González-Soto *et al*., 2015). In general, the strategies for the management of *Fusarium* wilt include the use of resistant cultivars, chemical control and use of natural antagonistic organisms (e.g., microorganisms). But, the excessive use of agrochemicals may produce soil pollution with detrimental effects in humans (Djébali and Belhassen, 2010). On the other hand, the biological control represent excellent alternative for control of *Fusarium* wilt in cotton plants due to their low environmental impact. In this sense diverse microorganisms have been reported to have antagonistic effects against different *Fusarium* species (Sun *et al*., 2011; Sundaramoorthy and Balabaska, 2013). Antagonistic bacteria, specially belonging to the *Bacillus* genus are among the most used biological agents to fight against many plant pathogens (El-hamshary and Khattab,2008). *Bacillus* species showed different strategies to reduce the infection in the plants by pathogens, for example: activation of genes that participle in the systemic resistance and production of antibiotics (Kloepper et al., 2004; Kim et al., 2009; Kumar *et al*., 2011; Chen *et al*., 2012). The study of native microorganisms capable of producing an effective biocontrol of *Fusarium* wilt has focused on isolating mesophilic microorganisms from tropical and subtropical regions (Ruiz-Sanchez et al., 2014; Adame-Garcia *et al*., 2015; Fu *et al*., 2015). Nevertheless,

research that evaluating the diversity of autochthonous microorganisms in agricultural and native desert soils from Baja California, are scarce. Considering the above the objective of the present investigation was to characterize *Bacillus* spp., isolated of *Prosopis juliflora* rhizosphere a native plants from Northwestern Mexico and evaluate its antagonistic potential against three different *Fusarium* species: *F. oxysporum, F. solani* and *F. equiseti.*

2.3 Materials and Methods

2.3.1 Isolation of Microorganisms

Rhizosphere sections from *Prosopis juliflora* were collected in Baja California, México. One gram of soil sample was diluted in sterile distilled water (9 mL). The dilutions were homogenized by agitation and then were serially diluted up to 10^{-6} dilution. 1 mL from each dilution of 10^{-5} and 10^{-6} were spread on specific medium (Pikovskaya´s Agar) (Annex 1) and incubated at 30 ± 2°C for 3 days. Finalized the period of incubation, the phosphate solubilizing bacteria were selected based on the zone of clearing around the colonies. The colonies showing clear zone were picked and re-streaked onto Pikovskaya's Agar plates. The isolate showing maximum clear halo zone of P-solubilization was designated as *Bacillus* sp., strain ALICA and stored in 30% glycerol at -20°C for further studies.

2.3.2 Solubilization Efficiency of *Bacillus* sp., Strain ALICA

For estimating solubilization efficiency, the selected *Bacillus* sp., strain ALICA was spot inoculated at the center of Pikovskaya's agar media in triplicates and incubated at 30± 2°C. Diameters of colony and solubilization halo were measured after 1, 2, 3, 4, 5, 6 and 7 days. The solubilization index (SI) was evaluated according to Zhao *et al*. (2014); where SI = diameter of solubilization halo/diameter of colony.

2.3.3 Quantification of Soluble Phosphate and pH in Liquid Media

The determination of phosphate solubilization was realized in flasks with 100 mL of Pikovskaya's broth (pH 7.0) with 1 mL of phosphate solubilizing bacteria at 10^8 CFU/mL, approximately. Autoclaved un-inoculated Pikovskaya's broth served as control. The flasks were incubated for 7 days at 30°C on a shaker at 130 rpm. 10 mL of homogenized suspensions were sampled at days 0, 1, 2, 3, 4, 5, 6 and 7 post-incubation to follow the concentration of released soluble phosphorus and the pH changes. The cultures were collected by centrifugation (10,000 rpm) for 6 min at room temperature. Phosphate in culture supernatant was estimated using "QuantiChrom™Phosphate Assay Kit (DIPI-500)" (Hildebrand *et al*., 2009).

2.3.4 Molecular Identification of Strain ALICA by Amplification of 16s rDNA

Bacillus sp., strain ALICA was cultivated in 20 mL of Nutrient Broth media at 30°C in agitation 130 rpm for 24 h. DNA was isolated using the method proposed by Mendez-Trujillo *et al*. (2013) (Annex 2). The polymerase chain reaction (PCR) was implemented with 2 µL DNA previous obtain from strain ALICA as PCR template and 1.2 µL (10 mM) of each specific primer 27f/1495r according to Zhang *et al*. (2013). The PCR reaction was carried out using the program proposed by Mendez-Trujillo *et al*. (2013). The fragment of 16S rDNA was visualized under a UV transillumination imaging system. For sequencing, PCR product was sent to a laboratory of GENEWIZ® (South Plainfield, NJ 07080-USA) with forward primer 27f. The 16s rDNA gene sequences were compared with available nucleotide chains of bacterial lineage in NCBI GenBank and the neighborJoining tree was constructed using the MEGA7 program.

2.3.5 PCR Screening for Antibiotic Genes in Strain ALICA

Detection of the genes that encode for the production of antibiotics such as subtilosin and subtilisin was done by PCR using gene-specific primers. The subtilosin (Sbo) and subtilisin (Stn) specific primer used were: Sbo1 Forward (5´-TCGGTTTGTAAACTTCAACTGC-3´) and Sbo1Reverse (5´-GTCCACTAG ACAAGCGGCTC-3´) and Stn Forward (5´-CTTAAACGTCAGAGGCGGAG-3´) and Stn Reverse (5´-ATTGTGCAGCTGCTTGTACG-3´). A total volume of PCR reaction 30 µL: 1 µL 10 mM dNTP, 3 µL 10x PCR buffer, 2.5 µL 50 mM $MgCl_2$, 0.3 µL (5 units/µL) of Taq polymerase (BIORAD, USA), 2.4 µL (10 mM) of both primers and 2 µL template (20 ng of DNA). Amplification was performed in a DNA thermal cycler (BIORAD, USA) according to Mendez-Trujillo *et al*. (2013). The samples were electrophoresed in a 1.5 % (w/v) agarose gel containing ethidium bromide and purified as earlier described. The PCR products obtain were purified and analyzed using software provided by GenBank.

2.3.6 Antagonistic Activities of Dual Plate Assay

Antagonistic activity of *Bacillus* sp., strain ALICA was performed by the dual cultures method according to Elkahoui *et al*. (2012), against the following phytopathogenic fungi: *F. oxysporum, F. solani* and *F. equiseti*. Mycelial disc (6 mm diameter) of the fungal pathogen was inoculated at the center of a 9 cm diameter of PDA plate and the bacterial isolate was streaked at a distance of 2 cm from the center in a square pattern around the fungal disc. A fungal disc from each tested fungus was centered in PDA plate without bacteria served as control. All of treatments were done in triplicate. The inoculated petri dishes were incubated at 28 ±2°C and radial growth of the fungal colonies was recorded at 5 days. Data were expressed as growth inhibition (%) according to formula proposed by Trivedi *et al.* (2008).

2.3.7 Antifungal Activity of Cell Free Supernatant

The *Bacillus* sp., strain ALICA was inoculated into Erlenmeyer flask 200 mL containing 100 mL of nutrient broth media and incubated on a rotary shaker (130 rpm) 3 days at 30°C. The bacterial growth (Log phase) was collected by centrifugation at 10,000 rpm for 6 min. The supernatant previously obtained was filtrate using 0.22 µm membrane filter. To assess the effect of bacterial culture filtrate on the growth of *F. oxysporum, F. solani,* and *F. equiseti* the culture filtrate was added to warm sterilized potato dextrose agar medium at rate of 25% and poured into petri dishes (Abdulkareem *et al*., 2014). After solidification, a plug of mycelium of each pathogenic fungus (6 mm in diameter) was positioned at the center of the PDA dishes. PDA dishes without culture filtrate were inoculated with each fungus as control. Dishes were grown at 30°C for 120 h. Growth inhibition of each fungus was recorded in triplicate.

2.3.8 Statistical Analysis

Data were analyzed by analysis of variance (ANOVA) and the means were compared using post-hoc Tukey's HSD test with $P \leq 0.05$ being accepted as significant. The statistical software used was SPSS (Version 21). Results are reported as means ± SD (standard deviation).

2.4 Results

2.4.1 Isolation of Phosphate Solubilizing Bacteria

In the present study, the isolated bacterium ALICA showed significant (P<0.01) increase of solubilization index (2.38±0.09) during the firsts 72 h of exposure to PVK agar media (Fig. 1). However, within 96 to 168 h after exposure, solubilization index values were significantly (P≤0.440) lowest, 1.34 ± 0.02, compared with levels observed in the first 72 h of the experiment (Fig. 1).

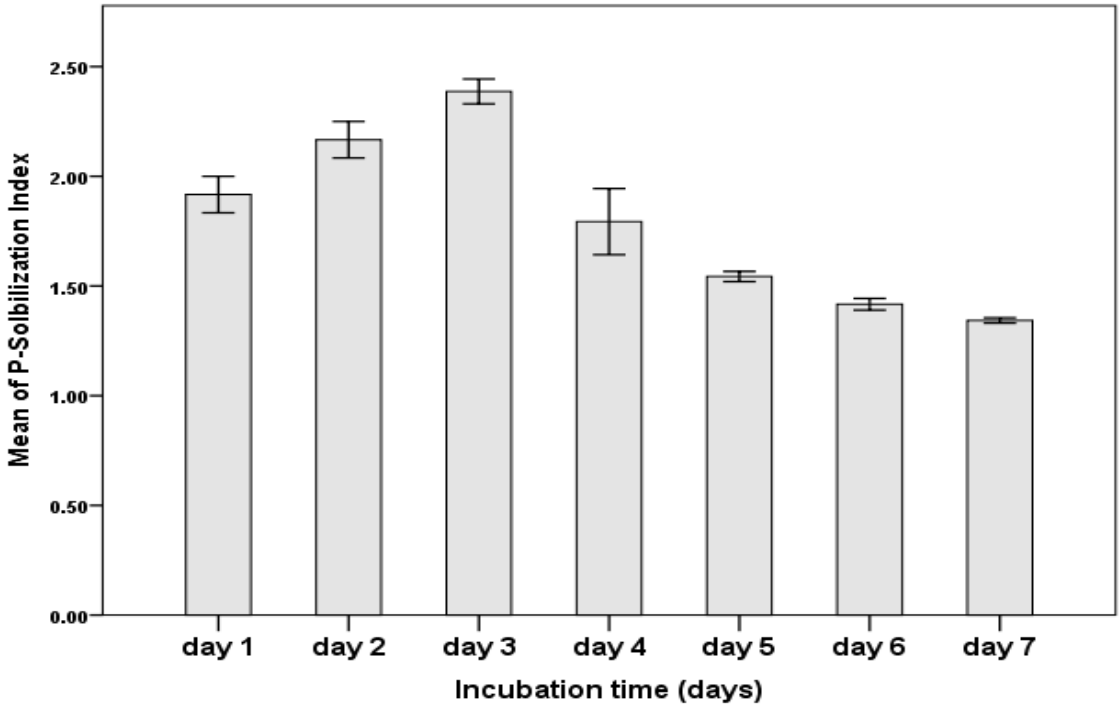

Fig. 1 Solubilization index of Ca_3 $(PO_4)_2$ in solid Pikovskaya's medium for bacterial isolate ALICA obtained from Mesquite rhizosphere, during 7 days of incubation at 28±2 °C. Error bars represent the standard errors of the means.

2.4.2 Quantitative Estimation of Phosphate Solubilization and pH in Liquid Media

The levels of soluble phosphorus and pH in liquid Pikovskaya's medium that contained known amounts of insoluble phosphate were analytically measured at different points during of the 7 days growth period at 30ºC. Our results showed that Bacillus sp., strain ALICA, significantly changed (*P*<0.01) the amount of P solubilized with the time. Whereas, the concentration of solubilized phosphate gradually increased from 1 to 3 days and decreased thereafter (Fig. 2). On the other hand, pH medium gradually decreased in the first 3 days and then slightly increased (Fig. 2). A significant negative correlation (r = -0.954; *p* <0.01) between P concentration and pH was observed. The maximum P-solubilization by *Bacillus* sp., strain ALICA (206.02±5.91 µg/mL) was recorded at the 3th day when the pH reached the lowest value (pH= 5.0±0.0, *p* <0.01). The pH value and soluble-P concentration in the un-inoculated control flasks remained almost the same as in day zero (p H=7±0.0, P= 16.14±1.34 µg /mL).

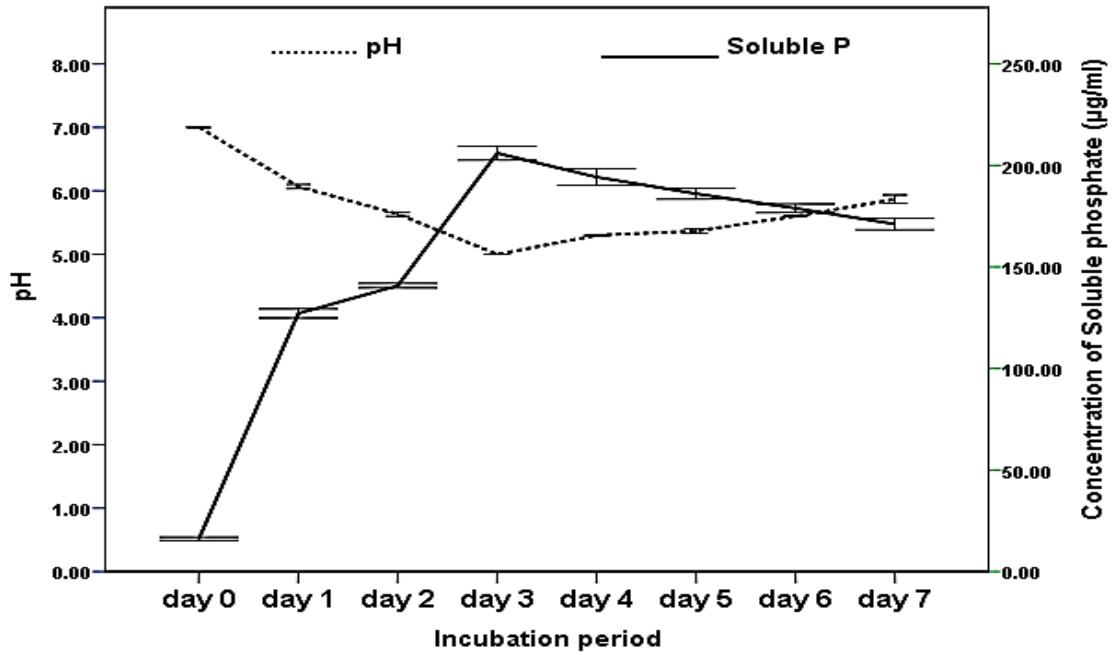

Fig. 2 Soluble phosphorus (µg/ ml) and pH in liquid medium Pikovskaya during 7 days of incubation with bacterial isolate ALICA in the presence of $Ca_3(PO_4)_2$. Error bars represent the standard errors of the means.

2.4.3 Molecular Identification of Isolate ALICA Based on its 16S rDNA Gene Sequence

The partial 16S rDNA sequence analysis was employed to identify the *Bacillus* sp., strain ALICA to the genus and specie levels. A 1096-bp PCR product from the 16S rDNA gene was amplified from the genomic DNA (Annex 3). Subsequent sequence analysis showed that strain ALICA shared 94% identity with *B. subtilis* strains deposited in GenBank. The gene sequence of ALICA was submitted to GenBank, NCBI data base and accession number was assigned (KX137176). Using DNA sequence of strain ALICA a neighbor joining tree was constructed and the result showed high similarity with members of the genus *Bacillus* (Fig. 3).

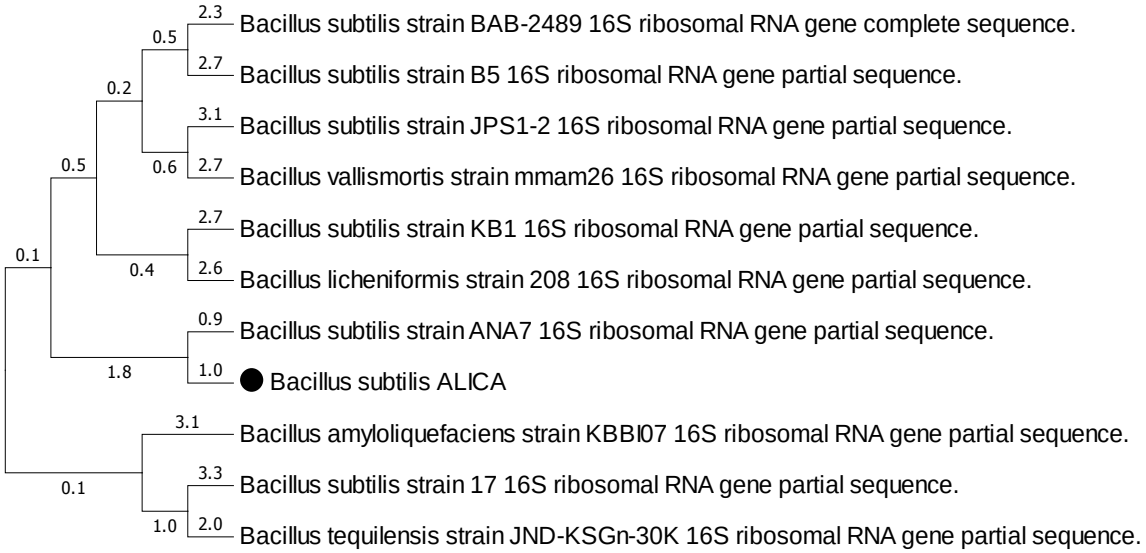

Fig. 3 Phylogenetic tree of bacterial isolate ALICA, based on partial 16S rDNA gene sequence. The dendrogram was constructed by the neighbor-joining method, using the MEGA.7 program.

2.4.4 PCR Screening for Antibiotic Genes of Strain ALICA

In the present study, *Sbo* and *Stn* genes were identified by PCR analysis and sequenced from *Bacillus* strain ALICA (Fig. 4). *Sbo* sequence (360 bp) showed homology to the subtilosin A gene sequences present in *B. amyloliquefaciens* strain MZ-40 (92%), B. *subtilis* strain B3 (92%) and *B. subtilis* strain IP (92 %) with accession numbers FJ151507, DQ452520 and JN118836, respectively. In this way, BLAST

analysis revealed that *Stn* (672 bp) matched closely with subtilisin gene presents in *B. subtilis* clone pGXAA2011 (97%), *B. mojavensis* strain A21 (98%) and *B. subtilis* strain DTQ-DR23 (90%) with accession numbers AY953434, KC02060 and EF061456, respectively.

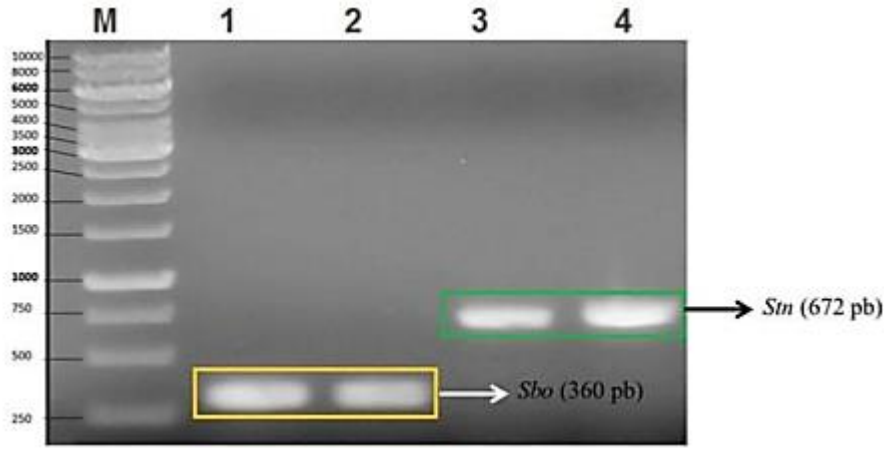

Fig. 4: PCR products of subtilosin (Sbo) and subtilisin (Stn) genes for duplicate from *B. subtilis* strain ALICA. Line MM = molecular marker; lines 1 and 2: subtilosin (Sbo) gene; lines 3 and 4: subtilisin (Stn) gene.

2.4.5 Antagonistic of Dual Plate Assay and Cell Free Culture Filtrate Antagonistic

In the present study, the results of dual plate assay demonstrated that *Bacillus* sp., strain ALICA had antagonistic effect on *F. oxysporum, F. solani* and *F. equiseti* after 5 days incubation (Fig. 5). The results revealed that strain ALICA showed broad spectrum antagonism against *F. solani* (47%), *F. equiseti* (45%) and *F. oxysporum* (32%), the maximum inhibition (%) in radial growth varied from 32 to 47 after 5 days of incubation (Fig. 5B and Table 1). With respect to effect of supernatant on radial growth of *Fusarium.* The results showed that the growth inhibition of *Fusarium* species were highly effective in cell-free culture filtrates as compared to dual culture (Fig. 5C). In this respect, our data showed that the greatest inhibition (%) in radial growth of *F. solani* (51%), *F. equiseti* (66%) and *F. oxysporum* (47%), caused by strain ALICA were

documented after 5 days of incubation on PDA supplemented with cell-free culture filtrate (Table 1).

Table 1 *In-vitro* inhibition of fungal growth by bacterial isolate ALICA on the basis of dual culture and culture filtrate techniques.

Pathogens	Percentage inhibition of radial growth	
	Dual culture	Culture filtrate
F. solani	47.87±1.67	51.40±1.28
F. equiseti	45.83±0.95	66.03±1.10
F. oxysporum	32.57±1.27	47.87±1.07

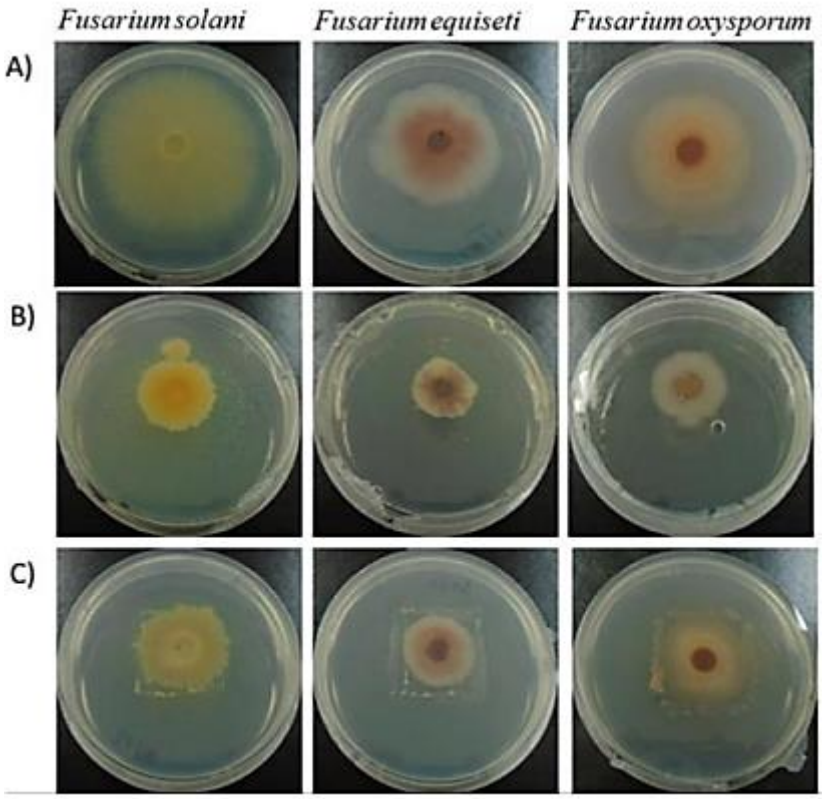

Fig. 5: Growth inhibitions of *F. solani, F. equiseti* and *F. oxysporum* as affected by (A) control without bacteria, (B) with cell free culture filtrate and (C) with bacterial isolate ALICA in dual culture assay.

2.5 Discussion

In this work, one new *B. subtilis* strain (ALICA) from *Prosopis juliflora* rhizosphere with capacities of P- solubilization and antagonistic activities against *Fusarium* species was successfully identified. The solubilization index and soluble P concentrations of isolate ALICA fluctuated during incubation days with maximum values at 3 days. These results are in line with those obtained by Jena and Rath (2013). The fluctuation observed in the solubilization index of strain "ALICA" during the period of incubation with Pikovskaya's agar and broth medium may be due to the varying type, amount, and diffusion rates of diverse organic compounds secreted by phosphate solubilizing microbes as previously mentioned by Li *et al.* (2015). In this concern, the fluctuations in solubilization index are due to the fact that this bacterium was in a state of phosphate deficiency and starvation which explains the rapid assimilation of tricalcium phosphate (TCP) within the first hours of incubation (Mardad *et al.* 2013). Our findings showed a negative relation between pH values and levels of soluble phosphorus in the culture media. This suggested the activation of metabolic products as organic acids that facility the conversion of insoluble phosphate to soluble form (Zhang *et al.,* 2013). In this regard, Marra-Leandro *et al.* (2015) proposed that organic acids biosynthesis cause one drop in pH values due to the release of protons and this reaction is an elementary principle of phosphate solubilization. This acidification caused by the production of organic acids by bacteria, which through their carboxylic groups chelate the cations (mainly Ca) bound to phosphate converting them into the soluble forms, and the negative relationship between pH and soluble-P indicates the significant role of these organic acids in mineral P solubilization (Chen *et al.,* 2006).

Therefore microorganisms as strain ALICA which decrease the medium pH during growth could be considered as efficient P solubilizer according to Li *et al.* (2015). On the other hand, the obtained result showed that in both assays (dual-culture and cell free supernatant), strain ALICA significantly inhibited the growth of pathogenic fungi such as: *F. solani, F. equiseti*, and *F. oxysporum* in comparison with control. Similarly, Ashwini and Srividya (2014) found that *B. subtilis* inhibited fungal growth of *Alternaria* (3) spp.

(55%), *Colletotrichum gloeosporioides* (57%), *Phytophthora capsici* (55%), *Rhizoctonia solani* (42%), *F. solani* (42%), *F. oxysporum* (40%) and *Verticillium* sp. (36%). This result may be recognized that growth inhibition of pathogenic fungi by *B. subtilis* might be due to the synthesis of antimicrobial compounds.

In addition to, *B. subtilis* probably suppresses the growth of pathogenic fungi as results of antifungal substances or by colonizing micro-sites faster than fungi (Elkahoui *et al.,* 2012). In this concern, Gao *et al.* (2015) reported that *Bacillus* species secrete proteins with antifungal activity; therefore the inhibitory effect is mainly due to the antifungal substances. *Bacillus* strains could produce a wide range of antifungal compounds, such as lytic enzymes, antifungal peptides and nutrient depletion (Berg *et al.,* 2001; Zhao *et al.,* 2013). Overall, there are several mechanisms to inhibit fungal growth by *B. subtilis.* However, our results demonstrate that this inhibition is probably due to production of antifungal compounds in the culture filtrate, because the cell free culture filtrates capable to suppress the fungal growth.

In this sense, the identification of antifungal antibiotic in microorganism is important for determining its competence to be a good biocontrol agent for plant diseases (Zhao *et al.,* 2014). Our result of the PCR amplification of the lipopeptide genes from DNA of *B. subtilis* strain ALICA, showed the presence of subtilosin *(Sbo)* and subtilisin *(Stn)* (Fig. 5), which showed the highest degrees of similarity to homologous sequences previously identified in other biocontrol strains when compared with GenBank sequences. This is important because the mainly restrictions of biological control is the use of a large quantity of "exotic" microorganisms with high inconsistency in the efficacy of one test to another and the negative effect on native microbial communities (Pereira *et al.,* 2009). In this sense considering the antimicrobial assays results of *B. subtilis* strain ALICA, this new strain could be applied as bio- fertilizer and bio-fungicide based on positive effect showed *in vitro* in desert ambient as Northwestern Mexico.

2.6 Conclusion

Our present investigation concludes that *B. subtilis* ALICA is potential phosphate solubilizing bacteria and biocontrol agent against phytopathogens. It showed antifungal

effects on three different *Fusarium* species *in vitro.* However, tests in the field are required to complete this work, in addition to evaluate other plant growth promoting features, extraction of antifungal compounds, mycolytic enzymes and the effect of biotic and abiotic factors on this strain.

2.7 References

Abdulkareem, M., H.M. Aboud, H.M. Saood and M.K. Shibly, 2014. Antagonistic activity of some plant growth rhizobacteria to *Fusarium graminearum. Int. J. Phytopathol.,* 3: 49-54

Adame-Garcia, J., R. Rodriguez-Guerra, L. Iglesias-Andreu, J. Ramos- Prado and M. Luna-Rodriguez, 2015. Molecular identification and pathogenic variation of *Fusarium* species isolated from *Vanilla planifolia*in Papantla Mexico. *Bot. Sci.,* 93: 669-678

Ashwini, N. and S. Srividya, 2014. Potentiality of *Bacillus subtilis* as biocontrol agent for management of anthracnose disease of chilli caused by *Colletotrichum gloeosporioides* OGC1. *Biotechnology,* 4: 127-136

Berg, G., A. Fritze, N. Roskot and K. Smalla, 2001. Evaluation of potential biocontrol rhizobacteria from different host plants of *Verticillium dahliae* Kleb. *J. Appl. Microbiol,* 91: 963-971

Chen, Y.P., P.D. Rekha, A.B. Arun, F.T. Shen, W.A. Lai and C.C. Young, 2006. Phosphate solubilizing bacteria from subtropical soil and their tricalcium phosphate solubilizing abilities. *Appl. Soil Ecol.,* 34: 33-41

Chen, Y., F. Yan, Y.R. Chai, H.X. Liu, R. Kolter, R. Losick and J.H. Guo, 2012. Biocontrol of tomato wilt disease by *Bacillus subtilis* isolates from natural environments depends on conserved genes mediating biofilm formation. *Environ. Microbiol.,* 15: 848-864

Djebali. N. and T Belhassen, 2010. Field study of the relative susceptibility of eleven potato *(Solanum tuberosum* L.) varieties and the efficacy of two fungicides against *Rhizoctonia solani* attack. *Crop Prot*., 29: 998-1002

El-hamshary, O.I.M. and A.A. Khattab, 2008. Evaluation of antimicrobial activity of *Bacillus subtilis* and *Bacillus* cereus and their fusants against *Fusarium solani. Res. J. CellMol. Biol.,* 2: 24-29

Elkahoui, S., N. Djebali, O. Tabbene, A. Hadjbrahim, B. Mnasri, R. Mhamdi, M. Shaaban and F. Limam, 2012. Evaluation of antifungal activity from Bacillus strains against *Rhizoctonia solani. Afr. J. Biotechnol,* 11: 4196-4201

Fu, R., F. Yu, Y. Gu, T. Xue, Y. Guo, Y. Wang, X. Wu, M. Du and W. Chen, 2015. Improvement of antagonistic activity of *Bacillus megaterium* MHT6 against *Fusarium moniliforme* using He-Ne laser irradiation. *Int. J. Agric. Biol.,* 17: 1141-1148

Gao, X., Y. Gong, Y. Huo, Q. Han, Z. Kang and L. Huang, 2015. Endophytic *Bacillus subtilis* Strain E1R-J Is a Promising Biocontrol Agent for Wheat Powdery Mildew. *Biomed. Res. Int.,* 2015: Article ID 462645

Gonzalez-Soto, T., D. Gonzalez-Mendoza, R. Troncoso-Rojas, A. Morales-Trejo, C. Cecena-Duran and O. Grimaldo-Juarez, 2015. Molecular identification of Fusarium species isolated from transgenic insect-resistant cotton plants in Mexicali valley, Baja California. *Genet. Mol. Res.,* 14: 11739-11744

Hildebrand, J.L., O.S. Bains, D.S.H. Lee and C.J. Kennedy, 2009. Functional and energetic characterization of P-gp-mediated doxorubicin transport in rainbow trout *(Oncorhynchus mykiss)* hepatocytes. *Comp. Biochem. Physiol.* C., 149: 65-72

Jena, S.K. and C.C. Rath, 2013. Optimization of Culture Conditions of Phosphate Solubilizing Activity of Bacterial sp. Isolated from Similipal Biosphere Reserve in Solid-State Cultivation by Response Surface Methodology. *Int. J. Curr. Microbiol. Appl. Sci.,* 2: 47-59

Kim, G.H. M.T. Lim, J.S. Hur, K.J. Yum and Y.J. Koh, 2009. Biological control of tea anthracnose using an antagonistic bacterium of *Bacillus subtilis* isolated from tea leaves. *Plant Pathol.* J., 25: 99102

Kloepper, J.W., C.M. Ryu and S. Zhang, 2004. Induced systemic resistance and promotion of plant growth by Bacillus spp. *Phytopathology,* 94: 1259-1266

Kumar, A., A. Prakash and B.N. Johri, 2011. *Bacillus* as PGPR in crop ecosystem. *In: Bacteria in Agrobiology: Crop Ecosystems*1st edition, pp: 37-59. Maheshwari, D.K. (ed.). Springer, New York, USA

Li, X., L. Luo, J. Yang, B. Li and H. Yuan, 2015. Mechanisms for solubilization of various insoluble phosphates and activation of immobilized phosphates in different soils by an efficient and salinity-tolerant *Aspergillus niger* Strain An2. *Appl. Biochem. Biotechnol.,* 175: 2755-2768

Lutfunnessa, R.J.F. and S. Shamsi, 2011. Fungal diseases of cotton plant *(Gossypium hirsutum* L.) in Bangladesh. *Dhaka Univ. J Biol. Sci.,* 20: 139-146

Mardad, I., A. Serrano and A. Soukri, 2013. Solubilization of inorganic phosphate and production of organic acids by bacteria isolated from a Moroccan mineral phosphate deposit. *Afr. J. Microbiol. Res.,* 7: 626635

Marra-Leandro, M., S.M. Oliveira-Longatti, R.F.S. de Soares Claudio, M de. Lima Jose, L. Olivares Fabio and M.S. Moreira Fatima, 2015. Initial pH of medium affects organic acids production but do not affect phosphate solubilization. *Braz. J. Microbiol.,* 46: 367-375

Mendez-Trujillo, V., L. Moreno-Ramirez, M. Carrillo-Beltran and D. Gonzalez-Mendoza, 2013. Fast Protocol for DNA Isolation of DNA from Bacterial Isolated from a Hyper-arid Environment. *J. Pure Appl. Microbiol,* 7: 1-4

Pereira, P., A. Nesci and M. Etcheverry, 2009. Impact of two bacterial biocontrol agents on bacterial and fungal culturable groups associated with the roots of field-grown maize. *Lett. Appl. Microbiol.,* 48: 493-499

Ruiz-Sanchez, E., M.A. Mejia-Bautista, J. Cristobal-Alejo, A. Valencia- Botin and A. Reyes-Ramirez, 2014. Antagonistic activity of *Bacillus subtilis* vs *Colletotrichum gloeosporioides* (Penz.). *Rev. Mex. Cienc. Agric.,* 5: 1325-1332

Sun, J.B., M. Peng, Y.G. Wang, P.J. Zhao and Q.Y. Xia, 2011. Isolation and characterization of antagonistic bacteria against *fusarium* wilt and induction of defense related enzymes in banana. *Afr. J. Microbiol. Res.,* 5: 509-515

Sundaramoorthy, S. and P. Balabaska, 2013. Evaluation of Combined Efficacy of *Pseudomonas fluorescens* and *Bacillus subtilis* in Managing Tomato Wilt Caused by Fusarium oxysporum f. sp. *lycopersici* (Fol). *Plant Pathol. J,* 12: 154-161

Teran-Vargas, A.P., J.C. Rodriguez, C.A. Blanco, J.L. Martinez-Carrillo, J. Cibrian-Tovar, H. Sanchez-Arroyo, L.A. Rodriguez-del-Bosque and D. Stanley, 2005. Bollgard cotton and resistance of tobacco budworm (Lepidoptera: Noctuidae) to

conventional insecticides in the Southern Tamaulipas, Mexico. *J. Econ. Entomol.,* 98: 2203-2209

Trivedi, P., A. Pandey, and L.M.S. Palni, 2008. *In vitro* evaluation of antagonistic properties of Pseudomonas corrugata. *Microbiol. Res.,* 163: 329-336

Zhang, A., G. Zhao, T. Gao, W. Wang, J. Li, S. Zhang and B. Zhu, 2013. Solubilization of insoluble potassium and phosphate by *Paenibacillus kribensis* CX-7: A soil microorganism with biological control potential. *Afr. J. Microbiol. Res.,* 7: 41-47

Zhao, K., P. Penttinen, X. Zhang, X. Ao, M. Liu, X. Yu and Q. Chen, 2014. Maize rhizosphere in Sichuan, China, hosts plant growth promoting *Burkholderia cepacia* with phosphate solubilizing and antifungal abilities. *Microbiol. Res,* 169: 76-82

Zhao, X., Z.J. Zhou, Y. Han, Z.Z. Wang, J. Fan and H.Z. Xiao, 2013. Isolation and identification of antifungal peptides from *Bacillus* BH072, a novel bacterium isolated from honey. *Microbiol. Res.,* 168: 598-606

CAPÍTULO III (CHAPTER III)

ANTIFUNGAL ACTIVITIES OF AUTOCHTHONOUS *Bacillus subtilis* ISOLATED FROM *Prosopis juliflora* AGAINST PHYTOPATHOGENIC FUNGI

3.1 Abstract

The ability of *Bacillus subtilis* ALICA to produce 3 mycolytic enzymes (chitinase, β-1,3-glucanase, and Protease), was carried out by the chemical standard methods. *Bacillus subtilis* ALICA was screened based on their antifungal activity in dual plate assay and cell-free culture filtrate (25%) against five different phytopathogenic fungi *Alternaria alternata, Macrophomina sp., Colletotrichum gloeosporioides, Botrytis cinerea* and *Sclerotium rolfesii*. The *B. subtilis* ALICA detected positive for chitinase, β-1,3 glucanase and protease enzymes. Fungal growth inhibition by both strain ALICA and its cell-free culture filtrate ranged from 51.36 to 86.3% and 38.43 to 68.6%, respectively. Moreover, hyphal morphological changes like damage, broken, swelling, distortions abnormal morphology were observed. Genes expression of protease, β-1,3 glucanase and lipopeptides (Subtilosin and Subtilisin) were confirmed their presence in the supernatant of strain ALICA. Our findings indicated that strain ALICA provided a broad spectrum of antifungal activities against various phytopathogenic fungi, and may be a potential effective alternative to chemical fungicides.

Key words: *Bacillus subtilis*, mycolytic enzymes, Biocontrol, Lipopeptides.

3.2 Introduction

In the Northwestern Mexico, the fungi are the most common plant pathogens, which cause large losses in the quantity and quality of crops yield and thus cause great economic losses (Holguín-Peña, 2005). Control of these fungi has been largely through the application of fungicides, which represents a quick solution to the phytosanitary problems. However these agrochemicals represent a risk to environmental by the

negative effects in the human and animal health (Solanki *et al*., 2015). On the other hand, biological control using beneficial autochthonous microorganisms is an eco-friendly alternative to chemical fungicide, which can protect the plant from pathogens by several mechanisms such as antibiosis, parasitism, competition, lytic enzymes, and induced systemic resistance (Saechow *et al*., 2017; Thakaew and Niamsup, 2013). The term “autochthonous microorganisms” refers to a group of beneficial microbes that are native to the area, thus the name autochthonous. Autochthonous microorganisms play an important role by protecting the normal host from invasion by microorganisms with a greater potential for causing disease (Thakaew and Niamsup, 2013). In this context, autochthonous microorganisms, specially belonging to the *Bacillus* genus are among the most used biological agents to fight against many plant pathogens (Ashwini and Srividya, 2014). *Bacillus* species (eg., *B. subtilis*) displayed diverse strategies to reduce the infection in the plants by pathogens: 1) production of extracellular antibiotics; and 2) production of mycolytic enzymes like chitinase, protease, and β-1,3 glucanase (Ashwini and Srividya, 2014; Solanki *et al*., 2012). *Bacillus subtilis* is a species commonly found in the environment, its taxonomy and that of related species has been extensively studied in the last two decades (Ruiz-Sanchez *et al*., 2016). However, though many different environmental isolates and strains of *B. subtilis* have been described, to date there is no report regarding the identification of native *B. subtilis* isolates from extreme arid condition present in Northwestern of Mexico, that elicit significant antagonistic activity against fungi that cause plants diseases.

The study of *B.subtilis* capable of producing an effective biocontrol of different phytopathogenic fungi has focused on isolating of several strains from tropical and subtropical regions (Ruiz-Sanchez *et al*., 2016; Adame-García *et al*., 2015). Nevertheless, research that evaluating the diversity of autochthonous microorganisms as *B.subtilis* in native soils from Northwestern, Mexico, specifically, Baja California, is scarce. Considering the above the present study was carried out to evaluate the antagonistic potential of *Bacillus subtilis* strain “ALICA” previously isolated from *Prosopis juliflora* rhizosphere a native plants from Northwestern of Mexico against *Alternaria alternata, Macrophomina sp., Colletotrichum gloeosporioides, Botrytis cinerea* and *Sclerotium rolfesii*.

3.3 Material and methods

3.3.1 Microorganisms

Bacillus subtilis strains “ALICA” (Gene bank number, KX137176) used in the present study was previously isolated from rhizosphere soil of *Prosopis juliflora* (Abdelmoteleb *et al*., 2017). The plant pathogenic fungi *Alternaria alternata, Macrophomina* sp., *Colletotrichum gloeosporioides, Botrytis cinerea* and *Sclerotium rolfesii* were kindly supplied by Dra. Rosalba Troncoso-Rojas from the Research Center in Food and Development (CIAD-Hermosillo, Mexico).

3.3.2 Enzymes assay

For the production of enzymes, the strain *Bacillus subtilis* ALICA was inoculated in 100 ml Erlenmeyer flasks containing 50 ml of synthetic broth medium with (%): K_2HPO_4 0.1, $MgSO_4.7H_20$ 0.01, NaCl 0.1, $(NH_4)_2SO_4$ 0.7 and lyophilized fungal mycelium 0.1. After 72 h incubation at 30 °C with rotary agitation 150 rpm, the culture was centrifuged at 10,000 rpm for 10 min at 4°C. The crude supernatant was used as enzyme source.

3.3.2.1 Chitinase assay

The chitinase activity was measured as described by Brants and Earle (2001), 4-methylumbelliferyl-β-D-N, N', N''-triacetylchitotrioside [4-MU-β-(GlcNAc) 3] (Sigma) solution was prepared as a substrate at a concentration of 1.3 µM in 50 mM sodium phosphate buffer pH 7 (Annex 4). The reaction mixture containing 10 µl of enzyme solution, 5 µl of the substrate and 35 µl of 50 mM sodium phosphate buffer pH 7 was performed at 37 ºC for 20 min. 150 µl of 0.2 M Na_2CO_3 was added to stop the enzymatic reaction. Fluorescence after the enzyme activity was measured by using a TBS-380 Mini-Fluorometer at 325 nm excitation and 446 nm emission wavelengths and compared against methylumbelliferone (4-MU) standard curve (Annex 5). Enzyme assays were

performed in triplicates. One unit of enzyme activity (U) was defined as the amount of enzyme able to release one ng of 4-methylumbelliferone (4-MU) per min.

3.3.2.2 β-1,3-glucanases assay

The β-1,3-glucanase activity was determined by measuring the reducing sugars released from laminarin as a substrate using 1% dinitrosalicylic acid (DNS) method (Miller, 1959). 500 µl of supernatant was mixed with 500 µl 0.5% Laminarin substrate which dissolved in 50 mM acetate buffer, pH 6.0 (Annex 6). After incubation at 40 ºC for 60 min the enzyme was inactivated by adding 1 ml of a 1% dinitrosalicylic acid solution and heating the preparation in a boiling water bath for 10 min. The absorbance was measured at a wavelength of 540 nm. The amount of reducing sugar released was calculated using glucose standard curve (Annex 7). One unit of β-glucanase activity is defined as the amount of enzyme required to produce 1 µg of glucose in 1 min under the experimental conditions used.

3.3.2.3 Detection of protease enzyme production

Protease activity was performed on SMA (skimmed milk agar) which prepared using a 10% (w/v) stock solution of skimmed milk powder autoclaved at 115 ºC for 10 min. while agar solution made separately and autoclaved at 121°C for 20 min. The tow solutions were mixed to a final concentration of 1% skimmed milk, while still hot, and poured into Petri plates. Tested strain spotted on SMA plates and incubated 3 days at 30°C, the formation of clear zone around the colony was considered as protease positive.

3.3.2.4 Protease assay

Overnight preculture cultivated in Nutrient Broth medium was inoculated at 1% in protease production media (50 ml in 100 ml Erlenmeyer flasks) contained (% w/v) : glucose 0.1, peptone 1, yeast extract 0.02, $MgSO_4$ 0.01, $CaCl_2$ 0.01, K_2HPO_4 0.05 (pH 7.0) and incubated 72 h at 30 °C on a rotary incubation shaker (150 rpm). After incubation, culture was harvested by centrifugation at 10,000 rpm for 10 min at 4 °C. The cell free supernatant was used as the enzyme source for protease assay and the protease activity was determined as described by Jayashree *et al*. (2014). One ml of

enzyme solution was added to 1 ml 2% (w/v) casein solution (dissolved in 50 mM phosphate buffer with pH 7) and incubated in water bath at 37°C for 20 min. The reaction was terminated with the addition of 2 ml of 0.4 M Trichloroacetic acid. After 30 min stand at room temperature, the reaction mixture was centrifuged at 10,000 rpm for 10 min. Aliquots of 0.5 ml supernatant were mixed with 2.5 ml of 0.4 M Na_2CO_3 and 0.75 ml of Folin–Ciocalteu's phenol reagent: water (1:3 v/v) and incubated at room temperature for 30 min in dark condition. The optical density of the solutions was determined at 660 nm and compared against a tyrosine standard curve (Annex 8). One unit of enzyme activity was defined as the amount of the enzyme that liberates 1µg of 7 tyrosine per min under the standard assay conditions. Specific activity was expressed as units/ mg protein.

3.3.2.5 Quantitative assay of protein

Protein content of the enzymes solution (Supernatant) was determined by using the Bradford method and bovine serum albumin as a standard (Annex 9).

3.3.3 Antifungal assay

The efficacy of *B. subtilis* strain "ALICA" was tested against *Alternaria alternata*, *Macrophomina* sp., *Colletotrichum gloeosporioides, Botrytis cinerea* and *Sclerotium rolfesii* on Potato Dextrose Agar (PDA) medium using dual plate method. Ten days old culture agar discs (6 mm) of pathogens were disposed at the center of Petri dishes and the bacterial strain was streaked in a square form around the agar disc at 2 cm distance from the center and incubated at 28° C until mycelial growth had fill plates containing the control (without bacteria). The reduction of fungal growth was monitored by measuring the diameter in millimeter of the colony. The percentage of growth inhibition of tested fungi was calculated according to the formula given by Trivedi *et al*. (2008), % growth inhibition= (R1 - R2/R1)*100. Where R1 = radial growth of control and R2= radial growth of the fungus in dual culture. At the end of the incubation period, the morphological changes of fungal mycelium were studied microscopically under optical microscope (40× magnification).

3.3.4 Antifungal activity of cell-free supernatants of *B. Subtilis*

Bacteria were grown on Nutrient broth at 30 °C, with constant shaking at 150 rpm and after 3 days of incubation, cells were removed by centrifugation at 10,000 rpm for 10 min at 4 °C. Supernatant was passed through a 0.22 µm membrane to obtain cell free filtrate. The antifungal activity of cell-free supernatant of *B. subtilis* strain "ALICA" on the growth of five pathogenic fungi was tested in Petri dishes containing the potato dextrose agar (PDA) medium. Twenty five milliliter of the culture filtrate mixed with 75 ml of the PDA medium was poured into Petri dishes. Thereafter, an inoculum (6 mm diam.) of each fungus was inoculated at the centre of PDA plate and incubated at 28 °C until the mycelia colony of the control had grown to almost fill the plate. Relative inhibition of fungal growth was evaluated by the percentage reduction in the growth of the mycelia in comparison to that on control plates without culture filtrate as described earlier.

3.3.5 Gene expression of biocontrol genes

Total RNA was extracted from the overnight culture of *B. subtilis* strain "ALICA" cells grown in nutrient broth media, according to the method of Mendez *et al*. (2011). After treatment of the RNA with DNAse I (Fermentas), cDNA was synthetized using iscript-cDNA-synthesis-kit (BIO RAD, USA). RT-PCR amplifications of the subtilosin, subtilisin, protease and β-1,3-glucanase genes were carried out using gene-specific primers (Table 2). PCR was carried out in 30 µl reaction volume containing 1µl 10 mM dNTPs, 3 µl 10x PCR buffer, 2.5 µl 50 mM $MgCl_2$, 0.3 µl (5 units/µl) of Taq polymerase (BIORAD, USA), 1.2 µl (10 mM) of each primer and 2 µL template cDNA. Amplification was performed in a DNA thermal cycler (BIORAD, USA) and consisted of an initial denaturation at 94 °c for 5 min; followed by 35 cycles; denaturation for 30s at 94 °C, annealing for 30s at 58°C, extension at 72°C for 1 min with final extension was at 72°C for 7 min. PCR fragments were analysed by agarose gel electrophoresis and ethidium bromide staining and changes in gene expression levels were assessed by visual inspection of band densities. The image analysis software ImageJ (Version 1.33u, available free at http://rsb.info.nih.gov/ij/) was used for semi-quantitative analysis of the

subtilosin, subtilisin, protease and β-1,3-glucanase gene expression and expressed in arbitrary units. In order to confirm that there was no significant contamination in the total RNA preparation, we synthesized first-strand DNA and performed control reactions in the absence of reverse transcriptase, for which we did not find bands.

Table 2. Sequences of primers used in the study

Genes	Primer name	Sequence	Reference
Subtilosin	Sbo1F	5´-TCGGTTTGTAAACTTCAACTGC-3´	Cao *et al*., (2012)
	Sbo1R	5´-GTCCACTAGACAAGCGGCTC-3´	
Subtilisin	Qk1F	5´-CTTAAACGTCAGAGGCGGAG-3´	Cao *et al*., (2012)
	Qk1R	5´-ATTGTGCAGCTGCTTGTACG-3´	
Protease	22mer (F)	5'-CATATGTTTGGGTACTCTATGG-3'	Sadeghi *et al*.,(2009)
	25mer (R)	5'-GGATCCTTATTGGCCGGGAACGGAA-3'	
β-1,3-glucanase	β-glucanase	F-5'-AATGGCGGTGTATTCCTTGACC-3'	Solanki *et al*., (2012)
	β-glucanase	R-5'-GCGCGTAGTCACAGTCAAAGTT-3'	

3.3.6 Statistical analysis

Statistical Package for the Social Sciences (SPSS) software version 21 was used to analyze the significant differences between different treatments using one-way ANOVA and post-hoc Tukey's HSD test (P<0.05). Results are indicated with the average of the values determined ± standard deviation (SD).

3.4 Results

3.4.1 Mycolytic enzymes

Quantification of lytic enzymes of *B. subtilis* ALICA used in this study produced various cell wall degrading enzymes chitinase, β-1,3-glucanase and protease. Results were recorded according to the U/mg protein produced in the enzyme assays.

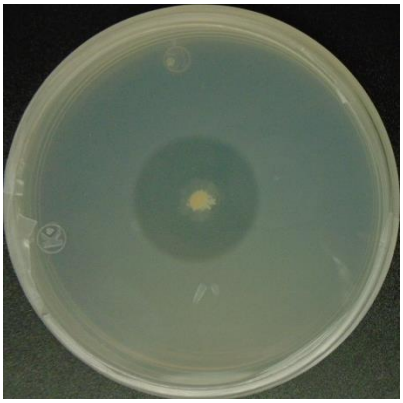

Fig. 6: Qualitative assay for protease activity on skimmed milk agar plate.

Chitinase and β-1,3-glucanase activities were induced using a lyophilized fungal mycelium amended medium. Protease enzyme production was detected preliminarily as formation of a clear zone around the colony on skim milk agar medium (Fig. 6), then quantified using standard methods. Data presented in Table (3) showed that *B. subtilis* ALICA produced significant activities of chitinase, β-1,3-glucanase and protease which were 138, 211.4 and 345.7U/ mg protein, respectively.

Table 3. Activity of hydrolytic enzymes of antagonistic *B. subtilis* strains ALICA

Enzymes	Chitinase	β-1,3 Glucanase	Protease
Activities (Unit/ mg protein)	138	211.4	345.7

3.4.2 Dual culture assay

The *B. subtilis* strain “ALICA” illustrated certain degree of antagonism in the dual-plate assays to all of the tested phytopathogenic fungi, *Alternaria alternata, Macrophomina* sp., *Colletotrichum gloeosporioides, Botrytis cinerea* and *Sclerotium rolfesii* (Figs. 7 and 8A). The results revealed considerable reductions in the growth of fungal mycelia as affected by *B. subtilis* strain ALICA. The results of the analysis of variance showed significant differences ($P < 0.05$) of growth inhibition among the different pathogens. The

maximum growth inhibition was 86.3 ± 0.69 % for *B. cinerea* and the minimum inhibition was 51.36 205 ± 1.32 % for *C. gloeosporioides*. During antagonism a damaged mycelia of tested fungi was observed under optical microscope. Morphological changes like damage, broken, swelling, distortions abnormal morphology and the material of the cell let out were found in the fungal mycelium grown with *B. subtilis* ALICA comparing to the control (Fig. 8B). Moreover, spores formation of pathogens was not observed in dual plates.

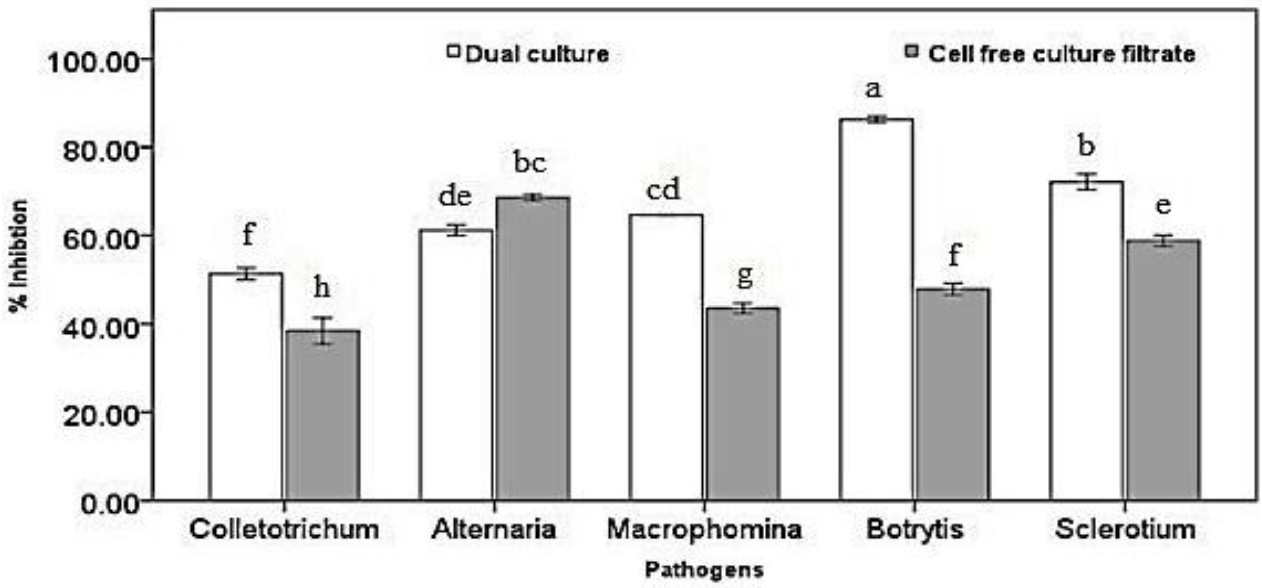

Fig. 7: Effect of *B. subtilis* ALICA and its cell free culture filtrate on mycelial growth of phytopathogenic fungi.The values are expressed as mean ± SD of the four replicated samples, and different letters on bars indicate significant difference analyzed by post-hoc Tukey's HSD test (P<0.05).

3.4.3 Inhibitory effects of *B. subtilis* ALICA cell-free culture filtrate on pathogens growth

The antifungal activity of *B. subtilis* ALICA cell-free culture filtrate against several phytopathogenic fungi is summarized in Figure 7 and 8A. It was remarkable that Cell-free culture filtrate at 25% in PDA plates decrease significantly ($P \leq 0.05$) the growth of all target fungi. In general, the effect of culture filtrate on mycelial growth inhibition was

less effective than dual culture for all tested fungi except *A. alternata*, which was more affected by cell-free culture filtrate as compared to dual culture. The highest significantly inhibition (68.6 ± 0.69 %) using cell-free culture filtrate was achieved for *A. alternata*, followed by *S. rolfesii* (58.8±1.2), *B. cinerea* (47.86±1.3%), *Macrophomina* (43.53±1.1 %), and *C. gloeosporioides* (38.43±2.9%) was the least affected by cell-free culture filtrate of *B. subtilis* strain "ALICA" as in the case of dual culture assay.

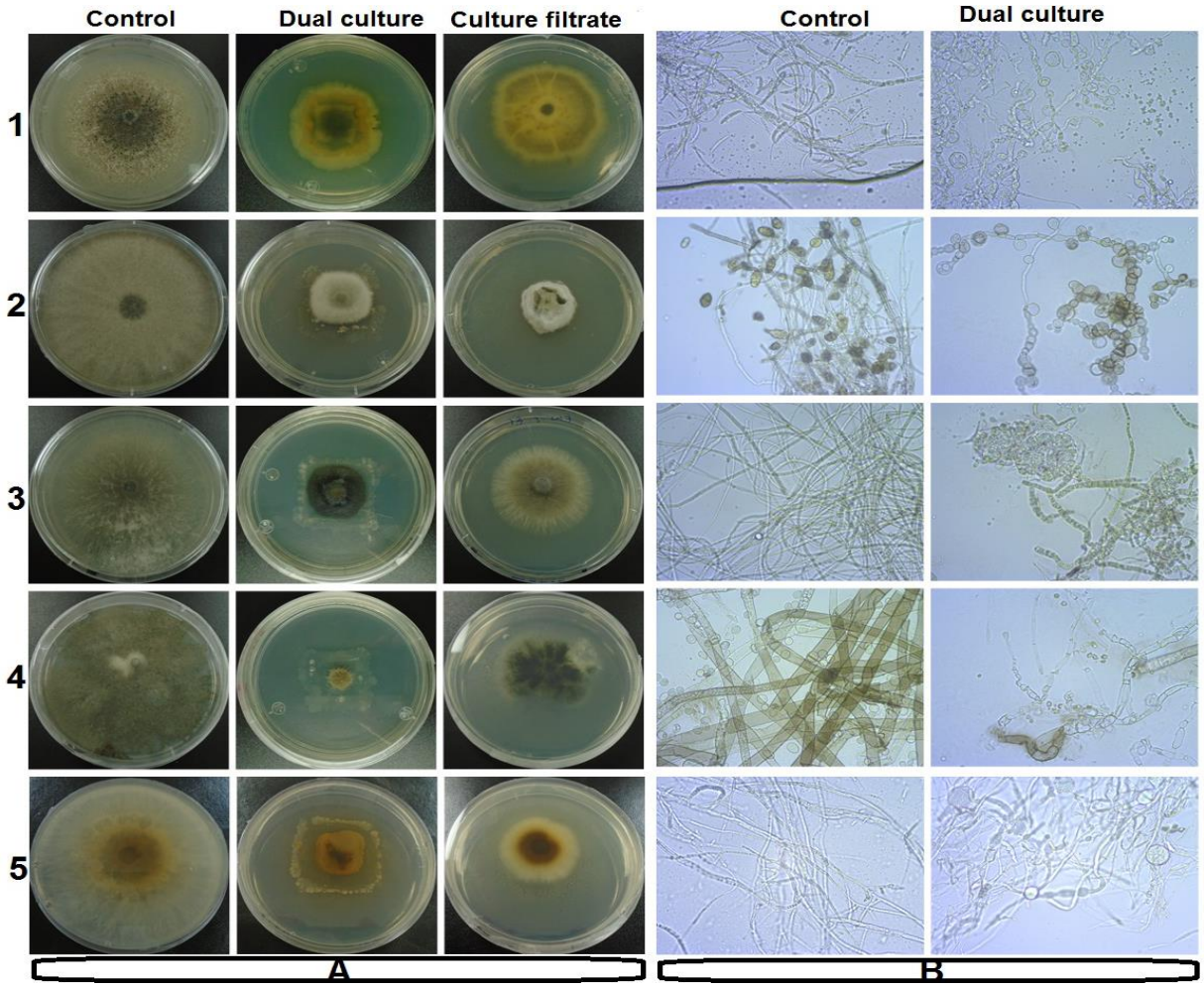

Fig. 8: (A): Antifungal activity of *B. subtilis* ALICA and its cell free culture filtrate against, 1= *Colletotrichum gloeosporioides,* 2= *Alternaria alternata,* 3= *Macrophomina sp.,* 4= *Botrytis cinerea* and 5= *Sclerotium rolfesii.* (B): Morphological changes of fungal mycelia upon interaction with *B. subtilis* ALICA in dual culture plates.

3.4.4 Gene expression of biocontrol genes

As illustrated in Fig. (9 A and B), the PCR amplification of biocontrol genes subtilosin, subtilisin, protease and β-1,3 glucanase in *B. subtilis* showed that all of the four genes have been expressed. Subtilosin and subtilisin gene expression showed one specific band at around 360 and 672 pb, respectively. On the other hand, protease gene amplification showed one specific band at around 290 bp length and amplification of β-1,3 glucanase gene was also specific on the 415 bp in *Bacillus subtilis* strain “ALICA”.

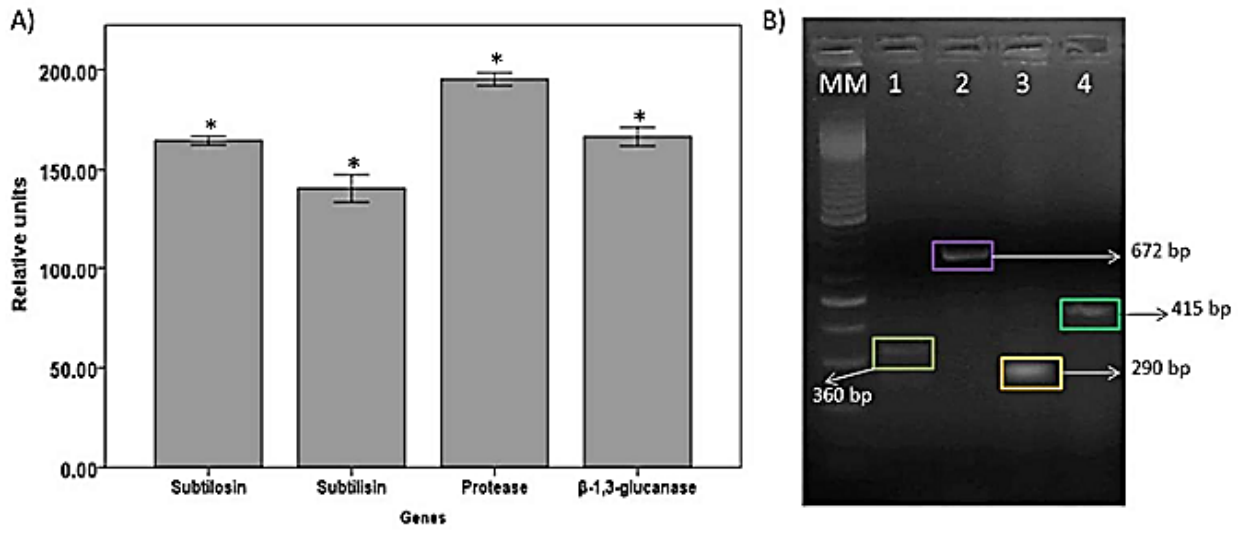

Fig. 9. Biocontrol genes quantification, using a RT-PCR assay expressed in arbitrary units (A), and B) PCR products visualized in 1% agarose gel electrophoresis and stained with ethidium bromide of *Bacillus subtilis* strain ALICA: lines 1 and 2: subtilosin (360 bp) and subtilisin (672 bp) gene; 3 and 4: protease (290 bp) and β-1,3 glucanase (415 bp). The values are expressed as mean ± SD of the four replicated samples. Asterisk indicates statistically significant differences between treatments ($P < 0.05$).

3. 5 Discussion

In the present study, a new *Bacillus subtilis* strain “ALICA” isolated from the rhizosphere of *Prosopis juliflora*, in Baja California, Mexico, with antagonistic activities against wide range of phytopathogenic fungi was evaluated. In the present study *B. subtilis* strain“ALICA” had a strong antagonistic activity against *Colletotrichum gloeosporioides; Alternaria alternata; Macrophomina* sp; *Botrytis cinerea* and *Sclerotium rolfesii* showing strong inhibitory activity against mycelial growth. These results contrast with previous report (Ashwini and Srividya, 2014) in which the inhibition of growth of phytopathogenic fungi by another *B.subtilis* strains was significantly minor compared with our results obtain in the present study.

On the other hand, mycelial growth inhibition of five tested fungi by the bacterial culture filtrate and the hyphal damages with no noticeable parasitism following the bacterial treatment as viewed by microscopy, suggest that bacterial antibiotics produced by *B. subtilis* strain “ALICA” might be responsible for the inhibition of the pathogen growth. In this sense, the gene expression of subtilosin and subtilisin, genes from “ALICA” support the hypothesis that antibiosis is the major action mode that exhibits this strain. In this context, recent studies have shown that the reason for antagonism between *Bacillus* spp and fungi may be the production of antifungal lipopeptides such as surfactin, subtilosin, or subtilisin (Tendulkar *et al*., 2007; Nielsen *et al*., 2000). On the other hand, *B. subtilis* strain “ALICA” expressed two hydrolytic enzymes, β-1,4-glucanase and protease, which possibly degrade the contents of the fungal cell wall, such as β-1,3-glucan and glucosidic bonds. Therefore, it is assumed that the cell wall lysis of the pathogenic fungi is due to the coordinated action of hydrolytic enzymes and antifungal lipopectides, such as subtilosin, subtilisin, protease and β-1,3 glucanase. Similarly Zhang *et al.* (2017) reported the inhibition of growth of *Gaeumannomyces graminis* var. *tritici* by *B. subtilis* Z-14 culture filtrate, indicating that the antifungal effects of *B. subtilis* Z-14 may be due to the secretion of diverse compounds in the culture filtrate. Finally, the strain “ALICA” used in the present study was isolated from the rhizosphere of *Prosopis juliflora*, obtained in Baja California, Mexico, where the phytopathogenic fungi has been present in last decades but has never been efficiently controlled. In this sense, “ALICA” could represent an effective biocontrol agent against *Colletotrichum gloeosporioides; Alternaria alternata; Macrophomina* sp; *Botrytis cinerea* and *Sclerotium rolfesii*.

However, these studies were conducted under *in vitro* conditions and further studies are required to investigate whether these results hold true under field conditions.

3.6 References

Abdelmoteleb A, Troncoso-Rojas R, Tzintzum-Camacho O, González-Mendoza D, Duran Ceceña C, Grimaldo-Juárez O, Aviles-Marin M, Duran-Hernández D. 2017. Biocontrol of *Fusarium* spp., Causal Agents of Damping-off in Cotton Plants by Native *Bacillus subtilis* Isolated from *Prosopis juliflora*. International Journal of agriculture & Biology, 19: 713–718. DOI: 10.17957/IJAB/15.0344.

Adame-García J, Rodríguez-Guerra R, Iglesias-Andreu L, Ramos Prado J, Luna-Rodríguez M. 2015. Molecular identification and pathogenic variation of *Fusarium* species isolated from *Vanilla planifoliain* Papantla Mexico. Bot Sci 93: 669-678.

Ashwini N, Srividya S. 2014. Potentiality of *Bacillus subtilis* as biocontrol agent for management of anthracnose disease of chilli caused by *Colletotrichum gloeosporioides* OGC1. 3 Biotech, 4: 127–136.

Brants A, Earle ED. 2001. Transgenic tobacco cell cultures expressing a *Trichoderma harzianum* endochitinase gene release the enzyme into the medium. Plant Cell Reports. 20: 73-78.

Holguín-Peña RJ, Arcos FG. 2005. First report of gray mold in tomato caused by *Botrytis cinerea* in Baja California, Mexico. Plant Dis, 89: 528-528.

Jayashree S, Annapurna B, Jayakumar R, Sa T, Seshadri S. 2014. Screening and characterization of alkaline protease produced by a pink pigmented facultative methylotrophic (PPFM) strain, MSF 46. Journal of Genetic Engineering and Biotechnology, 12:111–120.

Méndez V, Avelar E, Morales A, Cervantes M, Araiza A, González D. 2011. A rapid protocol for purification of total RNA for tissues collected from pigs at a slaughterhouse. Genetics and Molecular Research, 10: 3251-3255.

Miller GL. 1959. Use of dinitrosalicylic acid reagent for determination of reducing sugar. Analytical Chemistry, 31: 426-428.

Nielsen, T.H., Thrane, C., Christophersen, C., Anthoni, U., & Sørensen, J. 2000. Structure, production characteristics and fungal antagonism of tensin a new antifungal cyclic lipopeptide from Pseudomonas fluorescens strain 96.578. Journal Applied Microbiology, 89: 992–1001.

Ruiz-Sanchez E, Mejia-Bautista MA, Serrato-Diaz M, Reyes-Ramirez A, Estrada-Giron Y, Valencia-Botin AJ. 2016. Antifungal activity and molecular identification of native strains of *Bacillus subtilis*. Agrociencia 50: 133-148.

Saechow S, Thammasittirong A, Thammasittirong SNR. 2017. The Potential of *Bacillus subtilis* BAS114 for *In vitro* Biocontrol of Fusarium oxysporum. Advances in Environmental Biology, 11: 46-51.

Solanki MK, Singh RK, Srivastava S, Kumar S, Kashyap PL, Srivastava AK. 2015. Characterization of antagonistic-potential of two Bacillus strains and their biocontrol activity against Rhizoctonia solani in tomato. J Basic Microbiol 55: 82-90.

Solanki MK, Robert AS, Singh RK, Kumar S, Pandey AK, SrivastavaAK, Arora DK. 2012. Characterization of Mycolytic Enzymes of *Bacillus Strains* and Their Bio-Protection Role Against Rhizoctonia solani in Tomato. Current Microbiology, 65:330–336.

Tendulkar, S.R., Saikumari, Y.K., Patel, V., Raghotama, S., Munshi, T.K., Balaram, P., & Chattoo, B.B. 2007. Isolation, purification and characterization of an antifungal molecule produced by *Bacillus licheniformis* BC98, and its effect on phytopathogen *Magnaporthe grisea*. Journal Applied Microbiology, 103: 2331–2339.

Thakaew R., Niamsup, H. 2013. Inhibitory Activity of *Bacillus subtilis* BCC 6327 Metabolites against Growth of Aflatoxigenic Fungi Isolated from Bird Chili Powder. International Journal of Bioscience, Biochemistry and Bioinformatics, 3: 27- 32.

Trivedi P, Pandey A, Palni LMS. 2008. *In vitro* evaluation of antagonistic properties of *Pseudomonas corrugata*. Microbiological Research, 163: 329-336.

Zhang, D., Gao, T., Li, H., Lei, B., & Zhu, B. 2017. Identification of antifungal substances secreted by Bacillus subtilis Z-14 that suppress *Gaeumannomyces graminis* var. *tritici*. Biocontrol Science and Technology, 27 :237-251.

CAPITULO IV (CHAPTER IV)

Green Synthesis of Silver Nanoparticles Using *Pluchea sericea* a Native Plants from Baja California, Mexico and their Potential Application as Antimicrobials

4.1 Abstract

The use of natural plant extracts in the synthesis of nanoparticles provides advancement over chemical and physical methods, due to its cost effectiveness and environment friendly nature. In this study, silver nanoparticles (AgNPs) have been synthesized with simple and green technique using *Pluchea sericea* plant leaf extract as reducer as well as stabilizer. The characterization and properties of AgNPs were investigated using UV–visible spectroscopic techniques, energy dispersive X-ray spectrometers (EDS), zeta potential and dynamic light scattering. The UV–visible spectroscopic analysis showed the absorbance peak at 487 nm, which indicates the synthesis of silver nanoparticles. The experimental results showed silver nanoparticles having Z-average diameter of 59.20 nm with higher stability (-70.9 mV). The EDS analysis also exhibits presentation of silver element. Additionally, the different concentrations of AgNPs (25, 50, 75 and 100 %) showed antibacterial activity against *Acinetobacter calcoaceticus*. Finally, AgNPs from leaf extracts of *P. sericea* may be used for antimicrobial activity against *A. calcoaceticus*. However, further studies will be needed to fully understand the antimicrobial activity of AgNPs and to determine if the microorganism can develop resistance toward these nanoparticles.

Keywords: Silver nanoparticles, Plants extract, Biosynthesis, Antibacterial activity, Nanotechnology.

4.2 Introduction

Nanoparticles (NPs) are a group of materials with distinctive features and extensive applications in different fields of science and medicine (Matei *et al*.2008). Moral metal

nanoparticles have been extensively studied and different approaches have been engaged for the preparation of metal nanoparticles (Raveendran *et al*.2003). Among these metal nanoparticles, silver nanoparticles have attracted intensive research interest because of their important applications as antimicrobial, catalytic, and antifungal activity (Yang and Cui2008; Ji-Ho *et al*. 2009). Silver has been used as an antimicrobial agent for centuries; the recent resurgence in interest for this element particularly focuses on the increasing threat of antibiotic resistance caused by the abuse of antibiotics (Yıldız and Ibtisam 2010). However, there are some limitations in using Ag ions or Ag salts as antimicrobial agents. Probable reasons include the interfering effects of salts. This type of limitation can be removed using silver in nano form. It is generally recognized that silver nanoparticles may attach to the cell wall, thus disturbing the cell wall permeability and cellular respiration. The nanoparticles may also penetrate inside the cell causing damage by interacting with phosphorus and sulfur containing compounds, such as DNA and protein. Another possible contribution to the bactericidal properties of silver nanoparticles is the release of silver ions from particles (Yıldız and Ibtisam 2010). It is important and necessary to prepare AgNPs with safely methods. Various chemical and physical methods are known for the preparation of silver and other metal nanoparticles. These methods are very costly and toxic to the environment (Kalaiarasi *et al*. 2013). Silver nanoparticles are fabricated by the reduction of silver ions to neutral silver atoms. Silver ions are reduced by the use of reducing agents (Kaushik *et al*.2010). Biosynthesis of nanoparticles is nothing but the bottom up approach of nanoparticles synthesis. Phytochemicals present in the plants possess anti-oxidant or reducing properties which are responsible for the reduction of metal compounds. Methods used for the biosynthesis of metal nanoparticles are eco-friendly, biocompatible, nontoxic and clean (Sharma and Yangard 2009). In recent years, plant-mediated biological synthesis of nanoparticles is gaining importance due to its simplicity and great potential with natural reductants (Sivalingam *et al*. 2012). In this sense, the genus *Pluchea* belongs to one of the most diverse botanical family, Asteraceae. *Pluchea* counts about 80 species of small herbs and shrubs and a large number of these taxa (30–40) thrive in tropical regions. *Pluchea sericea* (Nutt.) *Caville*, commonly known as ‘cachanilla’ is an evergreen wild shrub growing in sandy or saline soils of the Baja California, Sonora and Chihuahua

deserts in Mexico (Villasen˜or and Villareal 2006). In Mexico, the study of *P. sericea* has focused principally in the evaluation and identification of secondary metabolites (e.g., flavonoids and phenolic compounds) with application in the pest control (Ail-Catzim *et al*. 2015). However, studies about the use of *P. Sericea* for the biosynthesis of AgNPs as a green chemistry method are scarce. In this study, we report the easy synthesis of silver nanoparticles by an environmental friendly procedure involving the in situ reduction of Ag by *P. sericea* extracts and the evaluation of their antimicrobial activity against *Acinetobacter calcoaceticus*. This organism is Gram-negative coccobacilli that have emerged from an organism of questionable pathogenicity to an infectious agent of importance to hospitals worldwide. This organism has the ability to accumulate diverse mechanisms of resistance, leading to the emergence of strains that are resistant to all commercially available antibiotics (Van Looveren and Goossens 2004).

4.3 Materials and methods

4.3.1 Biosynthesis of Silver Nanoparticles (AgNPs) from *Pluchea sericea*

To prepare the AgNPs, fresh and healthy leaves were obtained from *P. sericea* plants grown at Mexicali, (32º24′34″ N and 115º11′16″ W) Baja California, Mexico. Leaves sterilization was done in the laboratory by one rinse with 0.5 % NaOCl (Clorox) for 3 min, followed by an extensive rinse with deionized sterile water. Then, the leaves were dried for 24 h at room temperature. The extract solution was prepared by heating 20 g leaves in flask with 200 mL of distilled water for 30 min at 60ºC. For AgNPs synthesis, 0.2 mL of *P. sericea* leaf extract were added into 0.8 mL of aqueous solution of 10 mM silver nitrate and heated to 60ºC for 30 min. The color change was observed which stands as a preliminary identification of the formation of AgNPs (Azizi *et al*. 2013).

4.3.2 Characterization of AgNPs from *P. sericea*

An aliquot of the sample (1 mL) of the suspension were collected when finish of incubation period (30 min) to monitor the completion of bioreduction of Ag^{+} in aqueous

solution, followed by dilution of the samples with 3 mL of deionized water, and subsequent scan in UV visible (vis) spectra, between wavelengths of 400–500 nm in a spectrophotometer (Thermo Scientific BioMate 3 Spectrophotometer, USA), having a resolution of 1 nm according to Saxena *et al*. (2010).

4.3.3 Scanning Electron Microscope (SEM) and Energy Dispersive Analysis of X-ray Spectroscopy (EDS) Analysis of Silver Nanoparticles

A scanning electron microscope (SEM) JEOL 6010 was employed to characterize the size and morphology of the AgNPs at an accelerating voltage of 10 kV. Thin films of the sample were prepared on a carbon coated copper grid by just dropping a very small amount of the sample on the grid, extra solution was removed using a blotting paper, and then the film on the SEM grid were allowed to dry by putting it under a mercury lamp for 5 min. For EDS analysis, the AgNPs were dried and drop coated on to carbon film. EDS analysis was then performed using the oxford instrument Thermo EDS (Ramalingam *et al*. 2013).

4.3.4 Zeta Potential and Dynamic Light Scattering (DLS) Measurements

Surface zeta potentials were measured using the laser zetameter (C:\Mlcrotrac\FLEX 11.0.0.4\Databases\NANOPARTICULAS.MDB). The mean size and its zeta potential of the particles was obtained present in the sample. Dynamic light scattering (or photon correlation spectroscopy) is an important technique generally used to realize the size distribution pattern of very small particles present in suspension or solution. Measurements were made by means of dynamic light scattering (DLS) in the range of 0.1–1000 µm according to Singh *et al*. (2010).

4.3.5 Antibacterial Assays

The antibacterial assays were done on *A. Calcoaceticus* (Gram negative) by standard disc diffusion method (Bao *et al*. 2011). Nutrient agar medium was used to cultivate

bacteria. Fresh overnight cultures of inoculums (100 µL) of bacterial culture were spread on to nutrient agar plates. 20 µL of synthesized AgNPs solution with four different concentrations (25, 50, 75 and 100 %) were prepared in distilled water, and was added to a 7 mm sterile filter paper discs and allowed to dry. AgNPs containing discs were placed in plate and a control plate (discs with only *P. sericea* leaf extract) was separately prepared. The plates were incubated at 30±2 ºC for 24 h. After incubation, the formation of inhibition zone was checked and the diameter of zone was measured.

4.3.6 Statistical Analysis

Data were processed by analysis of variance with $p \leq 0.05$, with Tukey's test, using the Statistical Analysis System version 6.12 (SAS Institute1997).

4.4 Results and Discussion

4.4.1 Synthesis of Silver Nanoparticles

The preliminary confirmation for the formation of AgNPs was the visual observation of color change of the aqueous solution of *P. sericea* leaf extract. Before the addition of silver nitrate the culture was in yellow color and at 30 min of reaction, the color of the solution was changed to brown (Fig.10). The color change may be due to the excitation of the surface plasmon resonance (SPR) effect and the reduction of $AgNO_3$ (Azizi *et al*.2013). This property is largely governed and dependent upon the particle type, size, shape as well as the nature of the surrounding medium (Dhand *et al*. 2016). In this sense, our result suggested that the biomolecules in plant extract may be responsible for the reduction of $AgNO_3$ and stabilization of AgNPs. In this context, Muthukrishnana *et al*. (2015) reported that presence of triterpenes and methoxy groups in the leaf extract of *Ceropegia thwaitesii* may play key role in reduction and stability of AgNPs. Therefore,

the extract of *P. sericea* that is rich in polyphenols, such as flavonoids, triterpenes and sesquiterpenes molecules (Ail-Catzim *et al*. 2015), could act as reducing and stabilizing agents for AgNPs production. On the other hand, the UV–vis spectra obtained from *P. sericea* leaf extract and $AgNO_3$ show characteristic absorption band of AgNPs at 487 nm (Fig.11).

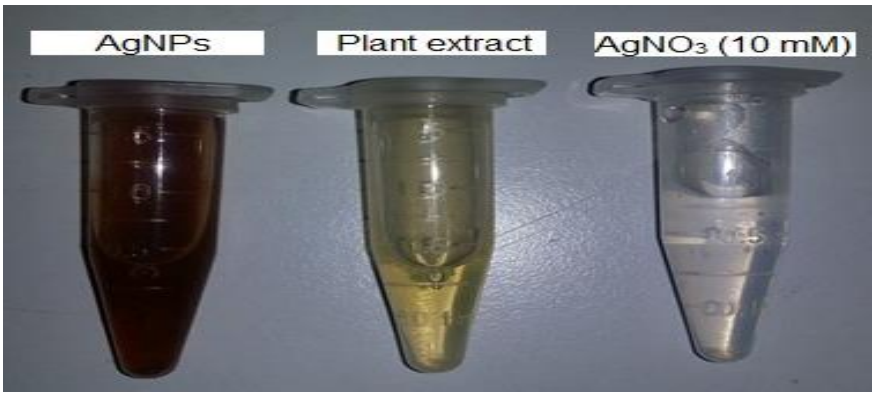

Fig.10. Synthesis of silver nanoparticles using plant extracts.

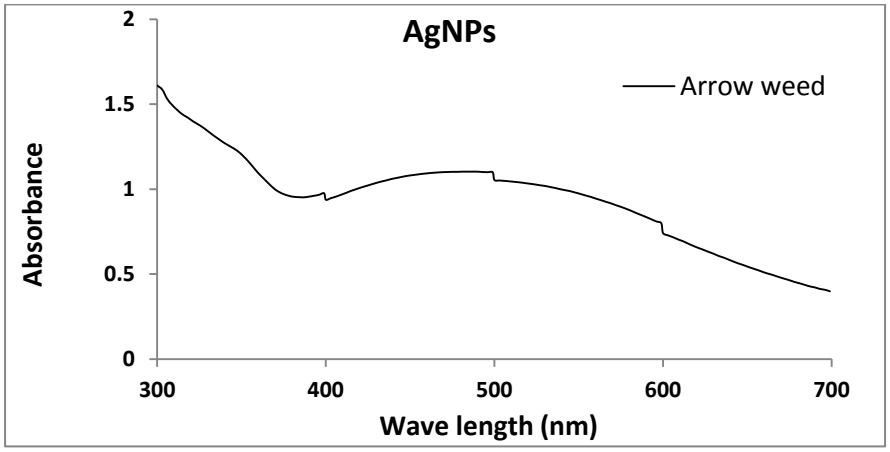

Fig.11. UV-vis spectra of the synthesized silver nanoparticles.

This was confirmed with the previous reports where spherical AgNPs showed the absorption bands at around 400–500 nm in the UV–visible spectra (Prathna *et al.* 2011). The results showed resemblance with the results of Baharara *et al*. (2014) who reported the synthesis of silver nanoparticles from *Achillea biebersteinii* flower extract with a strong absorption peak centered at 460 nm.

4.4.2 SEM and EDS Analysis

The morphology and size of silver nanoparticles analyzed using SEM is shown in Fig.12. In general, the SEM image shows that the majority of nanoparticles were in spherical shape with varying size as visually seen from the adjacent photographs. It can be seen that some of the particles are well dispersed and many of them have formed aggregates. In the microphotographs, it has also been seen that the synthesized silver nanoparticles were surrounded by other variety of compounds present in the extract (e.g., flavonoids, triterpenes and sesquiterpenes molecules) which may act as capping agent and provide stability to the silver nanoparticles. On the other hand, the EDS analysis gives qualitative as well as quantitative status of elements that may be involved in the formation of nanoparticles.

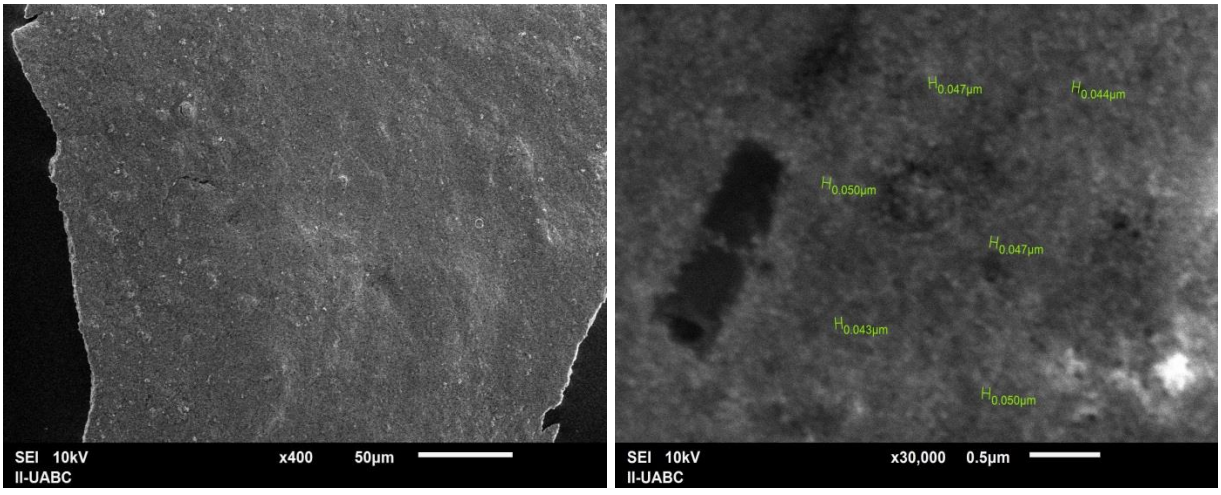

Fig.12. SEM image of silver nanoparticles from *P. sericea*

Figure (13) shows elemental profile of synthesized nanoparticles using leaf extracts and confirms the formation of silver nanoparticles. Figure (13) also showed higher counts at 3 keV due to silver nanoparticles. Generally, metallic silver nanocrystals show typical optical absorption peak approximately at 3 keV due to surface plasmon resonance (Baharara *et al*.2014). The elemental analysis of the silver nanoparticles shown in the figure revealed highest proportion of silver followed by C, Cl and O. The peaks are from the biomolecules bound to the surface of the silver nanoparticles and the graphite pad used as sample support. This finding was in accordance with Baharara *et al*. (2014) who reported that higher counts of AgNPs at 3 keV.

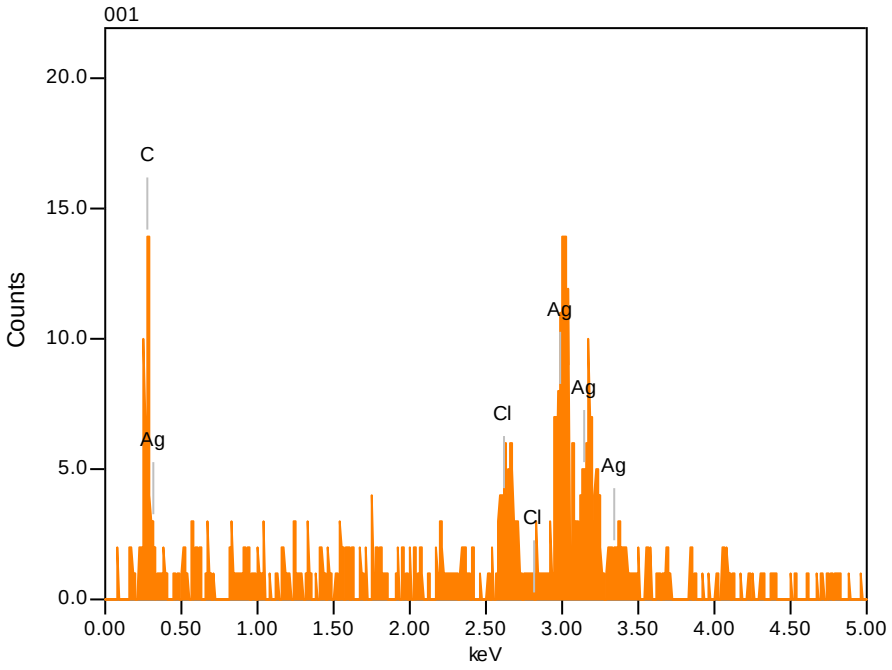

Fig.13. EDS image of silver nanoparticles produced from *Pluchea sericea*

4.4.3 Zeta Potential and Dynamic Light Scattering (DLS)

Particle size, size distribution and zeta potential were important characterizations of the silver nanoparticles because they govern the other characterizations, such as saturation solubility and dissolution velocity, physical stability, or even biological performances (Vishal and Agrawal 2011). The zeta potential value of the colloidal solution was determined to be -70.9 mV. The negative surface charge could be due to the adsorption

of bioactive components present in the aqueous extract onto the nanoparticles surface. The stability of the colloidal system is determined by the magnitude of the zeta potential (ζ). If the particles in suspension have a large negative or positive zeta potential then they will tend to repel each other and there will be fewer tendencies for the particles to come together and aggregate. The particles in suspension with ζ-potentials more positive than +30 mV or more negative than -30 mV are considered stable (Duman and Tunc¸2009). However, if the particles in suspension have low zeta potential values then there will be no force to prevent the particles coming together and aggregating. From Table (4) it is clear that the colloidal suspension was highly stable with a ζ-potential of -70.9 mV. These results are in agreement with those obtained by Umoren *et al*. (2014) who found that zeta potential of silver nanoparticles synthesized using red apple (*Malus domestica*) fruit extract was -65.07 mV. From the zeta potential value, it is evident that the nanoparticles prepared by leaf extract were found to stable without adding a different physical or chemical capping agent. Higher zeta potential indicates greater stability of the synthesized silver nanoparticles (Jebakumar and Sethuraman2012).

Table 4: Zeta-Potential analysis of silver nanoparticles synthesized from *P. sericea*

AgNPs synthesized Using *P. sericea*	**Average particle size**	**Mobility**	**Zeta potential**
	59.20 nm	-5.54 u/s/v/cm	-70.9 mv
	Charge	**Polarity**	**Conductivity**
	- 0.03313 fc	Negative	582 us/cm

The size distribution of the synthesized AgNPs is depicted in Fig. (14) It is observed that the particles obtained are polydisperse mixtures in the range 20.42–119.4 nm. The average size of the synthesized silver nanoparticles using *P. sericea* leaf extract is around 59.20 nm. In this concern, Umoren *et al*. (2014) showed that the particle size of the synthesized silver nanoparticles using red apple fruit extract was in the range 50–300 nm with average size 150 nm.

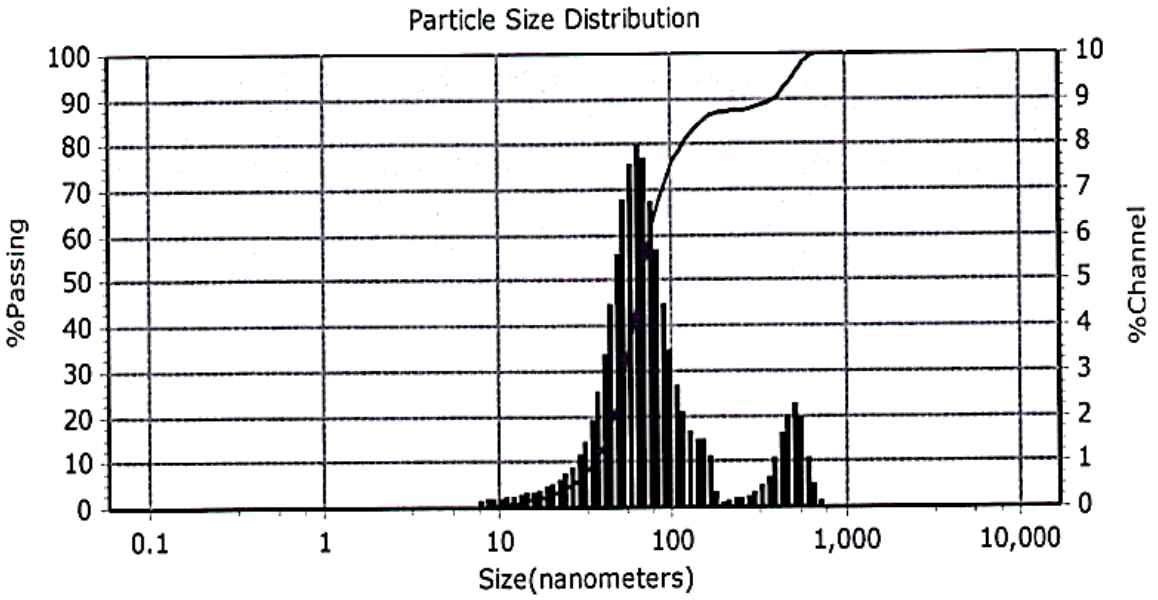

Fig.14. Particle size distribution of silver nanoparticles from dynamic light scattering measurements.

4.4.4 Antibacterial Activity

Acinetobacter species are receiving increasing attention as significant opportunistic pathogens, usually in the context of serious underlying disease (Dijkshoorn *et al*.2007). Disc diffusion is a distinguished and accustomed method to determine how is toxicity effect of a material in solution against to bacterial colonies (Parashar *et al*.2011). In this sense, our results showed that all concentrations of AgNPs from *P. sericea* present a clear zone of inhibition against tested bacteria compared with *P. sericea* leaf extract used as control (Fig.15). The results of antibacterial activity of prepared AgNPs evaluated from the disc diffusion method are given in Table (5).

Table 5. Inhibition of *Acinetobacter calcoaceticus* by nanoparticles from *P. sericea*

Microorganisms	Zone of inhibition (mm) with different concentrations of silver nanoparticles			
	25%	50%	75%	100%
P. sericealeaf extracts (control)	NA	NA	NA	NA
Acinetobacter calcoaceticus	8±0.23[a]	8.5±0.42[a]	9±0.85[b]	9±0.73[b]

The result showed that AgNPs solutions, low (25 and 50 %) and high (75 and 100 %), doses from extract of *P. sericea* had an antimicrobial activity (p<0.05) against *A. calcoaceticus*(zone of inhibition range 8.0–9.0 mm, respectively) with respect to control. Similar results were observed in *Proteus vulgaris*-MTCC 1771, *Bacillus subtilis* (MTCC 10619), and *A. calcoaceticus* treated with AgNPs obtained from *Abelia grandiflora* and *Urtica dioica* Linn (Sharma *et al.* 2014; Jyoti *et al*. 2015). Generally, inhibition of microorganism increased in a dose dependent manner in the presence of nanoparticles (Sharma and Yangard 2009).

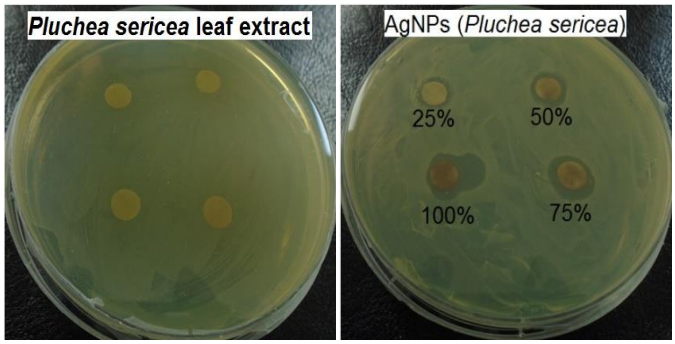

Fig. 15. Antibacterial activity of synthesized AgNPs against *Acinetobacter calcoaceticus.*

Nevertheless, in this study, the low and high dose rates were much closed. Therefore, the differences registered in 25 and 50 % doses of AgNPs were not significant. Analogous effect was observed when used high doses of AgNPs. On the other hand, the exact mechanism which silver nanoparticles employ to cause antimicrobial effect is not clearly known and is a debated topic. In this sense, several reports suggested that the synthesis of AgNPs could produce Ag ions which will damage the cell membrane, interrupt the metabolic activity, and subsequently lead to denaturation of protein, and finally cell death. AgNPs could also produce reactive oxygen species (ROS) (e.g., singlet oxygen, hydroxyl radical, and peroxide radical) which are toxic to the bacteria (Danilcauk *et al*. 2006; Kim *et al*. 2007). Finally, this new green method for the synthesis of AgNPs was established based on the use of plant extracts as reductants. The first step in this new synthesis was the selection of the plant extract with the best reductant characteristics. For this purpose, *Pluchea sericea* leaf was selected. This plant is abundant in Mexicali valley, therefore, they can be considered as low cost residues. This

feature makes it very attractive for economic, availability and reuse issues. The biosynthesis of AgNPs using *P. sericea* leaf is a simple, environmentally friendly, low-cost and non-toxic approach compared with chemical and physical methods that are very costly and toxic to the environment (Kalaiarasi *et al*.2013).

4.5 Conclusions

This study demonstrates that AgNPs can be synthesized through a green approach that is an inexpensive, pollution free, and eco-friendly method using *P. sericea* leaf extract as a bio-reducing agent. Additionally, the AgNPs from *P. sericea* showed antimicrobial activity against *A. calcoaceticus* bacteria at two different concentrations (25 and 75 %). Our findings indicate that AgNPs from *P. Sericea* may have potential benefits as biocontrol agents for human pathogens. However, further studies are needed to confirm their potential, determine their effect on human pathogens and identify the bioactive compounds in *P. sericea*.

4.6 References

Ail-Catzim CE, García López AM, Troncoso-Rojas R, González Rodríguez RE, Sánchez-Segura Y .2015. Insecticidal and repellent effect of extract of *Pluchea sericea* (Nutt.) on adults *Bemisia tabaci* (Genn.). Revista Chapingo. Serie Horticultura 21:33–41.

Azizi S, Namvar F, Mahdavi M, Ahmad M, Mohamad R .2013. Biosynthesis of silver nanoparticles using brown marine macroalga,Sargassum muticumaqueous extract. Materials 6:5942–5950.

Baharara J, Namvar F, Ramezani T, Hosseini N, Mohamad R .2014. Green synthesis of silver nanoparticles usingAchillea biebersteiniiflower extract and its anti-angiogenic properties in the rat aortic ring model. Molecules 19:4624–4634.

Bao Q, Zhang D, Qi P .2011. Synthesis and characterization of silver nanoparticle and graphene oxide nanosheet composites as a bactericidal agent for water disinfection. J Colloid Interface Sci, 360:463–470.

Danilcauk M, Lund A, Saldo J, Yamada H, Michalik J .2006. Conduction electron spin resonance of small silver particles. Spectrochim Acta Part A Mol Biomol Spectrosc 63:189–191

Dhand V, Soumya L, Bharadwaj S, Chakra S, Bhatt D, Sreedhar B .2016. Green synthesis of silver nanoparticles using *Coffea arabica* seed extract and its antibacterial activity. Mater Sci Eng C 58:36–43

Dijkshoorn L, Nemec A, Seifert H .2007. An increasing threat in hospitals: multidrug-resistantAcinetobacter baumannii. Nature Rev Microbiol 5:939–951

Duman O, Tunc¸ S .2009. Electrokinetic and rheological properties of Na-bentonite in some electrolyte solutions. Micropor Mesopor Mater 117:331–338

Jebakumar IET, Sethuraman MG .2012. Instant green synthesis of silver nanoparticles using *Terminalia chebula* fruit extract and evaluation of their catalytic activity on reduction of methylene blue. Process Biochem 47:1351–1357

Ji-Ho P, Luo G, Geoffrey M, Michael JS .2009. Biodegradable luminescent porous silicon nanoparticles for in vivo applications. Nat Mater 8:331–336

Jyoti K, Baunthiyal M, Singh A .2015. Characterization of silver nanoparticles synthesized usingUrtica dioicaLinn. leaves and their synergistic effects with antibiotics. J Radiat Res Appl Sci. doi:10.1016/j.jrras.2015.10.002

Kalaiarasi R, Prasannaraja G, Venkatachalama P .2013. A rapid biological synthesis of silver nanoparticles using leaf broth of *Rauvolfia tetraphylla* and their promising antibacterial. Indo Am J Pharm Res 3:8052–8062

Kaushik N, Thakkar S, Mhatre RY, Parikh MS .2010. Biological synthesis of metallic nanoparticles. Nanomed Nanotechnol Biol Med 6:257–262

Kim J, Yu K, Kim J, Park S, Lee H, Kim S, Park Y, Hwang C, Kim Y, Lee Y, Jeong D, Cho M .2007. Antimicrobial effects of silver nanoparticle. Nanomedicine 3:95–101

Matei A, Cernica I, Cadar O, Roman C, Schiopu V .2008. Synthesis and characterization of ZnO-polymer nanocomposites. IntJ Mater Form 1:767–770

Muthukrishnana S, Bhakya S, Kumar T, Rao MV .2015. Biosynthesis, characterization and antibacterial effect of plant-mediated silver nanoparticles using *Ceropegia thwaitesiian* endemic species. Ind Crops Prod 63:119–124

Parashar UK, Kumar V, Bera T, Saxena PS, Nath G, Srivastava SK, Giri R, Srivastava A .2011. Study of mechanism of enhanced antibacterial activity by green synthesis of silver nanoparticles. Nanotechnology 22:415104

Prathna TC, Raichur AM, Chandrasekaran N, Mukherjee A .2011. Biomimetic synthesis of silver nanoparticles by *Citrus limon* (lemon) aqueous extract and theoretical prediction of particle size. Colloids Surf B Biointerfaces 82:152–159

Ramalingam V, Rajaram R, Premkumar C, Santhanam C, Dhinesh P, Vinothkumar S, Kaleshkumar K .2013. Biosynthesis of silver nanoparticles from deep sea bacteriumPseudomonas aeruginosa JQ989348 for antimicrobial, antibioflim and cytotoxic activity. J Basic Microbiol 53:1–9

Raveendran P, Fu J, Wallen SL .2003. Completely green synthesis and stabilization of metal nanoparticles. J Am Chem Soc 125:13940–13941

Saxena A, Tripathi RM, Singh RP .2010. Biological synthesis of silver nanoparticles by using onion (*Allium cepa*) extract and their antibacterial activity. Dig J Nanomater Biostruct 5:427–432

SAS Institute .1997. SAS/STAT User's Guide. Release 6.03 edn. Cary, NC, USA

Sharma V, Yangard R .2009. Green synthesis and their antimicrobial activities. J Colloid Interface Sci 9:83–96

Sharma G, Jasuja ND, Rajgovind PS, Joshi SC .2014. Synthesis, characterization and antimicrobial activity of Abelia Grandiflora assisted AgNPs. J Microbial Biochem Technol 6:274–278

Singh A, Jain D, Upadhyay MK, Khandelwal N, Verma HN .2010. Green synthesis of silver nanoparticles using Argemone mexicana leaf extract and evaluation of their antimicrobial activities. Dig J Nanomater Biostruct 5:483–489

Sivalingam P, Antony JJ, Siva D, Achiraman S, Anbarasu K .2012. MangroveStreptomyces sp. BDUKAS10 as nanofactory for fabrication of bactericidal silver nanoparticles. Colloids Surf B Biointerfaces 98:12–17

Umoren SA, Obot IB, Gasem ZM .2014. Green synthesis and characterization of silver nanoparticles using red apple (*Malus domestica*) fruit extract at room temperature. J Mater Environ Sci 5:907–914

Van Looveren M, Goossens H .2004. Antimicrobial resistance of *Acinetobacter* spp. in Europe. Clin Microbiol Infect 10:684–704

Villasen˜or JL, Villareal JA .2006. El género *Pluchea* (Familia: Asteraceae, Tribu: *Plucheeae*) en México. Revista Mexicana de Biodiversidad 77:59–65

Vishal RP, Agrawal YK .2011. Nanosuspension: an approach to enhance solubility of drugs. J Adv Pharm Technol Res 2:81–87

Yang D, Cui D .2008. Advances and prospects of gold nanorods. Chem Asian J 3:2010–2022

Yıldız U, Ibtisam ET .2010. Development of a sensitive detection method of cancer biomarkers in human serum (75%) using a quartz crystal microbalance sensor and nanoparticles amplification system. Talanta 82:277–282

CAPITULO V. (CHAPTER V.)

Silver nanoparticles from *Prosopis glandulosa* and their potential application as biocontrol of *Acinetobacter calcoaceticus* and *Bacillus cereus*

5.1 Abstract

In the present study, the characterization and properties of silver nanoparticles from *Prosopis glandulosa* leaf extract (AgNPs) were investigated using UV–Vis spectroscopic techniques, energy dispersive X-ray spectrometers (EDS), zeta potential and dynamic light scattering. The UV–Vis spectroscopic analysis showed the absorbance peaked at 487 nm, which indicated the synthesis of silver nanoparticles. The experimental results showed silver nanoparticles had Z-average diameter of 421 nm with higher stability (−200 mV). The EDS analysis also exhibited presentation of silver element. Additionally, the different concentrations of AgNPs (25, 50, 75 and 100 mg/mL) showed antibacterial activity against *Acinetobacter calcoaceticus* and *Bacillus cereus*. Finally, AgNPs from leaf extracts of *P. glandulosa* may be used as an agent of biocontrol of microorganism of importance medical. However, further studies will be needed to fully understand the antimicrobial activity of silver nanoparticles obtain from *P. glandulosa*.

Keywords: Biosynthesis; silver nanoparticles; plant extracts; antibacterial activity

5.2 Introduction

Nanoparticles (NPs) are a group of materials with distinctive features and extensive applications in different fields of science and medicine (Reddy *et al*., 2014). Metal nanoparticles have been extensively studied and different approaches have been engaged for the preparation of these compounds. Among these metal nanoparticles, silver nanomaterials exhibit broad spectrum biocidal activity toward bacteria, fungi, and viruses (Alt *et al*., 2004). This has motivated its use in a large number of biomedical applications (Sanpui *et al*., 2011). In this sense, the nanoparticles may penetrate inside

the cell causing damage by interacting with phosphorus and sulfur containing compounds such as DNA and protein. Another possible contribution to the bactericidal properties of silver nanoparticles is the release of silver ions from the particles (Sadhasivam *et al*., 2010). At the present, various chemical and physical methods are known for preparation of silver and other metal nanoparticles. However, these methods are very costly and toxic to the environment (Nanda and Saravanan, 2009). On the other hand, the biological method provides a feasible alternative for the synthesis of nanoparticles. In this sense, the use of plants as the production assembly of silver nanoparticles has drawn attention, because of its rapid, eco-friendly, economical protocol and providing a single step technique for the biosynthetic processes (Jeong *et al*., 2005). Several plant extracts have been used to produce nanoparticles, such as *Cissus quadrangularis* or *Ficus benghalensis* (Valli and Vaseeharan, 2012; Saxena *et al*., 2012). In recent years, plant-mediated biological syntheses of nanoparticles have been gaining importance due to its simplicity and great potential with natural reductants (Kumar and Yadav, 2009). The genus *Prosopis* L., is characteristic of arid and semiarid zones, and its widespread distribution includes ecosystems in Asia, Africa, and the Americas (Pérez-García *et al*., 2012). In Mexico, the majority of the populations of the genus *Prosopis* are found in the north and center of the country, where they have formed forest extensions that are adapted to desert climate. Species such as *Prosopis glandulosa* Torr., dominate the vegetation mosaic in Baja California Mexico, primarily in an ecosystem known as mezquitales, which is characterized by a hyper-arid climate with almost no rainfall (0.6 mm year−1) (Carevic, 2014). These populations of the genus *Prosopis* have been the focus of scientific interest mainly because of their physiological and ecological adaptations to their hyper-arid environment. However, studies about the use of *P. glandulosa* for the biosynthesis of AgNPs as a green chemistry method are scarce. In the present study, we report the easy synthesis of silver nanoparticles by an environmental friendly procedure involving the in situ reduction of Ag by *P. glandulosa* extracts and the evaluation of their antimicrobial activity against *Acinetobacter calcoaceticus* and *Bacillus cereus*.

5.3 Material and methods

5.3.1 Biosynthesis of silver nanoparticles (AgNPs) from *P. glandulosa*

To prepare the AgNPs from *P. glandulosa*, healthy leaves of this plant were collected in Baja California, Mexico. The collected leaves were surface sterilized with 0.5% NaOCl (Clorox) for 1 min, followed by an extensive rinse with deionized sterile water. For sample preparation: *P. glandulosa* fresh leaves were cut into small pieces and dried using oven an electric oven for 12 h at 50 °C. Then 30 g of dried leaf of *P. glandulosa* was mixed with 300 mL of deionized water and heated at 70 °C for 30 min. About 50 mL of aqueous *P. glandulosa* leaf extract was then filtered thrice through Whatman No. 1 filter paper and centrifuged at 4000 rpm for 10 min to remove particulate matter and to get clear solutions which were then refrigerated (4 °C) for further use. For AgNPs synthesis 0.4 mL of aqueous *P. glandulosa* leaf extract were added into 0.16 mL of aqueous solution of 10 mM silver nitrate and heated to 60 °C for 30 min. The color change was observed which stands as a preliminary identification of the formation of AgNPs (Ahmed *et al*., 2016). Additionally, the AgNPs were purified by centrifugation at 10,000 rpm for 15 min to remove excess silver ions. The centrifugation process was repeated three times to remove all silver colloids with deionized water. After the sediment (AgNPs) was transferred to freeze dryer and the powder was used in antibacterial Assays.

5.3.2 Characterization of AgNPs from *P. glandulosa*

To determine the time point of maximum production of silver nanoparticles, the absorption spectra of the samples previously prepared with *P. glandulosa* leaf extract and silver nitrate were scanned in UV–Vis (vis) spectra, between wavelengths of 400–500 nm in a spectrophotometer (Thermo Scientific BioMate 3 Spectrophotometer, USA), having a resolution of 1 nm and using water as the blank.

5.3.3 Scanning electron microscopy and energy dispersive X-ray

A scanning electron microscope (SEM) (JEOL 6010; JEOL, Tokio, Japan) was employed to characterize the size and morphology of the AgNPs at an accelerating voltage of 10 kV according to the following procedure: a drop of AgNPs sample was transferred on to carbon coated copper grids. Then the film on the SEM grid was allowed to dry by putting it under a mercury lamp for 3 min and analyzed for size determination (Ramalingam *et al*., 2013). For EDS analysis, the AgNPs were dried and drop coated on to carbon film. EDS analysis was then performed using the oxford instrument Thermo EDS.

5.3.4 Zeta potential and dynamic light scattering

In order to find out the stability and size distribution of AgNPs obtained from *P. glandulosa*. Zeta potential was measured by using a Nanotrac Wave (Microtrac) according to Singh *et al*. (2010). Two thousand micro liter of sample was transferred in the clear disposable zeta cell for the measurement of zeta potential. Measurements were made by means of Dynamic Light Scattering (DLS) in the range of 0.1–1000 μm at 25 °C, using laser wavelength of 780 nm and a scattering angle of 90°. The DLS data were analyzed by the Microtrac FLEX operating software (Zhou *et al*., 2015).

5.3.5 Antibacterial assays

The antibacterial activity of the synthesized AgNPs was determined using the disk diffusion method. Two types of bacteria, including Gram-negative bacteria (*Acinetobacter calcoaceticus*) and Gram-positive bacteria (*Bacillus cereus*) were tested. Nutrient agar medium plates were prepared, sterilized and solidified. After solidification bacterial cultures were swabbed on these plates (each strain was swabbed uniformly onto individual agar plates). Sterile paper disks were placed on the agar plates. The plates were divided into three groups and each group included two types of bacteria (*A. calcoaceticus* and *B. cereus*); in the first group, 20 μL of sterile distilled water were applied to the disks as control. In the second group, 20 μL of different concentration of AgNPs, previously diluted with deionized water (25, 50, 75 and 100 mg/ mL) was added

to each disk. In the third group, 20 µL of leaf extract of *P. glandulosa* were applied to the disks (control). All the plates were incubated at 32 °C for 24 h. After incubation, the zone of inhibition, which appeared as a clear area around the disks, was measured.

5.4 Results

5.4.1 Biosynthesis of AgNPs-*P. glandulosa*

The green synthesis of AgNPs through *P. glandulosa* extracts were carried out and confirmed by visual observation. After the addition of the plant extract to the aqueous $AgNO_3$ solution, the color of the solution reaction changed from yellowish to a reddish brown color within 30 min of incubation at 60 °C (Fig. 16), indicating the formation of Ag-NPs. On the other hand, the UV–Vis spectroscopy is an important preliminary technique to ascertain the formation and stability of metal nanoparticles in aqueous suspension. Thus formation of AgNPs by reduction of aqueous Ag+ during exposure to the aqueous extract of *P. glandulosa* were followed and characterized by UV–Vis spectroscopy. As shown in Fig. (17), the surface plasmon resonance of the AgNPs was centered at approximately 487 nm.

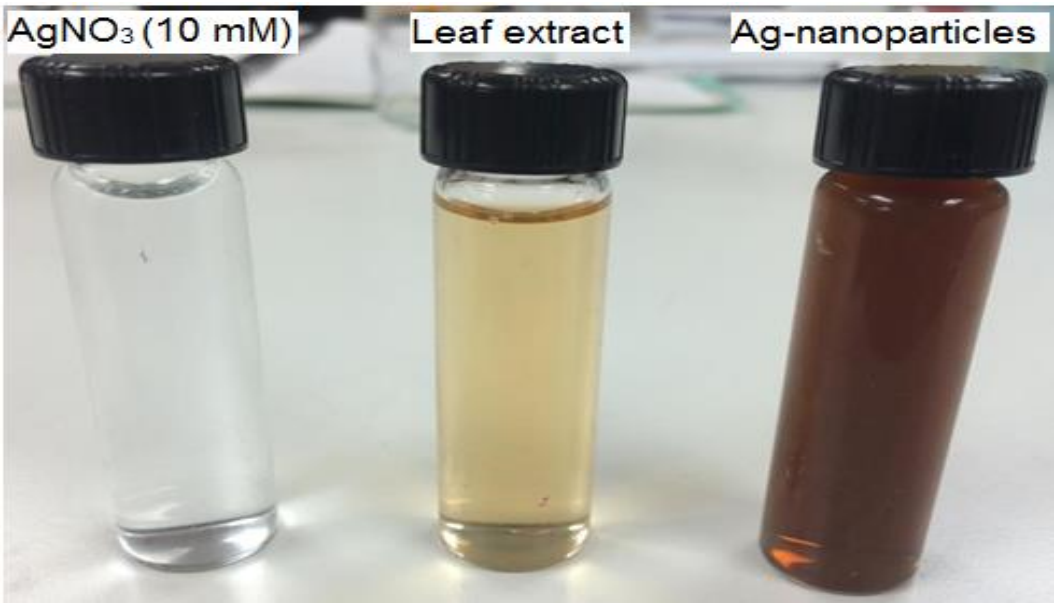

Fig.16. Synthesis of silver nanoparticles using plant extracts of *P. glandulosa*.

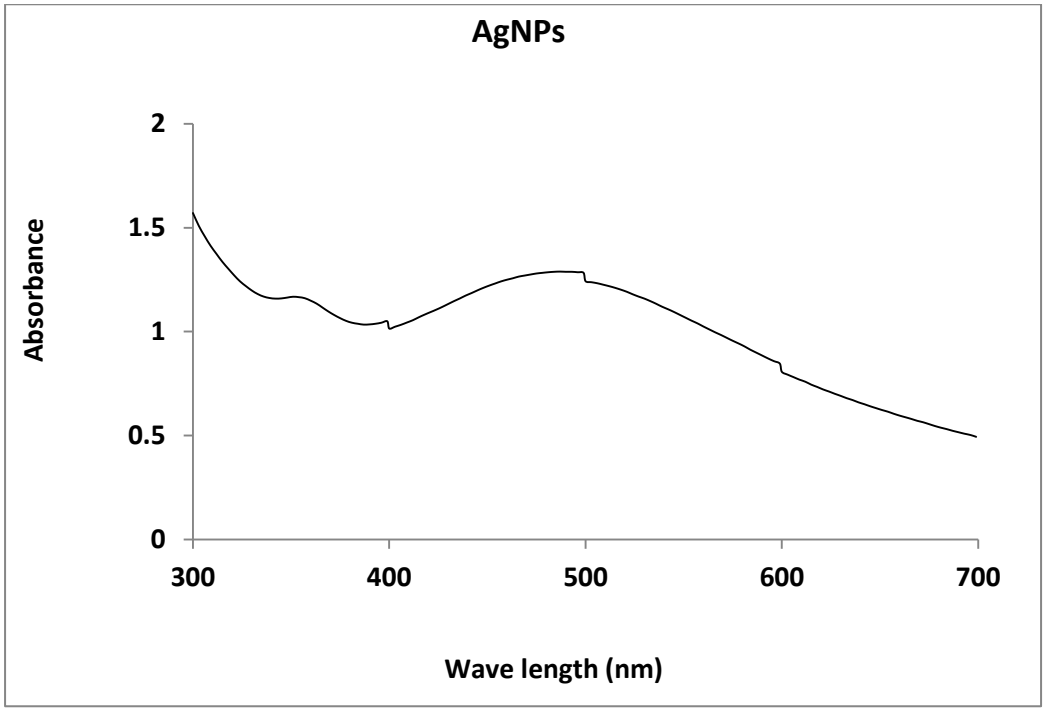

Fig. 17: UV–Vis spectra of the synthesized silver nanoparticles from *P. glandulosa*.

5.4.2 SEM and EDS analysis

SEM has been employed to characterize the size, shape and morphology of synthesized silver nanoparticles. SEM provided further insight into the morphology and size details of the silver nanoparticles. SEM image (Fig 18) recorded at high magnifications of the Ag nanoparticles synthesized by treating $AgNO_3$ solution with *P. glandulosa* leaf extract. In general, the SEM image shows that the majority of nanoparticles were in spherical shape with varying size as visually seen from the adjacent photographs. It can be seen that some of the particles are well dispersed and many of them have formed aggregates. On the other hand, the EDS analysis gives qualitative as well as quantitative status of elements that may be involved in formation of nanoparticles. The elemental profile of synthesized nanoparticles using extract of *P. glandulosa* shows higher counts at 3 keV due to silver, confirms the formation of silver nanoparticles (Fig. 19).

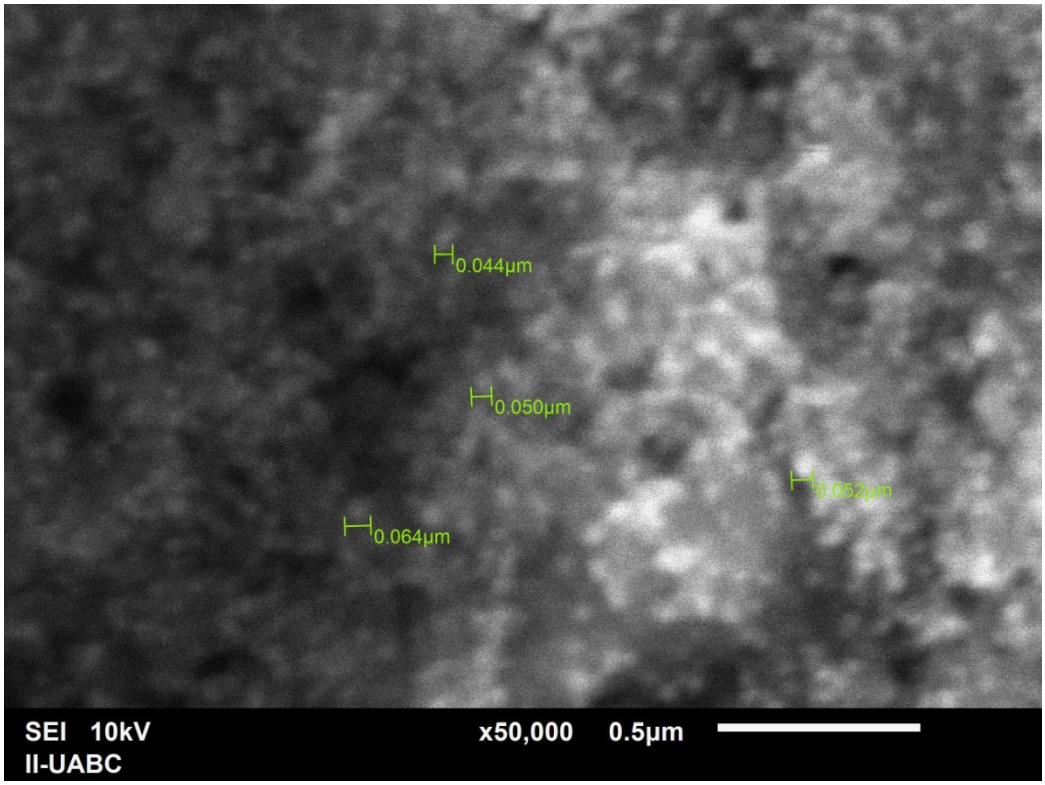

Fig. 18: SEM image of silver nanoparticles from *P. glandulosa*.

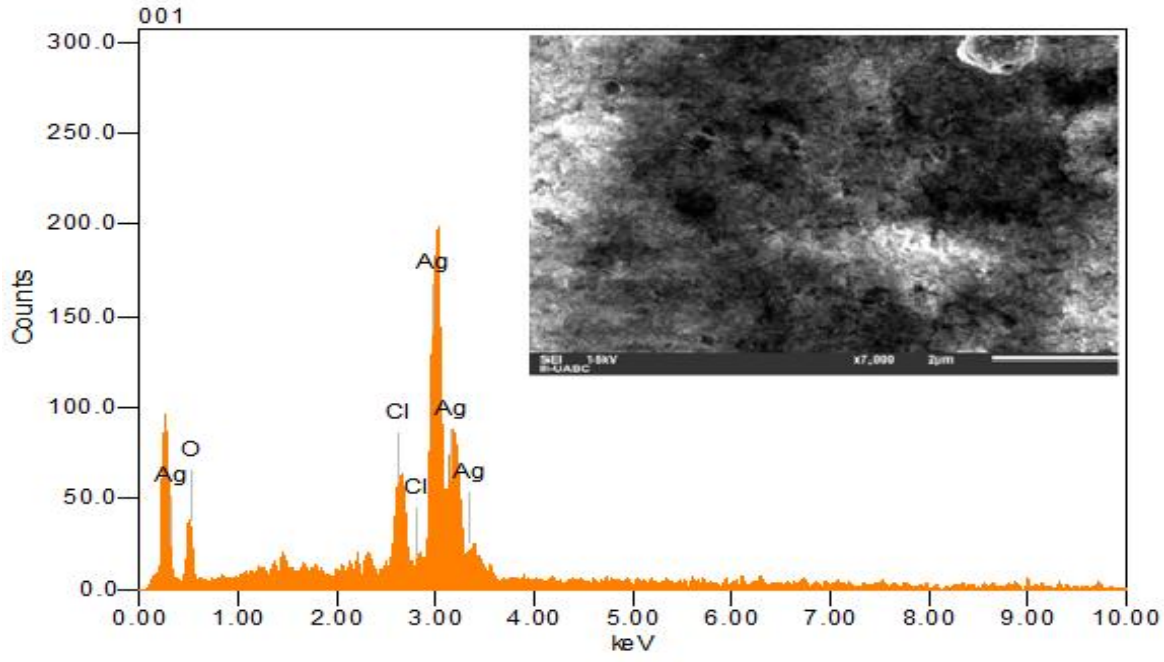

Fig. 19: EDS image of silver nanoparticles produced from *P. glandulosa*.

5.4.3 Zeta potential and DLS

Particle size, size distribution and zeta potential were important characterizations of the silver nanoparticles because they govern the other characterizations, such as saturation solubility and dissolution velocity, physical stability, or even biological performances (Visahl *et al*., 2011). As shown in Table (6), zeta potential was found to be −200.0 mV for synthesized AgNPs. On the other hand, the size distribution of the synthesized AgNPs is depicted in Fig. (20). It is observed that the particles obtained are polydisperse mixtures in the range of 32–600 nm with the average mean size (diameter) of 421 nm.

Table 6: Zeta-potential analysis of silver nanoparticles synthesized from *P. glandulosa*.

AgNPs synthesized Using *Prosopis juliflora*	**Average particle size**	**Mobility**	**Zeta potential**
	421.0 nm	-15.63 u/s/v/cm	-200.0 mv
	Charge	**Polarity**	**Conductivity**
	- 0.85541 fc	Negative	543 us/cm

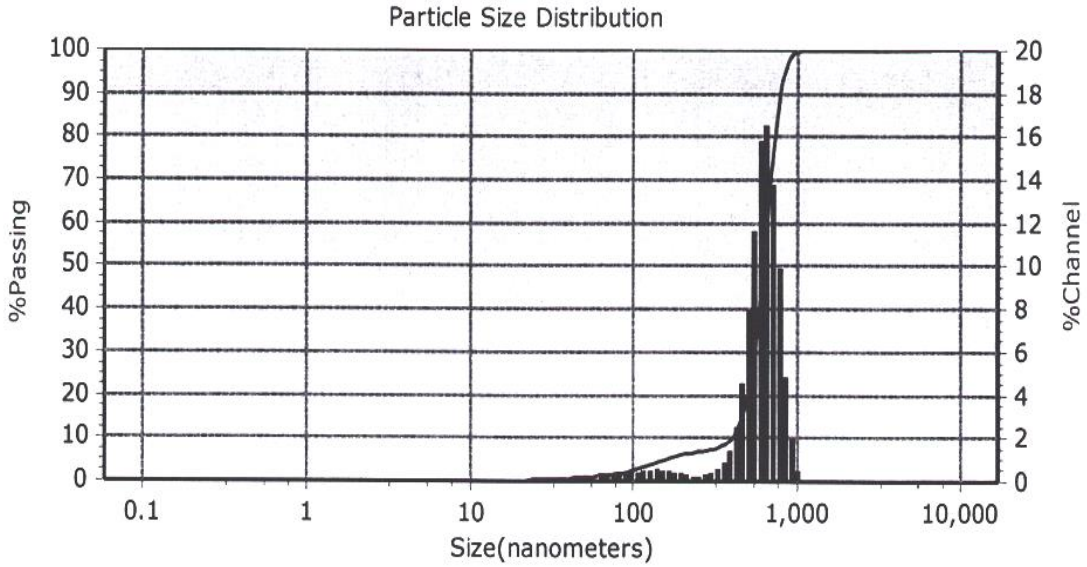

Fig. 20: Particle size distribution of silver nanoparticles from dynamic light scattering measurements.

5.4.4 Antimicrobial activity of synthesized silver nanoparticles

In the present study, the antibacterial activity of the synthesized AgNPs from *P. glandulosa* against *A. calcoaceticus* and *B. cereus* was investigated. Our results showed that all concentrations of AgNPs from *P. glandulosa* present a clear zone of inhibition against tested bacteria with respect to leaf extract of this plant used as control and the zone of inhibition increased with respect to the concentration of biosynthesized AgNPs used in the medium culture (Figure 21 and Table 7). In contrast, the leaf extract of *P. glandulosa* did not exhibit antimicrobial effect against tested bacteria (Figure 21).

Table 7: Inhibition of microorganisms by AgNPs from *P. glandulosa*.

Microorganisms	Zone of inhibition (mm) Silver nanoparticles			
	25%	50%	75%	100%
Bacillus subtilis	8	9	10	13
Acinetobacter calcoaceticus	9	10	9	12

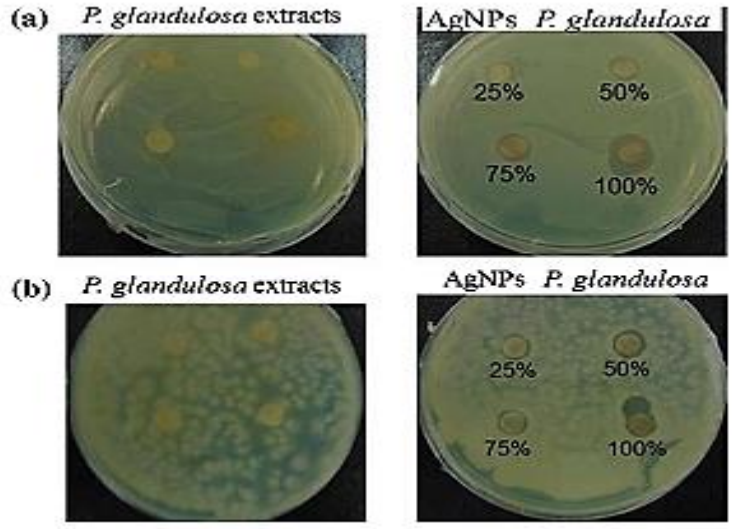

Fig. 21: Antibacterial activity of *P. glandulosa* extract and AgNPs from *P. glandulosa* (a) *Bacillus cereus* and (b) *Acinetobacter calcoaceticus*.

5.5 Discussion

In the present study, the silver nanoparticles exhibit reddish brown color in aqueous solution due to excitation of surface plasmon vibrations in silver nanoparticles (Shankar *et al*., 2004). Initially the reduction of Ag+ ions leads to the formation of silver atoms (Ag) which may follow by agglomeration into oligomer cluster. These clusters eventually lead to the formation of colloidal Ag particles (Ibrahim, 2015). Similar findings were reported by Raja *et al*., (2012) who used aqueous extract of fresh leaves of *P. juliflora* with 0.01 M $AgNO_3$ aqueous solution for the synthesis of AgNPs and they revealed that metabolites such as terpenoids or flavonoids could be responsible for the reduction and capping of AgNPs. The elemental analysis of the silver nanoparticles revealed highest proportion of silver followed by C, Cl and O. This result is consistent with the results reported by Ibrahim (2015), who found that higher counts of AgNPs synthesized using banana peel extract at 3 keV. On the other hand, our results showed that zeta potential was found to be −200.0 mV for synthesized AgNPs from *P. glandulosa*. Similar result were observed by Rai *et al*. (2006) and Tripathy *et al*., (2010), that mentioned that a zeta potential higher than 30 mV or lesser than −30 mV is indicative of a stable system. In this context, colloidal suspension of Ag nanoparticles synthesized using *Ceriops tagal* leaves extract and *Malus domestica* fruit extract were highly stable with a zeta potential of −34.18 mV (Dhas *et al*., 2013). The values of zeta potential for the AgNPs obtained in the present study indicate a long term stability of the colloids, which could be attributed to the presence of bioactive components present in the aqueous extract that cover nanoparticles stabilizing them. On the other hand, in the present study the average size of the particles obtains from *P. glandulosa* was of 421 nm. These findings are in agreement with previous studies realized by Palanisamy *et al*. (2014), who reported that the particle size of the synthesized silver nanoparticles using *Emblica officinalis* leaf extract was in the range 139–595 nm with average size 367 nm. The mechanism behind the activity of AgNPs from *P. glandulosa* against *A. calcoaceticus* and *B. cereus* is not yet fully explored and there are some common mechanisms behind up to date. However, there are various theories suggested about the action of AgNPs on microbes to cause the antimicrobial effect. One possibility of growth-restriction may be a chance

of the generation of free radicals by AgNPs positioned at surface which may have been thrashed lipid membrane followed by destruction of microorganisms (Sharma *et al*., 2014 & Morones *et al*., 2005). Another fact is that the DNA has sulfur and phosphorus as its major components; the nanoparticles can act on these soft bases and destroy the DNA which would definitely lead to cell death (Morones *et al*., 2005). However, further studies are needed to confirm their potential of AgNPs from *P. glandulosa* in the biocontrol of the microorganisms evaluated.

5.6 Conclusions

The biosynthesis of silver nanoparticles using *Prosopis glandulosa* is a simple, environmentally friendly, low cost and non-toxic approach. The fabricated nanoparticles showed antimicrobial activity against *B. cereus* and *A. calcoaceticus* at different concentration. Our findings indicate that AgNPs from *P. glandulosa* may have potential benefits as biocontrol agents for human pathogens. However, further studies are needed to confirm their potential, determine their effect on human pathogens and identify the bioactive compounds in *P. glandulosa*.

5.7 References

Ahmed S, Saifullah M, Babu LS, et al. 2016. Green synthesis of silver nanoparticles using *Azadirachta indica* aqueous leaf extract. J Radiat Res Appl Sci. 9:1–7.

Alt V, Bechert T, Streinrucke P, et al. 2004. An in vitro assessment of the antibacterial properties and cytotoxicity of nanoparticulate silver bone cement. Biomaterials. 25:4383–4391.

Carevic FS. 2014. The role of ecophysiological studies in the genus *Prosopis*: implications for the conservation of drought-prone species. Idesia. 32:77–81.

Dhas SP, Mukerjhee A, Chandrasekaran N. 2013. Phytosynthesis of silver nanoparticles using *Ceriops tagal* and its antimicrobial potential against human pathogens. Int J Pharm Pharm Sci. 5:349–352.

Ibrahim HMM. 2015. Green synthesis and characterization of silver nanoparticles using banana peel extract and their antimicrobial activity against representative microorganisms. J Radiat Res Appl Sci. 8:265–275.

Jeong SH, Yeo SY, Yi SC, et al.2005. The effect of filler particle size on the antibacterial properties of compounded polymer/ silver fibers. J Mater Sci. 40:5407–5411.

Kumar V, Yadav SK. 2009. Plant-mediated synthesis of silver and gold nanoparticles and their applications. J Chem Technol Biotechnol. 84:151–157.

Morones JR, Elechiguerra JL, Camacho A, et al. 2005. The bactericidal effect of silver nanoparticles. Nanotechnology. 16:2346–2353.

Nanda A, Saravanan M. 2009. Biosynthesis of silver nanoparticles from *Staphylococcus aureus* and its antimicrobial activity against MRSA and MRSE. Nanomedicine. 5:452–456.

Palanisamy K, Kalaiselvi PA, Gabriel M, et al. 2014. *Emblica officinalis* leaf extract mediated green synthesis of antibacterial silver nanoparticles against human pathogens. World J Pharm Sci. 3:2019–2032.

Pérez-García EA, Meave JA, Cevallos-Ferriz SRS. 2012. Flora and vegetation of the seasonally dry tropics in Mexico: origin and biogeographical implications. Acta Bot Mex. 100:149–193.

Rai A, Singh A, Ahmad A, et al. 2006. Role of halide ions and temperature on the morphology of biologically synthesized gold nanotriangles. Langmuir. 22:736– 741.

Tripathy A, Raichur AM, Chandrasekaran N, et al. 2010. Process variables in biomimetic synthesis of silver nanoparticles by aqueous extract of *Azadirachta indica* (Neem) leaves. J Nanopart Res. 12:237–246.

Raja K, Saravanakumar A, Vijayakumar R. 2012. Efficient synthesis of silver nanoparticles from *Prosopis juliflora* leaf extract and its antimicrobial activity using sewage. Spectrochim Acta, Part A. 97:490–494.

Ramalingam V, Rajaram R, Premkumar C, *et al*. 2013. Biosynthesis of silver nanoparticles from deep sea bacterium *Pseudomonas aeruginosa* JQ989348 for antimicrobial, antibioflim and cytotoxic activity. J Basic Microbiol. 53:1–9.

Reddy NJ, Nagoor V, Rani D., *et al*. 2014. Evaluation of antioxidant, antibacterial and cytotoxic effects of green synthesized silver nanoparticals by piper longum fruit. Mater Sci Eng C Mater Biol Appl. 34:115–122.

Sadhasivam S, Shanmugam P, Yun K. 2010. Biosynthesis of silver nano-particles by *Streptomyces hygroscopicus* and antimicrobial activity against medically important pathogenic microorganisms. Colloids Surf B. 81:358–362.

Sanpui P, Chattopadhyay A, Ghosh S. 2011. Induction of apoptosis in cancer cells at low silver nanoparticle concentrations using chitosan nanocarrier. ACS Appl Mater Interfaces. 3:218–228.

Saxena A, Tripathi RM, Zafar F, et al. 2012. Green synthesis of silver nanoparticles using aqueous solution of *Ficus benghalensis* leaf extract and characterization of their antibacterial activity. Mater Lett. 6:791–794.

Shankar SS, Rai A, Ahmad A, *et al*. 2004. Rapid synthesis of Au, Ag, and bimetallic Au core-Ag shell nanoparticles using Neem (*Azadirachta indica*) leaf broth. J. Colloid Interface Sci. 275:496–502.

Sharma G, Jasuja ND, Rajgovind P. et al. 2014. Synthesis, characterization and antimicrobial activity of *Abelia grandiflora* assisted AgNPs. J Microb Biochem Technol. 6: 274–278.

Singh A, Jain D, Upadhyay MK, et al. 2010. Green synthesis of silver nanoparticles using *Argemone Mexicana* leaf esctract and evaluation of their antimicrobial activities. Dig J Nanomater Biostruct. 5:483–489.

Valli JS, Vaseeharan B. 2012. Biosynthesis of silver nanoparticles by *Cissus quadrangularis* extracts. Mater Lett. 82:171–173.

Visahl RP, Agrawal YK. 2011. Nanosuspesion: an approach to enhance solubility of drugs. J Adv Pharm Technol Res. 2:81–87.

Zhou C, Qi W, Lewis EN, et al. 2015. Concomitant Raman spectroscopy and dynamic light scattering for characterization of therapeutic proteins at high concentrations. Anal Biochem. 472:7–20.

CAPITULO VI. (CHAPTER VI.)

Inhibition of *Fusarium solani* in transgenic insect-resistant cotton plants treated with silver-nanoparticles from *Prosopis glandulosa* and *Pluchea sericea*

6.1 Abstract

The phyto-synthesis of nanoparticles is a green chemistry approach that combines nanotechnology and bioactive compounds of plants. The aim of this study was to evaluate the effect of silver nanoparticles (AgNPs) from *Prosopis glandulosa* and *Pluchea sericea* on the control of *Fusarium solani* previous inoculated in the rhizosphere of transgenic insect-resistant cotton plants. The results showed that the weekly application of AgNPs from *P. glandulosa* and *P. sericea* caused a diminution of fungal propagules in the soil after 30 days of treatment. The AgNPs from *P. glandulosa* was more efficient in the reduction of infection points in the roots of the plants infected with *F. solani* compared with AgNPs from *P. sericea*. Additionally, the application of AgNPs from both plants showed a significant increase of optimum quantum yield (Fv/Fm), stomata conductance (g_s) and number of lateral roots in transgenic insect-resistant cotton plants after 30 days of exposure when compared to control. Based on our results, AgNPs from *P. glandulosa* and *P. sericea* could inhibit growth of *Fusarium solani*. However, more extensive and elaborate studies are needed to explain the different mechanism that participle in the inhibition of growth of fungus using nanoparticles from these plants.

Key words: Biocontrol, Native plants, Phytonanoparticles, Antifungal activity, Green synthesis

6.2 Introduction

Cotton (*Gossypium hirsutum* L.) is the most economically important crop in the global textile industry and constitutes more than half of all textile fiber consumption worldwide

(Karademir *et al*., 2011). A great achievement in cotton breeding was the development of transgenic pure-line varieties or hybrids containing the crystal (cry) genes of *Bacillus thuringiensis* (Bt) encoding insecticidal proteins (δ-endotoxin) that provide protection from lepidopteran pests (Terán-Vargas *et al*., 2005). The adoption of *Bt* transgenic cotton varieties in countries as Argentina, Brazil, Colombia and Mexico helped to reduce the cost of insecticide applications and increased yield of this crop (Terán-Vargas *et al*., 2005). For example, Mexico has adopted this new technology, and nine years after commercial release, *Bt* transgenic cotton reached 133,000 hectares (ha) planted in Mexico in 2015/16 according to the Agri-food and Fisheries Information Service (SIAP) of the Secretariat of Agriculture, Livestock, Rural Development, Fishing and Food (https://www.gob.mx/siap/acciones-y-programas/produccion-agricola-33119). However, the presence of fungal phytopathogens during the development of plants is very important because these organisms can lead to wilt or root rot disease that cause substantial losses to farmers (Abd-Elsalam, 2003). *Fusarium* wilt is an important disease presents in cotton plants in diverse countries, this diseases is caused by *Fusarium solani* (Gonzalez-Soto *et al*., 2015). These pathogens cause root rot, damping-off symptoms, reduction in size of leaves and bolls, which affect the yield and fiber quality (Gonzalez-Soto *et al*., 2015).

Diverse studies reported the use of different control measures for *Fusarium* species associated with plants, these measures include the application of agronomic control techniques, genetic resistance and use of chemical or biological antagonists (Aquino-Martinez *et al*., 2008; Baffoni *et al*., 2015). Currently environmental hazards caused by use of fungicides and the unpredictable results of biological control have been widely debated (Adesina *et al*., 2007). Therefore, researchers are searching for alternative measures that together with biological control and optimal use of fungicides provide major control of fungal diseases in plants (Baffoni *et al*., 2015). In this sense the use of antimicrobial activity of the nano-particles could be presented as a potential alternative for reducing the use of chemicals in agriculture. For example, silver nanoparticles (AgNPs) display diverse modes of inhibitory action against various pathogens such as fungal and bacterial species (Yamanaka *et al*., 2005; Lamsal *et al*., 2011). In this sense, the AgNPs may be used with relative safety for control of fungal diseases in plants

compared to synthetic fungicides. As the applications of AgNPs against *Fusarium* species associated with transgenic insect-resistant cotton has not been reported. Thus, the main objective of the present study was to evaluate the inhibition of fungal growth of *F. solani* in transgenic insect-resistant cotton treated with silver phyto-nanoparticles from *P. juliflora* and *P. sericea*.

6.3 Materials and methods

6.3.1 Germination of transgenic insect-resistant cotton

Bollgard® cotton transgenic seeds were provided by producers of the cotton product system of Baja California, Mexico. The seeds were superficially disinfected by immersion in a 0.5% sodium hypochlorite solution for 3 min followed by washes with sterile deionized water. After disinfection, the seeds were placed in single pots (0.3 L) containing a commercial potting soil mix combined with quartz sand and peat moss sterilized by autoclaving at 121°C for 2 h. The seeds were subjected to a photoperiod of 12 h light: dark photoperiods with 60 % of relative air humidity (Gonzalez-Mendoza *et al*., 2013).

6.3.2 Synthesis of silver nanoparticles

The silver nanoparticles from leaf extract of *P. glandulosa and P. sericea* used in the present study were previous obtained by Abdelmoteleb *et al*. (2016, 2017). The bioreduction of Ag^{+} ions was observed by color change from yellow to brown, indicating the formation of AgNPs at room temperature. The silver nanoparticles formed in the reaction solution showed a particle sizes average from 421 (*P. glandulosa*) to 59.20 nm (*P. sericea*) according to Abdelmoteleb *et al*. (2016, 2017). The AgNPs of *P. glandulosa* and *P. sericea* used in this experiment were previously diluted by deionized water at 100 ppm.

6.3.3 *Fusarium solani* inoculant formulation

Fusarium solani T-ICA04 previously had been isolated from two different sites of transgenic insect-resistant cotton growing in fields of Baja California (32° 24´ 12.26´´ **N**, 115° 9´ 13.60´´ **W** and 32° 28´ 5.63´´ **N**, 115° 12´ 11.94´´**W**). This strain was characterized molecularly and deposited in the Genbank with the following accession number: KJ620372. The formulation of inoculant was produced in potato-dextrose (PDB) broth for 5 days at 28° ± 2°C. The conidial suspension was then quantified by the aid of a automated cell counter (TC20^{TM} Bio-Rad) and diluted with water. Suspensions obtained were mixed uniformly with soil mix combined with quartz sand and peat moss. The soil was allowed to dry for about 3 weeks at room temperature (about 25- 28 °C). The amount of *Fusarium* propagules was evaluated by the dilution plate method on PDA agar (Gonzalez-Soto *et al*., 2015).

6.3.4 Inoculation with *Fusarium solani* and exposure to silver nanoparticles

Once the seedlings developed a few roots, they were transplanted to single pots (0.2 L) containing a commercial potting soil mix combined with quartz sand and infested soil with *F. solani* (prepared as described above) was added in the proportion of 3:1 v/v, to the uninfected soil to obtain a final concentration of $1x10^5$ count g^{-1} soil of *Fusarium solani* propagules. After the inoculation, the seedlings were divided into three groups: 1) inoculated (control); 2) inoculated + AgNPs from *P. glandulosa* and 3) inoculated + AgNPs from *P. sericea*. The groups 2 and 3 with *F. solani* inoculant were weekly irrigated with AgNPs (100 ppm) from *P. glandulosa* and *P. sericea*, respectively. The control plants (group 1) were irrigated only with deionized water. The amount of *Fusarium* propagules in each treatment was evaluated at 30 days after application of AgNPs (Gonzalez-Soto *et al*., 2015). All groups was replicated 10 times and grown in a growth chamber with a photoperiod of 12 h light: dark photoperiods with 60-70 % relative humidity.

6.3.5 Evaluation of physiological parameters

The stomata conductance (g_s) of young fully expanded leaves were measured at 30 days after exposure to treatments with AgNPs from *P. glandulosa* and *P. sericea*, using a potable leaf porometer (SC-1, Decagon, USA) according to Gonzalez-Mendoza *et al*. (2013). On the other hand, the chlorophyll fluorescence was measured using a potable Chlorophyll Fluorometers (OS30p, Opti-Sciences). It was represented optimum quantum yield (Fv/Fm) evaluated at 27ºC and time range was 10µs-3 sec. For each studied parameter (*gs* and Fv/Fm), 10 individual leaves young, completely developed, healthy were measured within each treatment.

6.3.6 Evaluation of morphological parameters

After thirty days of inoculation with *F. solani*, lateral roots (LR) of each seedling treatment were evaluated. The lateral root was classified according to the number of roots of 2nd orders using a stereomicroscope. This variable is an essential and continuous process in the formation of root systems and for the importance of the evaluation in the present study.

6.3.7 Number of lesions produced by the pathogen

The brown lesions characteristic of the infection of *F. solani*, observed on the system Radical (Espinosa-Victoria *et al*., 2004), was quantified at 30 days after inoculation with the pathogen, with the aid of a stereoscopic microscope in 10 seedlings of each treatment.

6.3.8 Statistical analysis

The experiment was set up in a completely randomized design with 10 replications. The significant differences between the AgNPs treated and control samples were analyzed using the Kruskal–Wallis test (Statistical Package version 5.5, Statsoft, USA).

6.4 RESULTS AND DISCUSSION

Data showed that addition of AgNPs from *P. glandulosa* and *P. sericea* had different effect on the amount of *Fusarium* propagules in the soil of the different treatments (Fig. 22 A). For example, the highest decrease of fungal propagules was observed after the addition of AgNPs from *P. glandulosa* to infected soil (Fig. 22 B).

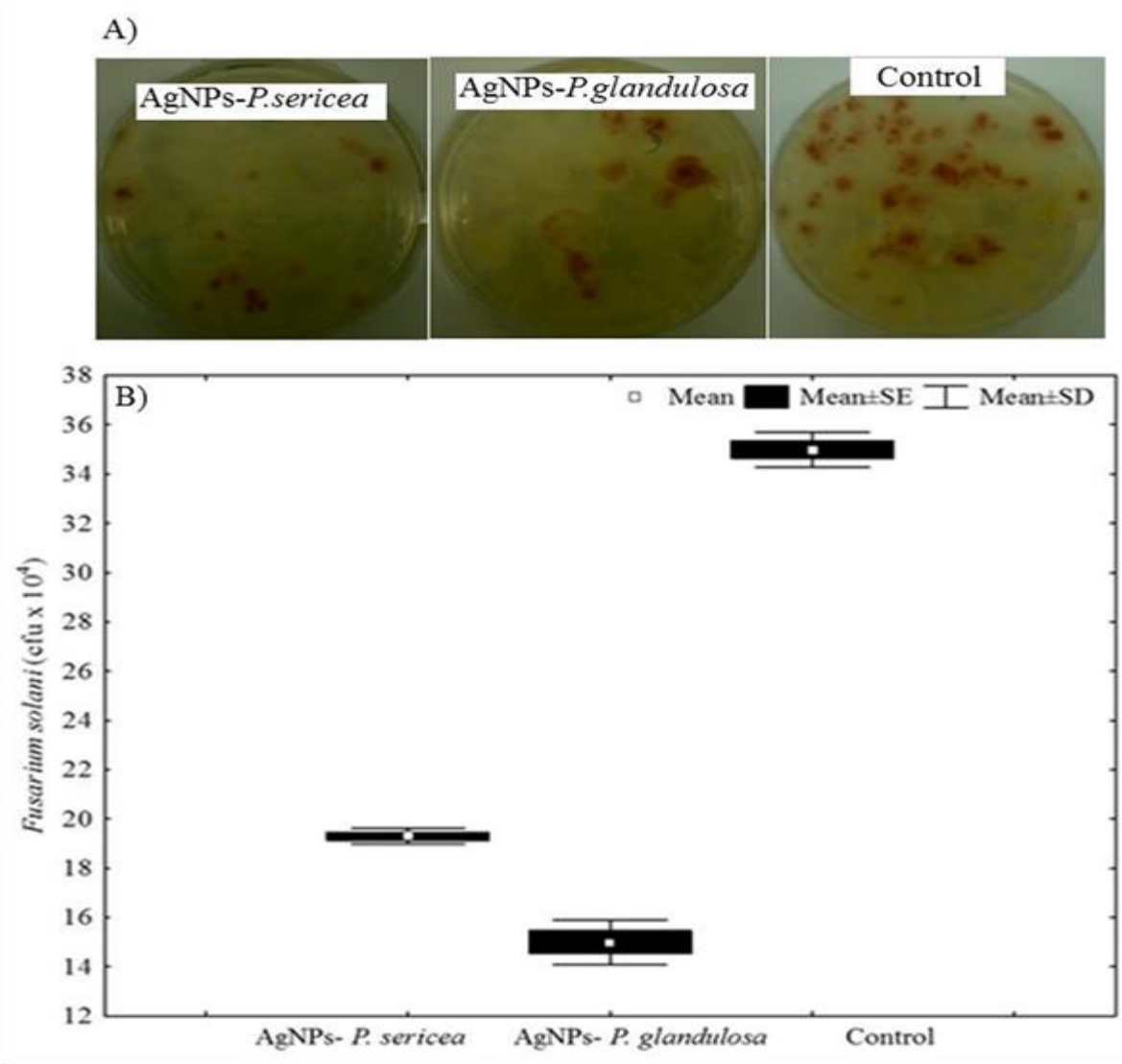

Fig. (22): A) Density of fungal propagules after 30 days of exposition to AgNPs from *P. sericea* and *P. glandulosa*; B) Effects of AgNPs-nanoparticles from *P. sericea* and *P. glandulosa* on population of *Fusarium solani* in rhizosphere of cotton plants after 30 days of treatment. (Values are expressed such mean ± S.D., n=10).

In this sense, the addition of AgNPs from *P. sericea* stimulated decrease of *Fusarium* population but in minor proportion. In contrast, highest number of *Fusarium* colonies was obtained from the control samples where AgNPs from the plants were not added (Fig. 22 B).

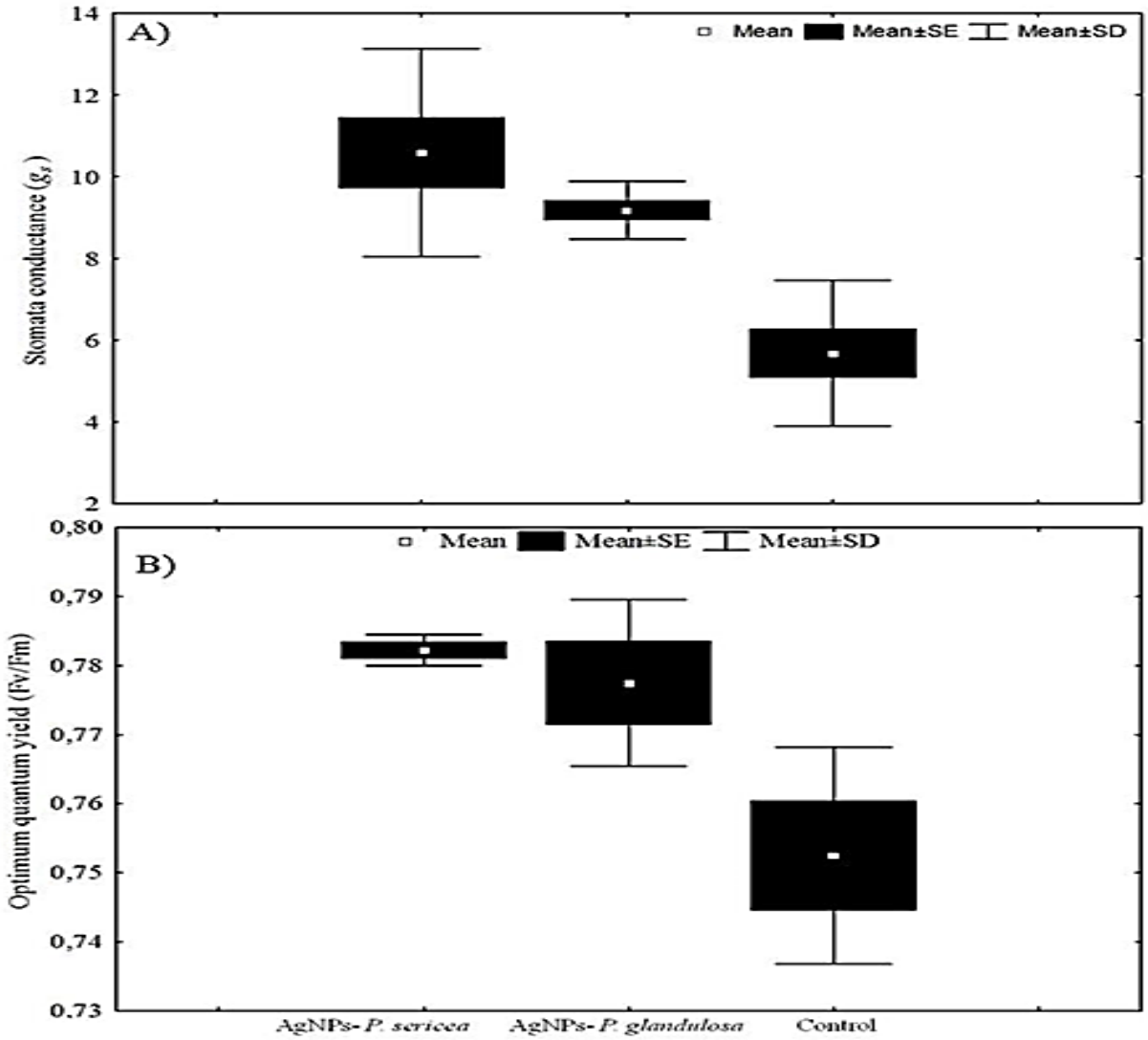

Fig (23): Effects of AgNPs from *P. sericea* and *P. glandulosa* on stomata conductance (A) and optimum quantum yield (B) in leaves of cotton plants after 30 days of treatment. (Values are expressed such mean ± S.D., *n*=10).

On the other hand, the transgenic insect-resistant cotton plants inoculated with *F. solani*, and treated with AgNPs from *P. glandulosa* and *P. sericea*, exhibited significantly changes in the optimum quantum yield (Fv/Fm) values with respect to control (Fig. 23 B). The effect of AgNPs from both plants showed a significantly increasing of stomata conductance (g_s) after 30 days of exposure (Fig 23 A). In contrast, the transgenic insect-resistant cotton plants inoculated only with *F. solani* exhibited significantly reduction in Fv/Fm and *gs* values compared with the plants treated with AgNPs (Fig 23).

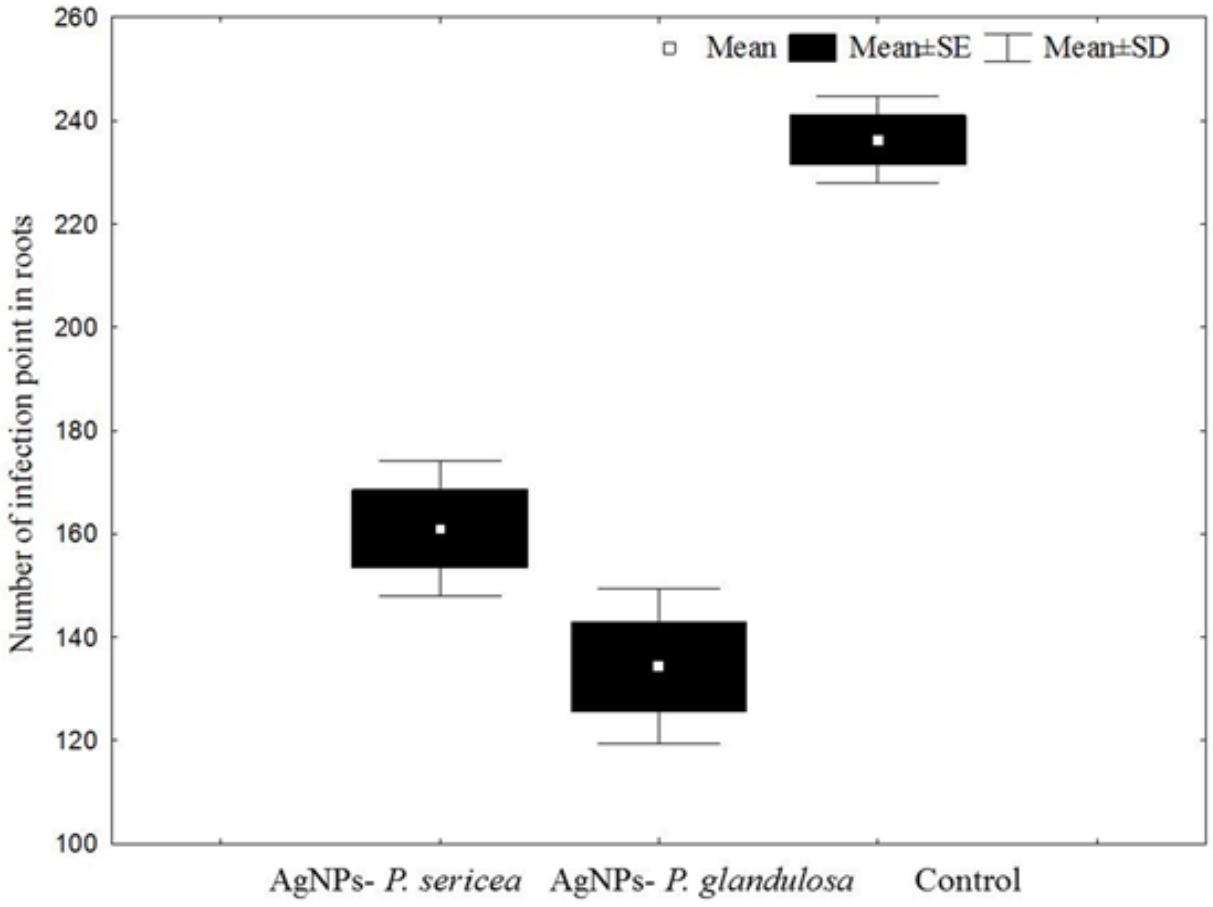

Fig (24): Modification in the number of infection points in roots of cotton plants after 30 days of treatment with AgNPs from *P. sericea* and *P. glandulosa* (Values are expressed such mean ± S.D., *n*=10).

In the present study, both AgNPs from *P. glandulosa* and *P. sericea* caused decreased infection point in roots when compared with control plants ($P \leq 0.05$) after 30 days of exposure (Fig. 24). AgNPs from *P. glandulosa* was more efficient in the reduction of infection points in the plants infected with *F.solani* compared with AgNPs from *P. sericea*. On the other hand, the effect of AgNPs from both plants showed a significant increase of number of lateral roots in transgenic insect-resistant cotton plants after 30 days of exposure when compared to control ($P \leq 0.05$) (Fig. 25 A and B).

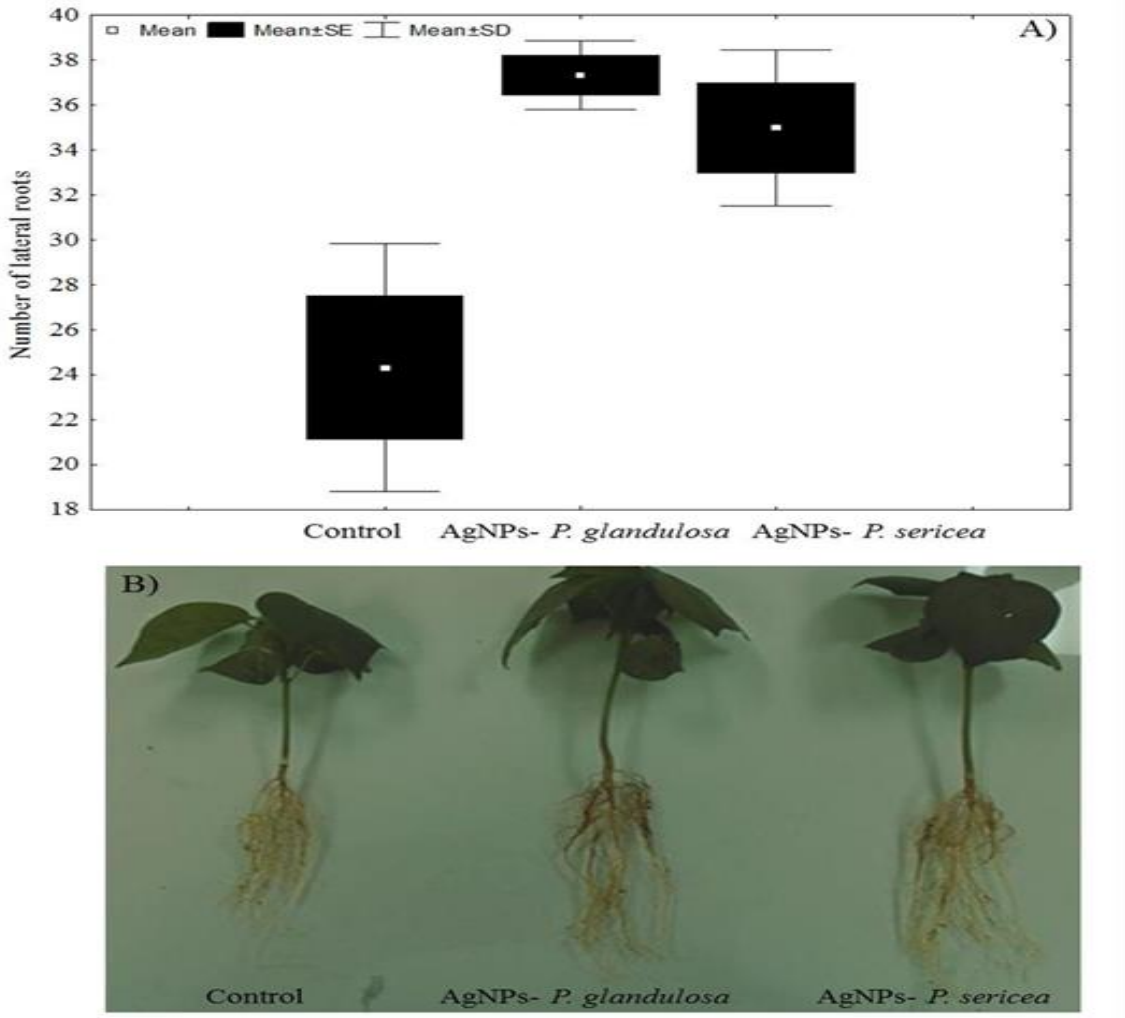

Fig (25): A) Effects of AgNPs from *P. sericea* and *P. glandulosa* on the number of lateral roots of cotton plants after 30 days of treatment; B) lateral roots of cotton plants after 30 days of exposition of AgNPs from *P. sericea* and *P. glandulosa*. (Values are expressed such mean ± S.D., *n*=10).

Previous studies indicated that the antifungal activity *in vitro* of AgNPs influence colony formation of spores and disease progress of different plant pathogenic fungi (Kim *et al.,* 2012). The results clearly demonstrated that the silver nanoparticles obtained from these native-plants have a potential to inhibit *F. solani.* However, the mechanism behind this activity is not yet fully explored. In this sense, there are various theories suggested about the action of AgNPs on fungal phytopathogens. For example, certain authors reported that the AgNPs produce free radicals which can cause damage to protein and lipids membrane followed by destruction of microorganisms (Jung *et al*., 2010; Aguilar-Méndez *et al*., 2011; Kim *et al*., 2012). In this respect, further studies are required to confirm their potential of AgNPs from *P. glandulosa* and *P. sericea* for the control of the *Fusarium solani* principally under field conditions. On the other hand, silver nanoparticles are known to produce positive and negative effects on growth and physiological parameters in plants (Stampoulis *et al*., 2009; Zuverza-Mena *et al.,* 2016; Jasim *et al*., 2017). Similarly, Raliya *et al*. (2015) found that the application of nanoparticles from different metals on tomato seedlings after one week caused an abnormal proliferation of root hairs compared to the control group. The effect on lateral roots observed in the present study could be explained by the hormesis effects, which is an adaptive response at the concentrations of nanoparticles used and by inhibition of development of pathogenic fungus in the roots by the nanoparticles employed (Nascarella and Calabrese, 2012; Xia *et al*., 2016). On the other hand, previous studies have shown that infection of plants by *Fusarium* sp., result in a diminution of optimum quantum yield (Fv/Fm) and stomata conductance (gs) as results of reduced water and nutrients uptake by roots (Ye *et al*., 2004). In this sense, our study showed that the optimum quantum yield (Fv/Fm) and stomata conductance (gs) was significantly increased in cotton plants treated with nanoparticles-Ag from *P. glandulosa* and *P. sericea*, suggesting that the use of nanoparticles prevented the *F. solani* invasion in the roots favoring the water transport in the cotton plants. On the other hand, the increase of optimum quantum yield (Fv/Fm) and stomata conductance (gs) in cotton plants with respect to control, were in contrast with the report of Da Costa and Sharma (2016) who reported a decrease of Fv/Fm and *gs* as result of nanoparticles exposure in *Oryza*

sativa. However, Li *et al.* (2013) observed that use of nanoparticles on watermelon, increased the seedling germination and enhanced physiological parameters. Considering the earlier works, the effect of nanoparticles can vary for different morphological and physiological attributes on plants.

6.5 CONCLUSION

In conclusion, the uses of Ag-nanoparticles from *P. sericea* and *P. glandulosa* could inhibit growth of *F. solani* and showed considerable antifungal activity in cotton plants infected with *F. solani*. Therefore, the application of nanoparticles as nano-fungicides is relatively a new approach in agricultural sectors. Therefore, more elaborate studies are needed to explain different mechanism of growth inhibition of fungus using nanoparticles from the plants and evaluate economic feasibility of application in field.

6.6 REFERENCES

Abdelmoteleb, A., B. Valdez-Salas, C. Ceceña-Duran, O. Tzintzun-Camacho, F. Gutiérrez-Miceli, O. Grimaldo-Juarez and D. González-Mendoza. 2017. Silver nanoparticles from *Prosopis glandulosa* and their potential application as biocontrol of *Acinetobacter calcoaceticus* and *Bacillus cereus*. Chem. Spec. Bioavailab. 29:1-5.

Abdelmoteleb, A., B. Valdez-Salas, M. Carrillo-Beltran, D.Duran-Hernandez and D. Gonzalez-Mendoza. 2016. Green Synthesis of Silver Nanoparticles Using *Pluchea sericea* a Native Plants from Baja California, Mexico and their Potential Application as Antimicrobials. Iran J. Sci. Technol. Trans. A Sci. (*in press*, doi:10.1007/s40995-016-0019-6)

Abd-Elsalam, K.A. 2003. Non-gel based techniques for plant pathogen genotyping. Acta Microbiol. Pol ., 52: 329-341

Adesina, M.F., A. Lembke, R. Costa, A. Speksnijder and Smalla, K. 2007. Screening of bacterial isolates from various European soils for *in vitro* antagonistic activity towards *Rhizoctonia solani* and *Fusarium oxysporum*: site-dependent composition and diversity revealed. Soil Biol. Biochem., 39: 2818–2828.

Aguilar-Méndez, M.A., E.S. Martín-Martinez, L. Ortega-Arroyo, G. Cobián-Portillo and Sánchez-Espíndola, E. 2011. Synthesis and characterization of silver nanoparticles: effect on phytopathogen *Colletotrichum gloesporioides*. J. Nanopart. Res., 13:2525–2532

Aquino-Martinez, J.G., L.M. Vazquez-Garcia, & Reyes-Reyes, B.G. 2008. Biocontrol *in vitro* e *in vivo* de *Fusarium oxysporum* Schlecht.f. sp. Dianthi (Prill. Y Delacr.) snyder y Hans con hongos antagonistas nativos de la zona florícola de villa Guerrero. Rev. Mex. Fitopatol., 26: 127-13

Baffoni, L., F. Gaggia, N. Dalanaj, A. Prodi, P. Nipoti, A. Pisi, B. Biavati, D. and Gioia, Di. 2015. Microbial inoculants for the biocontrol of *Fusarium* spp. in durum wheat. BMC Microbiology, 15: 242.

Da Costa, M.V.J. and Sharma, P.K. 2016. Effect of copper oxide nanoparticles on growth, morphology, photosynthesis, and antioxidant response in Oryza sativa. Photosynthetica 54: 110-119.

Espinosa-Victoria, D., D. González-Mendoza, J. Placencia-de la Parra, and García-Espinosa, R. 2014. Reducción de la incidencia de *Phytophthora capsici* Leo en el sistema radical de plántulas de chile pre-micorrizadas con *Glumus intraradices*. TERRA Latinoamericana, 22: 317-326.

González Soto, T., D. González-Mendoza, R. Troncoso-Rojas, A. Morales-Trejo, C. Ceceña-Duran and Grimaldo-Juárez, O. 2015. Molecular identification of *Fusarium* species isolated from transgenic insect-resistant cotton plants in Mexicali valley, Baja California. Genet. Mol. Res., 14: 11739 – 11744.

Gonzalez-Mendoza, D., F. Escoboza-Garcia, J.M. Santamaria and Zapata-Perez, O. 2013. Copper stress on photosynthesis of black mangle (*Avicennia germinans*). An. Acad. Bras. Cienc., 85:665–70.

Jasim. B., R. Thomas, J. Mathew and Radhakrishnan, E.K. 2017. Plant growth and diosgenin enhancement effect of silver nanoparticles in Fenugreek (*Trigonella foenum-graecum* L.) Saudi Pharm. J., 25: 443–447

Jung, J.H., S.W. Kim,J.S. Min, Y.J. Kim, K. Lamsal, K.S. Kim and Lee, Y.S. 2010. The effect of nano-silver liquid against the white rot of the green onion caused by *Sclerotium cepivorum*. Mycobiology, 38: 39–45.

Karademir, C., Karademir, E. and Gencer, O. 2011. Yield and fiber quality of F 1 and F 2 generations of cotton (*Gossypium hirsutum* L.) under drought stress conditions. Bulg. J. Agric. Sci., 17:795–805.

Kim, S.W., J.H. Jung, K. Lamsal, Y.S. Kim, Y. S. Min and Lee, S. 2012. Antifungal effects of silver nanoparticles (agnps) against various plant pathogenic fungi. Mycobiology, 40: 53–58.

Lamsal, K., S. W. Kim, J.H. Jung, Y.S. Kim, K.S. Kim and Lee, Y.S. 2011. Application of silver nanoparticles for the Control of *Colletotrichum* Species *in vitro* and pepper anthracnose disease in field. Mycobiology, 39: 194–199.

Li, J., P.R. Chang, J. Huang, Y. Wang & Yuan, H. 2013. Physiological effects of magnetic iron oxide nanoparticles towards watermelon. J. Nanosci. Nanotechnol., 13: 5561-5567

Nascarella, M.A. and Calabrese E.J. 2012. A Method to Evaluate Hormesis in Nanoparticle Dose-Responses. Dose-Response, 10: 344–354.

Raliya, R., R. Nair, S. Chavalmane, W.N. Wang, and Biswas P. 2015.Mechanistic evaluation of translocation and physiological impact of titanium dioxide and zinc oxide nanoparticles on the tomato (*Solanum lycopersicum* L.) plant. Metallomics., 7:1584–1594.

Showalter, A.M., S. Heuberger, B.E. Tabashnik and Carrière, Y. 2009. A primer for using transgenic insecticidal cotton in developing countries. Int. J. Trop. Insect Sci., 9:22.

Stampoulis, D., S.K. Sinha and White, J.C. 2009. Assay-dependent phytotoxicity of nanoparticles to plants. Environ. Sci. Technol., 43: 9473–9479.

Terán-Vargas, A. P., J. C. Rodríguez, C. A. Blanco, J. L. Martínez-Carrillo, J. Cibrián-Tovar, H. Sánchez-Arroyo, L. A. Rodríguez-Del-Bosque, and Stanley D. 2005. Bollgard cotton and resistance of tobacco budworm (Lepidoptera: *Noctuidae*) to conventional insecticides in the Southern Tamaulipas, Mexico. J. Econ. Entomol. 98: 2203-2209.

Xia, Z.K., Q.H Ma, S.Y Li, D.Q. Zhang, L. Cong, Y.L. Tian and Yang, R.Y. 2016.The antifungal effect of silver nanoparticles on *Trichosporon asahii* . J. Microbiol. Immunol. Infect.., 49:182-188

Yamanaka, M., K. Hara and Kudo, J. 2005. Bactericidal actions of a silver ion solution on *Escherichia coli*, studied by energy-filtering transmission electron microscopy and proteomic analysis. Appl. Environ. Microbiol., 71:7589–7593

Ye, S.F., J.Q. Yu, Y.H. Peng, J.H. Zheng, and Zou. L.Y. 2004. Incidence of *Fusarium* wilt in *Cucumis sativus* L. is promoted by cinnamic acid, an autotoxin in root exudates. Plant Soil., 263:143–150.

Zuverza-Mena, N., R. Armendariz, J.R. Peralta-Videa and Gardea-Torresdey, J.L. 2016. Effects of silver nanoparticles on radish sprouts: root growth reduction and modifications in the nutritional value. Front. Plant Sci., 7:90.

ANNEXES

Annex 1. Pikovskaya´s Agar

Pikovskaya's Agar medium (Pikovskaya 1948) containing (g/ L):

Tricalcium phosphate (TCP) as sole phosphorus source 5.0;

Glucose, 10.0

$MgSO_4.7H_2O$, 0.1

KCl, 0.2;

$(NH_4)_2SO_4$, 0.5

Yeast extract, 0.5

NaCl, 0.2

$MnSO_4.4H_2O$, 0.2

$FeSO_4$, 0.05

Agar, 20

Distilled water, 1000 ml

The pH was adjusted to 7.0 ± 0.2 and 0.1g/L of Bromocresol Purple was added as a pH indicator dye.

Annex 2. DNA Extraction from Bacteria

One ml of overnight grown culture was centrifuged at 10,000 rpm for 10 min. The pellet was re-suspended in 0.3 ml Extraction buffer [3% SDS (w/v) containing 0.5 mM EDTA, 1.0 M NaCl, and 0.3 mM hydroxymethyl-hydrochloride (Tris-HCl, pH 8.0)] with vortex. Then 0.3 ml of phenol/ chloroform mixture (1:1, v/v) were added, vortex gently and incubated for 5 min at 65^{o}C. The mixture was allowed to cool down to room temperature and centrifuged at 12,000 rpm, for 10 min at 4°C. The supernatant was transferred to a new microtube, 0.6 volume of cold absolute isopropanol was added and the contents mixed thoroughly, then incubated at -20°C for 30 min. Precipitated DNA pellet was collected by centrifugation at 13,000 rpm for 10 min, at 4°C. The supernatant was discarded and the pellet air dried followed by suspension in 30 µL DEPC-treated MiniQuantum (deionized) water, and stored at -20°C until further use.

Annex 3. Nucleotide sequences of the *Bacillus subtilis* strain ALICA isolated from *Prosopis juliflora* in the Valley of Mexicali, B.C.

Bacillus subtilis ALICA

GenBank: KX137176.1

gnannatant gnngtcgagc ggacagatgg gagcttgctc nctgatgtta gcggcggacg ggtgagtaac acgtgggtaa cctgcctgta agactgggat aactccggga aaccggggct aataccggat gcttgtttga accgcatggt tcaaacataa aaggtggctt cggctaccac ttacagatgg acccgcggcg cattancaaa atggtgaggt aacggntcac caaggcaacg atgcgtagcc gacctgancg ggntccaact cnnantggga ctgagacacg gcccanannn nnacgggag

Annex 4. Sodium phosphate buffer 50 mM , pH 7

1- Solution **A**: 0.1 M of NaH_2PO_4 (MW= 120), dissolve 0.6 g in distilled water and then raised the volume to 50 ml with distilled water.
2- Solution **B**: 0.1 M of Na_2HPO_4 (MW= 142), dissolve 0.71 g in distilled water and then raised the volume to 50 ml with distilled water.
3- Add 19.5 ml of solution **A** to 30.5 ml of solution **B**, and then add 50 ml distilled water.
4- Conserve the buffer at 4°C.

Annex 5. 4-methylumbelliferone (4-MU) standard curve

4-MU standard curve was prepared in the dark condition

1- Preparation of sodium carbonate solution (0.2 M), dissolve 21.1989 g of Na_2CO_3, (MW=105.99) in distilled water and then raised the volume to 1000 ml with distilled water
2- Preparation of 4-MU stock solution 1 mM (**A**): 0.02022 g of 4-MU (MW= 198.2, 98%) and raised the volume to 100 ml with distilled water.
3- 4-MU stock solution 10000 nM (**B**): 1 ml of stock solution A and raised the volume to 100 ml with sodium carbonate solution (0.2 M).
4- Using the stock solution B, prepare 100 ml each of the following 4-MU standards using Na_2CO_3 solution (0.2 M) as a diluent. Each tube should be labeled with name and concentration (nM).

Desired Concentration	Volume of stock solution (**B**) (ml)	Volume of Na_2CO_3 solution (0.2 M) (ml	Total Volume (ml)
500 nM	5	95	100
400 nM	4	96	100
300 nM	3	97	100
200 nM	2	98	100
100 nM **Stock solution C**	1	99	100
50 nM	50 of sol. **C**	50	100
10 nM	1 of sol. **C**	90	100

5- Read the fluorescence of solutions 500, 400, 300, 200, 100, 50 and 10 nM (50 µl) using a TBS-380 Mini-Fluorometer at 325 nm excitation and 446 nm emission wavelengths.

Observations: it is necessary to calibrate with sodium carbonate solution (0.2 M) as blank and after that calibration with 4-MU 500 nm. Prepare the solutions very quickly (no more than I hr.), to prevent them from degrading. Work in full darkness.

Tube No.	Concentrations	Spectrofluorometrically reads
1	10	9.353
2	50	47.52
3	100	96.52
4	200	203.9
5	300	291.2
6	400	400.6
7	500	497.4

Plot the standard curve of the absorbance (y- axis) against the concentration (x-axis).

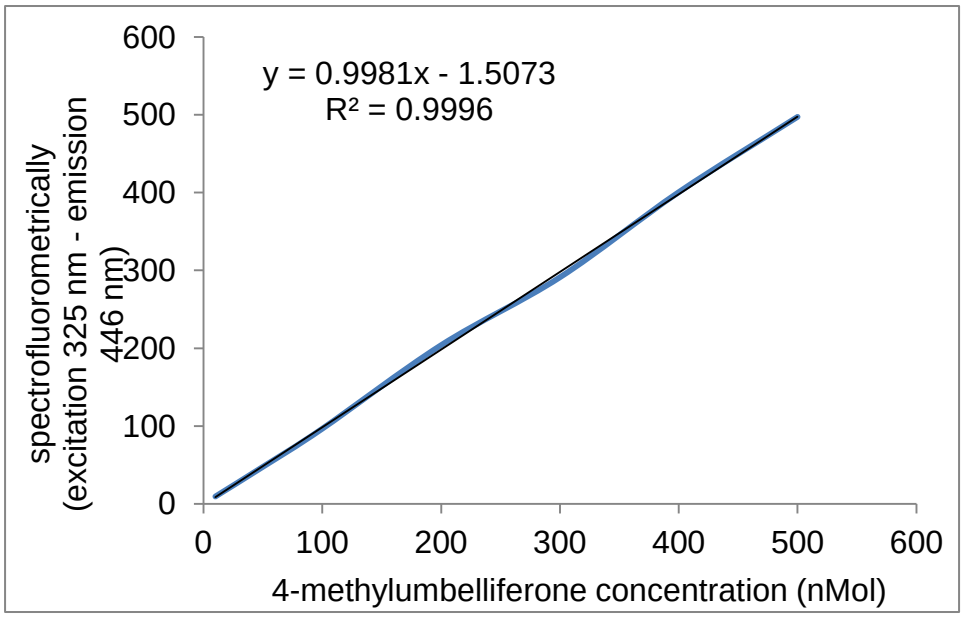

Annex 6. Acetate buffer 100 mM , pH 5.5

1- Solution **A**: 0.2 M Acetic acid glacial (MW= 60.05), dissolve 0.5775 g in distilled water, and then raised the volume to 50 ml with distilled water.
2- Solution **B**: 0.2 M sodium acetate (MW= 82.03), g in distilled water and then raised the volume to 50 ml with distilled water.
3- Mix 4.8 ml of solution **A** + 45.2 of solution **B** + 50 ml of distilled water.
4- Add 1 ml 2-mercaptoethanol.

Annex 7. Glucose standard curve

Glucose standard curve was prepared in the dark condition

1- Prepare stock solution of glucose 1 mg/ ml (1000 µg/ ml): dissolve 0.1 g glucose in deionized water (DW) and then raised the volume to 100 ml with DW.

2- Using the stock glucose standard solution, prepare 10 ml each of the following glucose standards using DW H_2O as a diluent. Each tube should be labeled with name and concentration (µg/ml glucose).

Desired Concentration	Volume Stock (ml)	Volume DW H_2O (ml)	Total Volume (ml)
500 (µg/ml)	5	5	10
450 (µg/ml)	4.5	5.5	10
400 (µg/ml)	4	6	10
350 (µg/ml)	3.5	6.5	10
300 (µg/ml)	3	7	10
250 (µg/ml)	2.5	7.5	10
200 (µg/ml)	2	8	10
150 (µg/ml)	1.5	8.5	10
100 (µg/ml)	1	9	10
0 (µg/ml) Blank	0	10	10

3- Mix 1 ml of each concentration with 1 ml 3,5-dinitrosalicylic acid (DNS) 1 % (DNS 1g, 25 ml NaOH 4%, 20 g sodium potassium tartrate, and then raised the volume to 100 ml with distilled water). Shake well and then place them in a boiling water bath for 10 minutes.

4- Cool the tubes thoroughly, Read the extinction (Optical density) of the colored solutions at 540 nm using the solution (0 µg/ml glucose) as a blank (control).

Tube No.	Concentration (µg/ml)	Absorbance (At 540 nm)
1	100 (µg/ml)	0.1
2	150 (µg/ml)	0.279
3	200 (µg/ml)	0.483
4	250 (µg/ml)	0.653
5	300 (µg/ml)	0.805
6	350 (µg/ml)	0.989
7	400 (µg/ml)	1.158
8	450 (µg/ml)	1.325
9	500 (µg/ml)	1.494

5- Plot the standard curve of the absorbance (y- axis) against the concentration (x-axis).

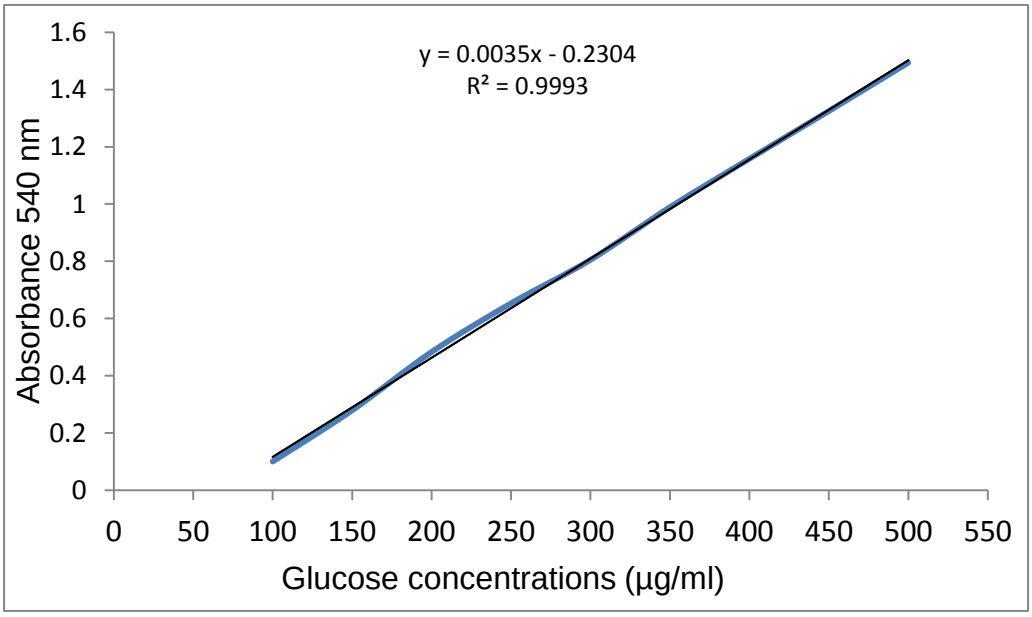

6- Use this plot to estimate the concentration of your unknown glucose sample. Express your results in µg/ml.

Annex 8. Tyrosine standard curve

Prepared in full darkness

1- Stock solution of tyrosine (1 mg/ ml): dissolve 0.01 g of tyrosine in a little of alkaline solution (NaOH, pH=9), and then raised the volume to 10 ml with distilled water.
2- From the stock solution, prepare the dilution series using distilled H_2O as a diluent. Each tube should be labeled with name and concentration (µg/ml tyrosine).

Desired concentration	Stock solution volume (µl)	Distilled water volume (µl)	Total volume (µl)
50 (µg/ml)	50	950	1000
100 (µg/ml)	100	900	1000
150 (µg/ml)	150	850	1000
200 (µg/ml)	200	800	1000
250 (µg/ml)	250	750	1000
300 (µg/ml)	300	700	1000
350 (µg/ml)	350	650	1000
400 (µg/ml)	400	600	1000
450 (µg/ml)	450	550	1000
500 (µg/ml)	500	500	1000

3- Mix 0.5 ml , 0.5ml Distilled water and 1 ml 0.4 M Trichloroacetic acid
4- 0.5 ml previous mix (previous step), 2.5 ml of 0.4 M Na_2CO_3 (4.2396 g of Na_2CO_3 in distilled water to 100 ml) and 0.75 ml of Folin–Ciocalteu's phenol reagent: water (1:3 v/v).
5- Read the absorbance of dilution series at 660 nm

Tube No.	Concentration	$A_{660\ nm}$
1	50 (µg/ml)	0.114
2	100 (µg/ml)	0.227
3	150 (µg/ml)	0.345
4	200 (µg/ml)	0.46
5	250 (µg/ml)	0.591
6	300 (µg/ml)	0.717
7	350 (µg/ml)	0.844
8	400 (µg/ml)	0.927
9	450 (µg/ml)	1.034
10	500 (µg/ml)	1.17

Plot the standard curve of the absorbance (y- axis) against the concentration (x-axis).

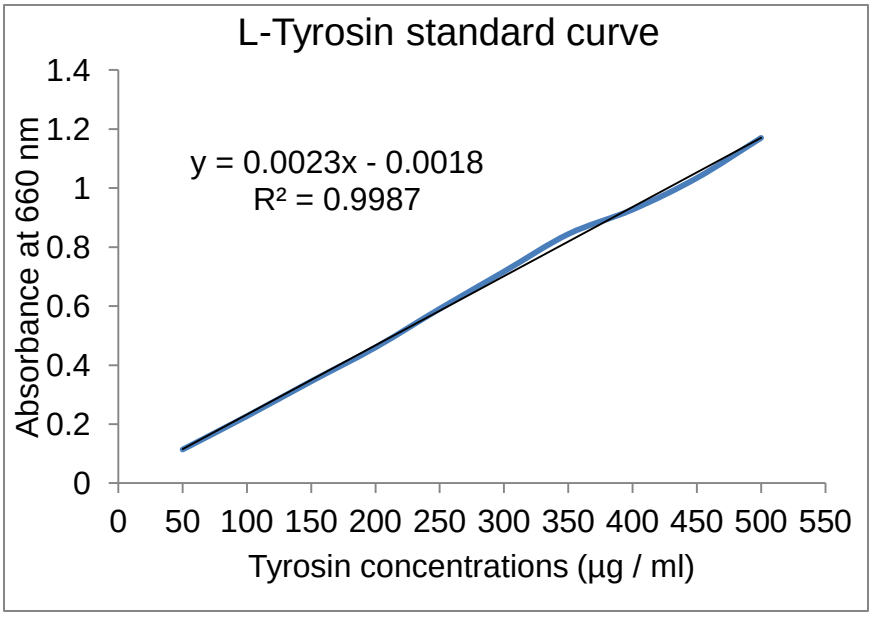

Annex 9. Albumin standard curve and protein assay

It was carried out in full darkness

1- Stock solution of albumin (100 µg/ ml): dissolve 1 mg albumin in deionized water (DW) and add DW to 10 ml.
2- The dilution series were prepared from the stock solution as following:

standards	Stock solution volume (µl)	Distilled water volume (µl)	Bradford reagent volume (µl)	Desired concentration
Blank	0	1600	400	0 (µg/ ml)
Std 1	60	1540	400	3 (µg/ ml)
Std 2	120	1480	400	6 (µg/ ml)
Std 3	180	1420	400	9 (µg/ ml)
Std 4	240	1360	400	12 (µg/ ml)
Std 5	300	1300	400	15 (µg/ ml)

3- Incubate 5 minutes at room temperature.
4- Read the absorbance at 595 nm.

Standard no.	Concentration (µg/ ml)	Absorbance at 595 nm		
1	3	0.22	0.26	0.266
2	6	0.418	0.424	0.419
3	9	0.59	0.608	0.568
4	12	0.731	0.73	0.718
5	15	0.847	0.843	0.851

Plot the standard curve of the absorbance (y- axis) against the concentration (x-axis).

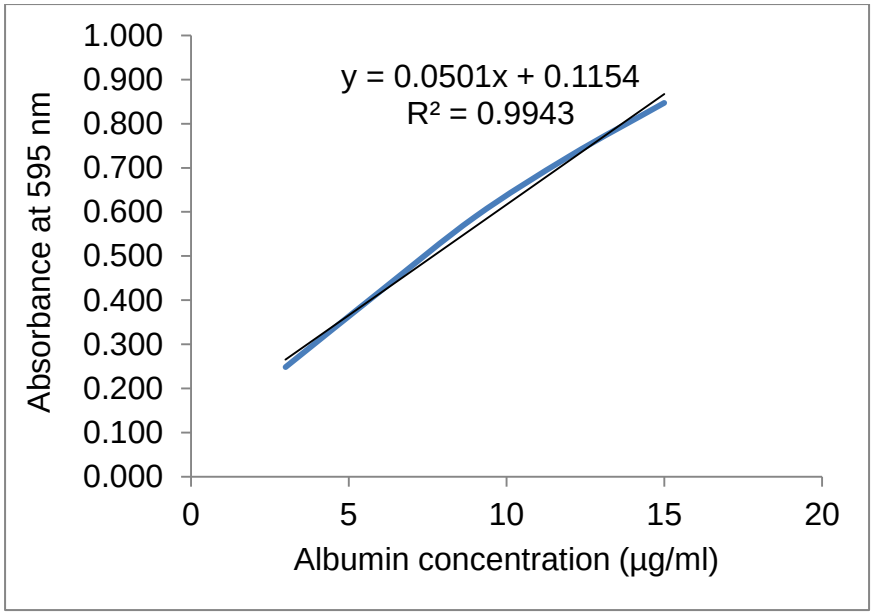

5- To measure the samples: 1 ml of sample + 600 ml DW +400 ml Bradford reagent and incubate 5 minutes at room temperature then read the absorbance at 595 nm and compare it with the standard curve to obtain the concentration of protein in the sample (with consideration of dilution factor).